UNIVERSITY OF CALIFORNIA SAN DIEGO

SAN DIEGO STATE UNIVERSITY

TWEAK-Fn14-RelB Signaling Cascade Promotes Stem Cell-like Features that Contribute to Post-Chemotherapy Ovarian Cancer Relapse

A dissertation submitted in partial satisfaction of the requirements for the degree of Doctor of Philosophy

in

Chemistry

by

Ryne Holmberg

Committee in charge:

University of California San Diego

Professor Gourisankar Ghosh
Professor Michael Gilson

San Diego State University

Professor Tom Huxford, Chair
Professor Carrie House
Professor Scott Kelley
Professor Christal Sohl

2023

The dissertation of Ryne Holmberg is approved, and it is acceptable in quality and form for publication on microfilm and electronically.

_____

_____

_____

_____

_____

_____
Chair

University of California San Diego

San Diego State University

2023

Dedication

This work is dedicated to my two wonderful children, Ellie and Micah, for their health and happiness.

16-bit Intel 8088 chip

with an Apple Macintosh
you can't run Radio Shack programs
in its disc drive.
nor can a Commodore 64
drive read a file
you have created on an
IBM Personal Computer.
both Kaypro and Osborne computers use
the CP/M operating system
but can't read each other's
handwriting
for they format (write
on) discs in different
ways.
the Tandy 2000 runs MS-DOS but
can't use most programs produced for
the IBM Personal Computer
unless certain
bits and bytes are
altered
but the wind still blows over
Savannah
and in the Spring
the turkey buzzard struts and
flounces before his
hens.

-Bukowski

Table of Contents

List of Figures

List of Tables

List of Abbreviations

ARD	Ankyrin Repeat Domain
CDDP	Cis-diamminedichloroplatium(II). AKA Cisplatin.
CSC	Cancer Stem Cells (see also: TIC)
Fn14	*Fibroblast growth factor-inducible immediate-early response protein 14. (TNFRSF12A, TWEAKR)*
HGSOC	High Grade Serous Ovarian Cancer
HO-8910PM	Highly metastatic derivation of HO-8910, a human ovarian cancer cell line
MCP-1	Monocyte Chemoattractant Protein-1.
NACT	Neoadjuvant Chemotherapy.
NF-κB	Nuclear Factor Binding the kappa light chain in B Cells
OC	Ovarian Cancer
OS	Overall Survival
PDTC	Pyrrolidine Dithiocarbamate, an inhibitor of NF-κB signaling. Blocks canonical signaling but not non-canonical.
PFS	Progression Free Survival
RFS	Relapse Free Survival
TIC	Tumor Initiating Cells (see also: CSC)
TNFSF	Tumor Necrosis Factor Superfamily
TWEAK	TNF-like Weak Inducer of Apoptosis
VBCF004	Primary cell line derived from the ascites of an HGSOC patient.

Acknowledgments

Chapter 1 includes material as it appears in Molecular Cancer Research 2023. My coauthors are Mikella Robinson, Samuel F. Gilbert, Omar Lujano-Olazaba, Jennifer A. Waters, Emily Kogan, Candyd Lace R. Velasquez, Denay Stevenson, Luisjesus S. Cruz, Logan J. Alexander, Jacqueline Lara, Emily M. Mu, Jared Rafael Camillo, Benjamin G. Bitler, Tom Huxford, and Carrie D. House. The dissertation/thesis author was the primary investigator and author of this paper.

In addition, I would like to thank Tom Huxford for his unending mentorship, support, and guidance throughout this journey. I would also like to thank Carrie House for taking me in and for modeling what it means to be a scientist. I would also like to thank the many labmates, from many labs, who have helped with experiments, data handling, writing, emotional support, and many other things. Bless you all.

Vita

2011 Bachelor of Science, Point Loma Nazarene University

2023 Doctor of Philosophy, University of California San Diego

San Diego State University

Abstract of The Dissertation

TWEAK-Fn14-RelB Signaling Cascade Promotes Stem Cell-like Features that Contribute to Post-Chemotherapy Ovarian Cancer Relapse

by

Ryne Holmberg

Doctor of Philosophy in Chemistry

University of California San Diego, 2023

San Diego State University, 2023

Professor Tom Huxford, Chair

Ovarian cancer is the most lethal gynecological cancer in the United States. Despite responding well to initial treatment, most patients relapse within 24 months. This relapse may be caused by cancer stem-like cells (CSCs) which resist initial chemotherapy and seed new heterogeneous tumors. Non-canonical NF-κB has previously been implicated in supporting CSCs, but the mechanism by which it does this is not understood. In this study we show that TWEAK and its receptor Fn14 are strong inducers of the non-canonical NF-κB pathway and that they are both enriched after chemotherapy. We go on to show that TWEAK/Fn14/RelB signaling enhances

CSC features and phenotypes, including spheroid formation, asymmetric division, *SOX2* expression, and the expression of EMT genes *VIM* and *ZEB1*. We also show that TWEAK treatment in combination with carboplatin enriches the CSC marker CD117, both by promoting CSC formation and by sensitizing non-CSCs to apoptosis. Inhibition of the TWEAK/Fn14/RelB axis in i.p. mouse model significantly prolonged overall survival when given as maintenance therapy post-chemotherapy. These results implicate TWEAK and Fn14 as factors which contribute to ovarian cancer relapse which could be explored for therapeutic development.

Chapter 1: TWEAK-Fn14-RelB Signaling Cascade Promotes Stem Cell-like Features that Contribute to Post-Chemotherapy Ovarian Cancer Relapse

1. Introduction

1.1 Ovarian Cancer

Ovarian Cancer is the most lethal gynecological malignancy in the United States, and the second most lethal overall among women.[1] One of the causes of this high mortality rate is that the disease is often diagnosed in stage III or IV due to a lack of early symptoms or screening.[2] Early symptoms are typically mild and are therefore overlooked. Screening for ovarian cancer is not part of a standard healthcare regimen and screening techniques are largely ineffective, having no overall effect on mortality rates.[3,4] In addition to a lack of early detection, relapse is a particular problem in HGSOC. Despite responding well to initial platinum-based therapies, over 80% of patients relapse within 24 months, with the new tumors being chemoresistant and aggressive. Between the late stage of diagnosis and high relapse rates, there is a desperate need both for improved early detection as well as treatments focused on relapse.

Epithelial carcinomas make up about 90% of all ovarian tumors. These tumors are classified into subtypes based on the type of epithelial cell within the female reproductive tract which gave rise to the initial tumor. These subtypes are serous, mucinous, endometrioid, clear cell, and transitional cell carcinomas. Distribution of these subtypes are: 52% serous, 10% endometrioid, 6% mucinous, 6% clear cell, and the remaining 26% being either rare subtypes or unspecified. In addition to the epithelial subtypes, there are also two types of non-epithelial ovarian

cancer: germ cell and sex cord-stromal tumors. These make up about 5% of ovarian cancer tumors.[5]

Additionally, ovarian tumors are divided into two categories: Type I and Type II tumors. Type I tumors develop from a precursor lesion and are strongly associated with KRAS, BRAF, and ERBB2 mutations, but have only 8% TP53 mutation. Type II tumors on the other hand develop directly from the surface epithelium or serous tubal intraepithelial carcinomas (STIC). The mutational drivers are inverted, with >80% mutation rate for TP53 while KRAS, BRAF, and ERBB2 mutations are rare.[6] Type I subtypes include low grade serous, mucinous, endometrioid, clear cell, and transitional cell carcinomas. Type II tumors include high grade serous, undifferentiated carcinomas, and carcinosarcomas.[2,7] Type II high grade serous makes up most cases of ovarian cancer. Despite their name, most HGSOC cases begin in the fallopian tubes and not the ovaries.[8–12] This same subtype is also responsible for 70-80% of all ovarian cancer deaths.[13]In addition to the above, tumors can be categorized by the mutational drivers which lead to tumor initiation.

Ovarian Cancer Staging

Like most cancers, ovarian cancer is divided into 4 stages based primarily on three criteria: local size and spread, presence in the lymph nodes, and the presence of distant metastases. Staging is a complicated assessment based on a combination of physical examination, biopsy, imaging, as well as examination during surgery, if applicable, and consists of several substages. Simply, Stage I signifies that the cancer is localized to the ovary or fallopian tube and is not detectable in lymph nodes. Stage II signifies that the ovarian cancer is in both ovaries/fallopian tubes and has spread to local organs such as the uterus, bladder, colon, or rectum, but is still not spread to lymph nodes or distant sites. The presence of a primary peritoneal tumor and/or ascites, defined as an abnormal

buildup of fluid in the abdomen, are also indicative of Stage II. Stage III signifies that there is further spread of the cancer, either into lymph nodes or into sites more distant than those listed in Stage II. Stage IV ovarian cancer has spread all over the body, commonly including all lymph nodes, the spleen, liver, and intestine.[14]

Ovarian Cancer Stem-like Cells (CSCs)

Although ovarian cancer typically responds well to traditional chemotherapy, over 80% of patients relapse within 24 months with the new tumors being chemoresistant.[15,16] One suggested cause of this recurrence is a small population of cancer cells within the tumor known as Cancer Stem-like Cells (CSCs), also referred to as Tumor Initiating Cells (TICs). The key features of CSCs are that they are quiescent, chemoresistant, and are capable of asymmetric division and long-term self-renewal.[17] These features allow a small portion of tumor cells to survive initial chemotherapy and create new heterogenous tumors.

CSCs make up only about 0.01-1% of all cells within the tumor and are themselves a heterogeneous population.[18,19]. These populations are challenging to define and distinguish from bulk tumor cells. Because of this scarcity, it is important to have good markers for identifying CSCs. Ovarian CSCs are identified by a combination of cell-surface markers, functional assays, and gene expression profiles, and mouse models such as limiting dilution and transplantation. The cell-surface markers used to identify CSCs in ovarian cancer include CD117 (c-kit), CD133, CD24 and CD44, and ROR1, or some combination thereof.[19–24] In addition to surface markers, proteins such as Lin28 and Myc have been associated with the CSC phenotype.[25–27] Functional assays such as spheroid forming ability and ALDH1/2 activity (usually by ALDEFLUOR assay) are also used to identify CSCs. Owing to their stem-like nature, CSCs also express the master stem-cell

regulators *OCT4*, *SOX2*, and *NANOG*, although recent work has demonstrated that of these three, *SOX2* is the most consistent indicator in ovarian cancer.[21,23,28–30]

EMT

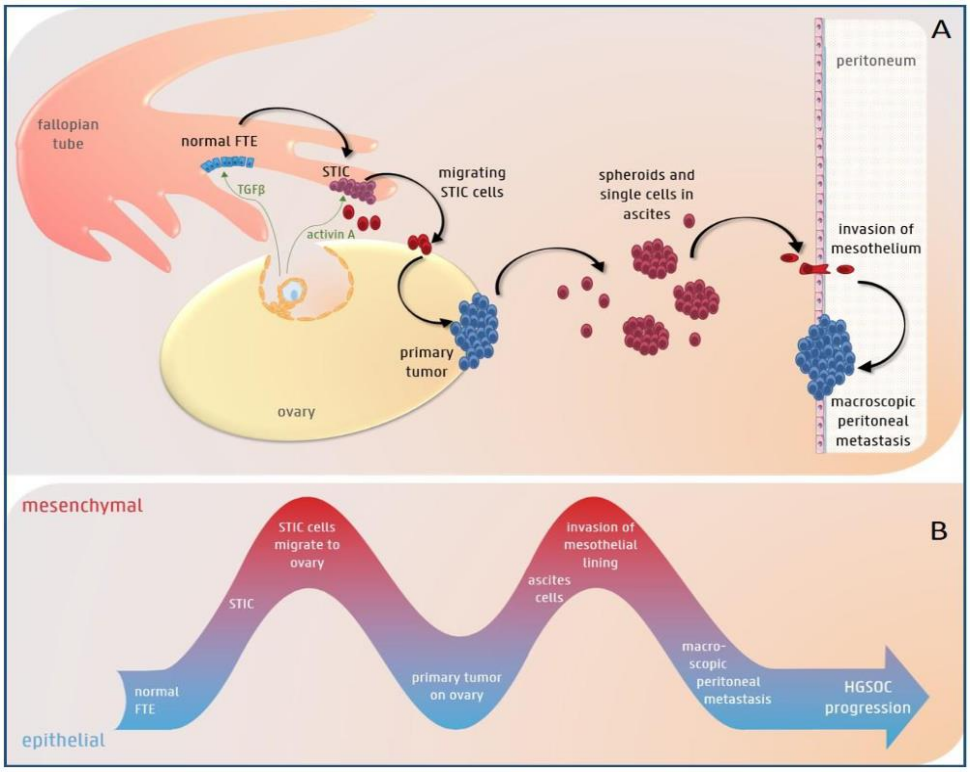

Figure 1 *– The potential role of EMT plasticity during HGSOC progression.*[31]

The epithelial to mesenchymal transition (EMT) is, as the name suggests, the processes of epithelial cells turning into mesenchymal cells. Epithelial cells are laid out in a tight 'brick wall' of apical-basal polarized cells which maintain adherens junctions, tight junctions, and desmosomes to keep cells together. Mesenchymal cells, on the other hand, have front-rear polarity, have less-rigid shapes, are detached from neighboring cells, and most importantly, are mobile through the ECM.[31,32] Progression through the EMT causes epithelial cells to gain more mesenchymal-like

phenotypes. This was first identified in embryonic development but also occurs in normal wound healing and in disease states such as organ fibrosis and cancer.[33]

In the context of cancer, the main effect of the EMT is the generation of cells which can move through and survive detached from the basement membrane. Detachment from the membrane allows the cells to be more mobile, which is necessary for spread, both locally and for distant metastases (**Figure 1**).[31,34] The EMT is a necessary part of many, if not all, cancer's progression.[35] The EMT is a reversible process, as these cells are capable of reverting to their epithelial state in a process known as the mesenchymal to epithelial transition (MET). MET progression allows mobile cancer cells to re-attach to an epithelial layer and form new tumors. During cancer progression, cells may revert back and forth between epithelial and mesenchymal states several times.[31]

The entire process is regulated by a relatively small number of EMT transcription factors (EMT-TFs), such as ZEB1, SNAIL/SLUG, and TWIST. These in turn regulate hundreds of target genes involved in the EMT. Many of these genes and gene products are used as markers for progression of the EMT. The markers used in this study are VIM, CDH1, and ZEB1.

Vimentin (VIM) is a type III intermediate filament that is the main structural component of mesenchymal cells. It is abundant in mesenchymal cells and is one of the most common markers for mesenchymal state.[36,37] Cadherin 1 (E-Cadherin, CDH1) is a calcium-dependent cell adhesion protein. It binds cells to one another in the epithelial layer and is therefore an epithelial marker. Loss of CDH1 loosens the connections between cells, allowing them to become more mobile. Zinc-finger E-box-binding homeobox factor 1 (ZEB1) is an EMT transcription factor (EMT-TF) which controls hundreds of target genes but is known to promote EMT over MET. For example,

ZEB1 represses the transcription of CDH1 while promoting vimentin by recruiting chromatin modifying proteins to their promoters.[35]

Treatment of Ovarian Cancer

Current standard of care for ovarian cancer involves surgery to debulk the tumor followed by chemotherapy to kill any remaining cancer cells.[38] For early stage I cases where the tumor has not spread, surgery may be sufficient by itself. In more advanced cases chemotherapy may be required prior to surgery to shrink the tumors to a more manageable size. Standard chemotherapy drugs used are a combination of carboplatin and paclitaxel, though cisplatin and docetaxel are also sometimes used. In addition to this regular regimen, treatment of stage III and IV disease usually includes additional drugs given as maintenance therapy to prevent relapse. Current maintenance drugs include the anti-angiogenesis antibody bevacizumab and three PARP inhibitors; niraparib, rucaparib, and olaparib.[38,39]

The most common adjuvant treatment in ovarian cancer are PARP inhibitors. PARP inhibitors are used in breast, ovarian, prostate, fallopian, and peritoneal cancers, and have been proposed as treatments for other cancers as well. Poly(ADP-ribose) polymerase (PARP) is a family of 17 enzymes which catalyze the transfer of ADP-ribose to target proteins. PARP1 and PARP2 are the enzymes of interest in ovarian cancer. One of their main functions is to detect and respond to single strand breaks (SSBs) in DNA. Along with DNA-PK, ATM, and p53, it is one of the early response proteins in DNA damage detection and repair. Detection of an SSB by PARP leads to production of PAR, which signals other members of DNA repair pathways.[40,41] Inhibition of PARPs leads to an accumulation of SSBs, which can become double strand breaks (DSBs) during replication. These DSBs are normally repaired by the homology-directed repair (HDR)

mechanisms, which is why PARP inhibitors are effective in cancers with BRCA1/2 mutations which have homologous repair deficiency (HRD).[42–44]

While PARP inhibitors and bevacizumab are the only current adjuvant treatments for HGSOC, other potential drug targets are being investigated. Targeting ALDH1 has had the most promising results to date. Disulfiram, an ALDH inhibitor, has shown significant anti-CSC activity in several cancers, including breast and prostate cancers. Disulfiram is FDA approved as a treatment for alcoholism, but because it is an ALDH inhibitor and ALDH is a marker for CSCs, it is being researched as potential treatment for ovarian cancer.[45,46] Disulfiram has been shown to sensitize tumor cells to radiation therapy while simultaneously protecting healthy cells.[47,48] It also has been shown to work synergistically with PARP inhibitors to suppress ovarian cancer, though not specifically CSCs.[46] Although it has received FDA approval for other uses, it has not yet been tested in a clinical environment as treatment for ovarian cancer.

Several other CSC marker proteins are also potential drug targets for specifically targeting CSCs. CD24 and CD44 have both been considered as targets and have shown some promising results both *in vitro* and *in vivo*, but no therapeutics are currently under development. CD24 has proven difficult to target due to its widespread expression. CD117 has been targeted using the kinase inhibitor imatinib, but it showed no efficacy in preventing relapse in phase 2 clinical trials and had similarly disappointing results when combined with docetaxel. The proposed reason for this failure is that only ~30% of ovarian tumors are $CD117^{+}$.[49,50] CD133 was investigated by using an anti-CD133 antibody. While the antibody does concentrate in ovarian tumors and has been used for imaging, it has not been further developed as a therapeutic.[39]

1.2 NF-κB

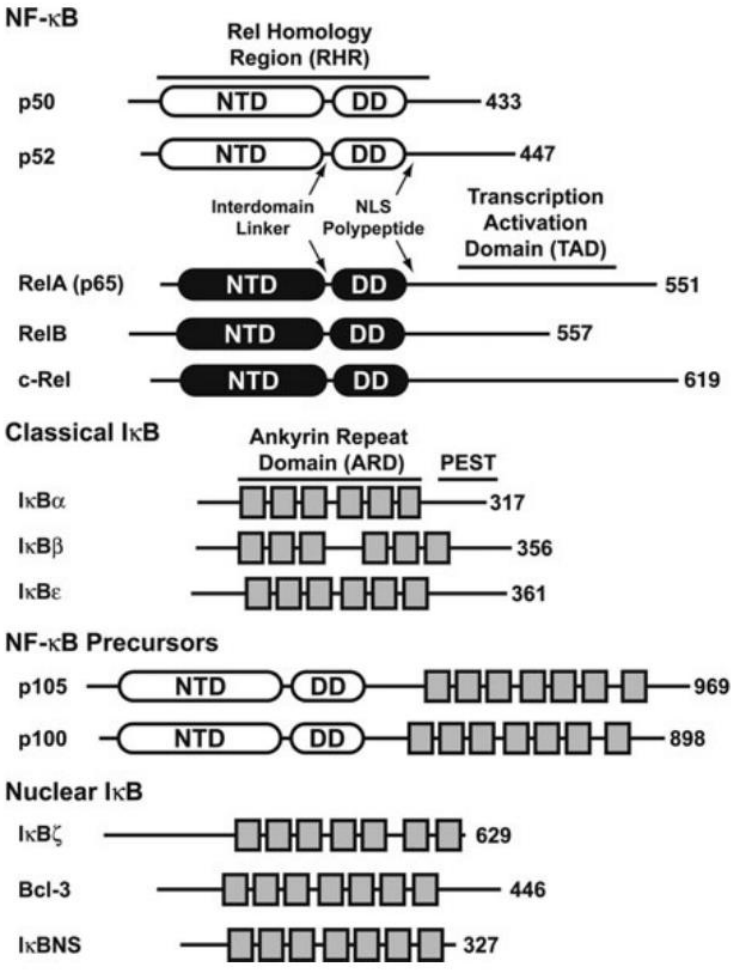

Figure 2 *– Domain organization of NF-κB and IκB proteins. The five NF-κB polypeptides are depicted in schematic form with the arrangement of the elements and domains discussed in the text identified and human numbering indicated. The IκB proteins are divided into classical IκB, NF-κB precursors, and nuclear IκB. From Huxford et. al.*[51]

NF-κB is a family of eukaryotic transcription factors that regulate the expression of diverse stress response genes including many key effectors of cell survival and inflammation. The signal transduction pathway that activates NF-κB has been the subject of extensive study for almost 40 years. NF-κB was first discovered by Ranjan Sen and David Baltimore in 1986 as a constitutively nuclear heterodimeric protein factor with affinity for a specific 10 base pair DNA element present within the intronic enhancer of the immunoglobulin kappa light chain in cultured B cells.[52] Soon after its discovery, however, it was observed that NF-κB is present in most, if not all, cells as part

of an inactive cytoplasmic complex with a member of the IκB family of transcription factor inhibitor proteins.[53] Control over NF-κB activity is, therefore, a consequence of selective removal of IκB proteins from inactive, cytoplasmic NF-κB:IκB complexes.[54]

NF-κB is aberrantly regulated or constitutively active in many tumors, including ovarian, and contributes to progression of a variety of cancers.[55] NF-κB can potentially affect the expression of hundreds of target genes. The NF-κB signal transduction pathway is wide ranging and pervasive and participates in crosstalk with several other signaling cascades including STAT3, p53, NRF2, JNK, Wnt, Notch, MAPK/ERK, PI3K, and Hedgehog.[56] Despite extensive efforts, selective targeting of NF-κB with small molecule therapeutics has not proven clinically beneficial. This is in large part due to its wide-ranging effects.

NF-κB Transcription Factors

The NF-κB family is composed of five polypeptide subunits: RelA (p65), RelB, c-Rel, p50, and p52 that spontaneously assemble as function homo- and heterodimers (**Figure 2**). Each of these proteins contains a conserved roughly 300 amino acids long stretch near their N-terminal ends known as the Rel Homology Region (RHR). Contained within the RHR are the sequences necessary for binding to DNA targets, dimerization, noncovalent association with IκB proteins, and active nuclear localization. Although, through combinatorial association, 15 distinct dimer combinations are possible, the p50:RelA and the p52:RelB heterodimers are the most commonly discussed, as they are the primary functional NF-κB dimers activated in response to canonical and non-canonical NF-κB signaling, respectively. Not all of the potential combinations have been observed in cells, likely due to their incompatibility. For example, the RelB:RelB homodimer exhibits significantly lower stability *in vitro*, as does RelB:RelA and RelB:c-Rel heterodimers. On the other hand, some other less well studied NF-κB dimers are quite abundant and play very

important roles as well. For example, c-Rel-containing dimers are known to promote survival in neuronal cells.[57]

Structurally, the RHR of NF-κB transcription factors contains two distinct folded domains in addition to a Nuclear Localization Signal (NLS) peptide region. The two domains are the N-terminal domain, which corresponds roughly to the first 200 or so amino acids of the RHR, and the C-terminal dimerization domain, which consists of the final 100 or so amino acid residues. The two domains are joined by a flexible linker peptide of approximately 10 amino acids in length. The dimerization domain contains the interface which allows NF-κB proteins to dimerize with one another. Both domains are involved in binding to DNA, though base-specific contacts are mediated exclusively by amino acids from the N-terminal domain. The flexible NLS polypeptide, which is immediately C-terminal to the dimerization domain, contains a type I nuclear localization signal that is necessary for import into the nucleus. The NLS is masked upon association with IκB, rendering the inactive complexes cytosolic prior to pathway activation.[51]

RelA, RelB, and c-Rel each contain disordered transcriptional activation domains (TADs) C-terminal to their RHR. Consequently, NF-κB dimers that contain at least one of these subunits serve as activators of target gene expression. The p50 and p52 subunits, which are, in fact, the partially digested products of "NF-κB precursor" IκB proteins p105 and p100, respectively, lack C-terminal TADs. Consequently, NF-κB dimers composed exclusively of p50 and/or p52 do not promote target gene expression without involvement of some transcriptional co-activator.

IκB Inhibitor Proteins

There are currently eight factors recognized as inhibitors of NF-κB (IκB) proteins. The defining structural characteristic of IκB is the presence of an Ankyrin Repeat Domain (ARD) with affinity toward specific NF-κB subunits. The ARD is a helical repeat motif that is relatively

common among proteins involved in protein-protein interactions. Each repeating unit is approximately 33 amino acids in length and consists of a short helix-loop-helix followed by an extended loop and a tight beta-turn. Success repeats stack upon one another generating an elongated protein domain without a classic "hydrophobic core." IκB proteins typically contain 6-7 ankyrin repeats.

IκB proteins can be classified into three subgroups: classical IκB, NF-κB precursors, and nuclear IκB. The classical IκB sugbroup includes IκBα, IκBβ, and IκBε. These proteins are responsible for binding to and sequestering RelA- and c-Rel-containing NF-κB dimers such as the canonical p50:RelA heterodimer in the cytoplasm. IκBα is by far the best studied of the classical IκB proteins. Though IκBβ is present in equal amounts to IκBα in some tissues, and both IκBβ IκBε are capable of binding with high affinity to NF-κB dimers *in vitro*, their actual physiological roles are less well understood. The three classical IκB proteins all contain a regulatory N-terminal flexible region which contains the consensus sequence D<u>S</u>GXX<u>S</u>. The two serines in this region are phosphorylation sites for the IκB Kinase β subunit (IKKβ or IKK2). Dual phosphorylation of these sites leads to their recognition by the β-TrCP receptor subunit of an SCF-type E3 ubiqutin-protein ligase complex targeting the complex-associated IκB for polyubiquitinylation and, ultimately, proteolytic degradation by the 26 *S* proteosome.[51]

"NF-κB precursors" refers to p105 and p100. These fascinating proteins are *bona fide* IκB proteins that each possess a C-terminal ARD with binding specificity for NF-κB proteins and phosphorylation sites. Interestingly, the affinity of p105 and p100 does not overlap with classical IκB proteins. Consequently, p100 in particular is found to be associated with RelB. But even more interesting is the fact that p105 and p100 are post-translationally processed via the proteasome, leaving the functional NF-κB protein subunits p50 and p52, respectively. The processing of p105

to p50 is constitutively active and p105 is therefore typically short lived. In contrast, p100 remains intact and sequesters RelB in the cytoplasm until non-canonical NF-κB pathway activation causes the IκB Kinase α subunit (IKKα or IKK1) to phosphorylate it at two conserved serine residues leading to its polyubiqutinylation and partial processing to p52.

The nuclear IκB subgroup consists of Bcl-3, IκBζ, and IκBNS. These are the least well understood of the IκB proteins. The property that unites them and is that they each migrate to the nucleus when expressed in eukaryotic cells. They also show different binding affinity than classic IκB proteins with Bcl-3 selectively binding to p52 and IκBζ targeting p50. IκBζ has been shown to act as a regulator of NF-κB: it represses expression of some NF-κB-dependent genes and activates others [58–62]. IκBζ is typically absent in resting cells but is itself a primary transcript of NF-κB induction through TLR-4 or the IL-1R receptors. The role of IκBζ has been defined primarily by its involvement in the transcription of pro-inflammatory cytokines including CCL2, IL-6, IL-17, IFN-γ, and others.[61,63–66] In the right context however, it demonstrates strong anti-inflammatory effects, most significantly through the production of IL-10 and M2 macrophage polarization.[67] In addition to cytokine production, IκBζ is also a key regulator for H3K4 trimethylation and a regulator for the chromatin remodeling factor Brg1.[68–70] Furthermore, IκBζ has been implicated in several diseases including gliomas, psoriasis, dust mite allergies, and broader inflammatory diseases.[71–73].

IκB Kinase (IKK)

Regulation of NF-κB is largely dependent upon removal of IκB proteins from inactive NF-κB:IκB complexes. This process is governed by the IκB Kinase (IKK). IKK is an enzyme complex of three proteins: IKKα (IKK1), IKKβ (IKK2), and IKKγ (NEMO). IKKα and IKKβ are catalytically active kinases while IKKγ acts in a supporting role. IKKγ is traditionally thought of

as a scaffold protein that exerts its necessary effect on the complex by regulating subcellular localization. However, recent work has shown that in some instances IKKγ may also play a more direct role of allosteric control over IKKβ subunit activity.[52]

The IKK complex is the lynchpin of NF-κB signaling. It is responsible for phosphorylation of the regulatory serines on IκB proteins, which ultimately leads to transcription factor activation. Even though the complex contains two potentially catalytic protein kinases (IKKα and IKKβ), and the two protein kinase subunits are extremely highly similar from primary amino acid sequence to tertiary fold, only IKKβ is observed to phosphorylate classical IκB proteins *in vivo* in response to pro-inflammatory stimuli via the "canonical" NF-κB signal transduction pathway. No other kinases have been observed fulfilling this function. Interestingly, IKKα, the second kinase in the complex, can perform the function *in vitro,* but is not known do so *in vivo*.[74] It does, however, play an extremely important role in activating NF-κB in response to a subset of stimuli through a "non-canonical" NF-κB signaling pathway that does not require IKKγ.[54] IKK has additional functions in addition to its primary role in the NF-κB pathway. There are as many as 50 identified phosphorylation targets between IKKα and IKKβ, though not all have been verified *in vivo*.[75]

NF-κB Signaling

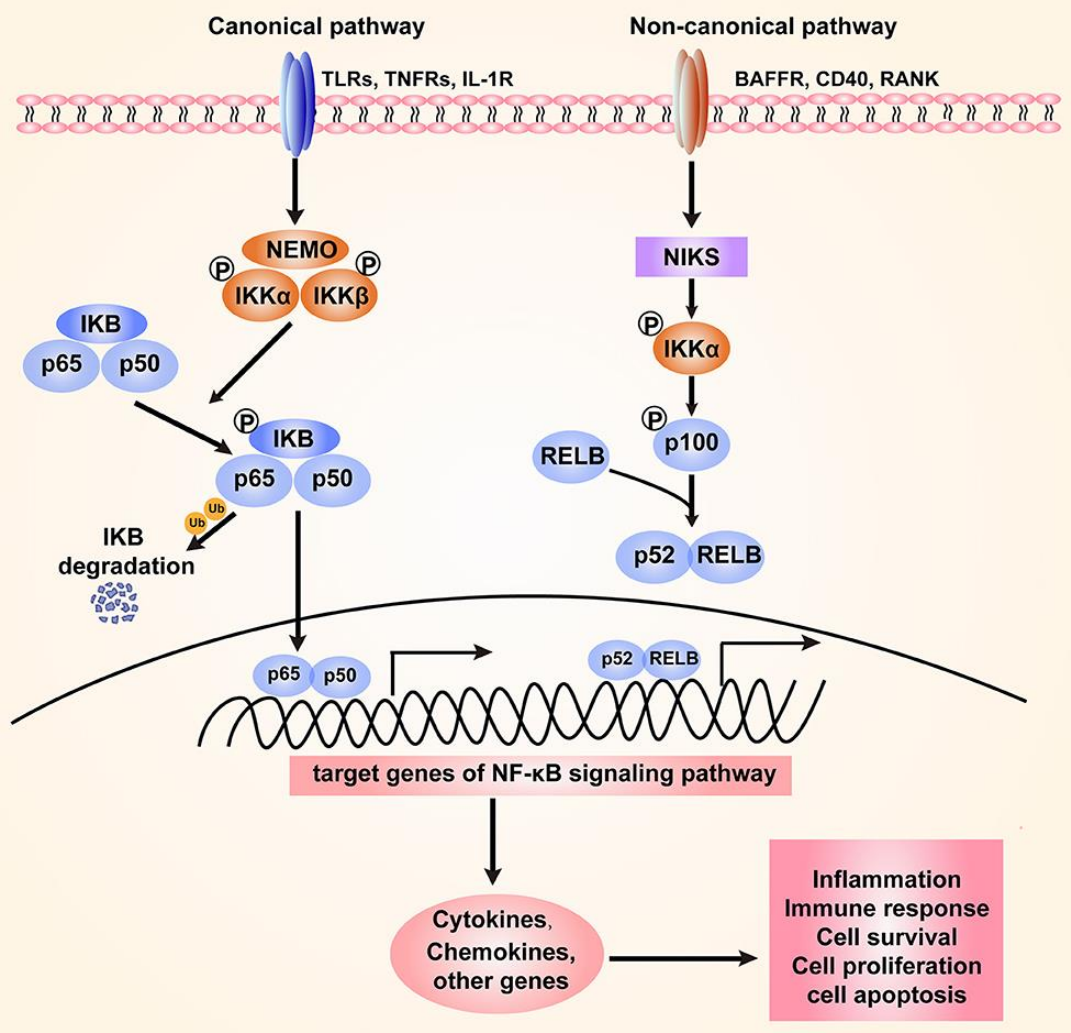

Figure 3 *- The two branches of the NF-κB pathway.*

NF-κB has, therefore, two distinct signaling pathways by which it can become activated and begin the process of elevating the expression of select target genes: the canonical (classical) and non-canonical (alternative) pathways (**Figure 3**). The different pathways are defined by the identities and mechanisms of their upstream signaling factors as well as by the specific NF-κB proteins that are induced. In canonical NF-κB signaling the NF-κB p50:RelA heterodimer is sequestered in the cytosol through its association with IκBα. Signaling through diverse plasma

membrane-associated or intracellular receptors leads to the IKKγ-dependent catalytic activation of the IKKβ subunit via dual site phosphorylation within the activation loop of its protein kinase domain. Induction of NF-κB proceeds through the dual phosphorylation of IκBα by IKKβ, leading to ubiquitin-dependent 26 *S* Proteasome-mediated degradation of IκBα. This in turn releases the p50:RelA heterodimer, allowing it to translocate to the nucleus where it performs its function as a transcription factor.

In non-canonical or alternative NF-κB signaling, the NF-κB complex is RelB in association with the of p100 NF-κB precursor. The c-terminal end of p100 acts like IκBα, sequestering the complex in the cytosol in the inactive state. Activation of BAFF, Lymphotoxin-b, CD40, TWEAK, or RANK receptors leads to an accumulation of the NF-κB inducing kinase (NIK), which under normal conditions is constitutively synthesized and then ubiquitinylated and degraded. Pathway activation prevents degradation of NIK, which leads to activation of IKKα kinase activity via activation loop phosphorylation. Notably, this action is independent of any role by IKKγ. Active IKKα is able to phosphorylate p100, leading to its partial proteasomal processing to p52 and yielding an unmasked NF-κB p52:RelB heterodimer, which then enters the nucleus to activated target gene expression.

Previous work has suggested that differential activation of NF-κB signaling promotes either TIC or not-TIC phenotypes in ovarian cancer. Broadly speaking, canonical NF-κB signaling is more critical for rapid proliferation, while non-canonical signaling is vital for quiescence, although both impart some drug resistance. It remains unknown what factor(s) lead to differential activation of these pathways in ovarian cancer.[76]

1.3 TWEAK/Fn14

Structure

TNF-like weak inducer of apoptosis, or TWEAK, (TNFSF12, APO3L) was originally reported by Chicheportiche et al. in 1997 as a weak inducer of apoptosis in HT-29 colon cancer cells sensitized with IFN-α or IFN-γ.[77] It was separately identified in 1998 by Marsters et al. as a ligand for the 'death receptor' APO3R because of its ability to induce apoptosis in cells with this receptor.[78] They therefore initially named it APO3L. Although this conclusion was reasonable at the time, it has since been demonstrated that TWEAK was likely acting on a different receptor as TWEAK does not have affinity for APO3.[79]

TWEAK is synthesized as a 249 AA type II transmembrane protein. It is composed of a 206 AA extracellular region, 25 AA transmembrane region, and an 18 AA intracellular domain. Like most of the TNFSF members, TWEAK forms a trimer on the cell surface and the biologically active form is released into the extracellular matrix upon proteolytic cleavage of the extracellular domain.[79]. Proteolysis takes place by furin cleavage between AAs 93-94, with AAs 90-93 containing the furin R-X-(K/R)-Rˇ cleavage site. Murine and human TWEAK are very similar, having 93% identity in the receptor binding domain.[77] TWEAK is a widespread cytokine, and mRNA and/or protein can be found throughout the body under basal conditions. It is expressed in the heart, pancreas, skeletal muscle, brain, colon, small intestine, lung, ovary, prostate, spleen, lymph node, appendix, and peripheral blood lymphocytes. It is also weakly expressed in several other tissues and has been detected in many different tumors.[80] Despite being widespread, the TWEAK/Fn14 pathway remains largely inactive often due to low expression of the receptor Fn14.[81]

The cognate receptor of TWEAK is fibroblast growth factor-inducible 14 (Fn14). Fn14 expression can be induced by FGF1 or FGF2 and it is ~14 kDa in size, making it the smallest receptor in the TNF Receptor Superfamily.[79] It is synthesized as a 129 AA type I transmembrane protein and processed to a 102 AA cell surface receptor by signal peptidase. The affinity of the TWEAK/Fn14 interaction is ~0.8-2.3 nM.[82,83] Notably, Fn14 lacks the death domain which is typical for TNFRs. Fn14 expression is induced upon injury and is therefore transient in wounds which heal but persistent in chronic disease.[81]

The only receptor other than Fn14 that is known to interact with TWEAK is CD163. CD163 is expressed exclusively on monocytes/macrophages and acts primarily as a scavenging receptor for soluble TWEAK, though alternative functions of the TWEAK/CD163 axis are being explored.[84–86] To the best of my knowledge, however, no signal transduction has been observed from this interaction.

TWEAK/Fn14 Signaling

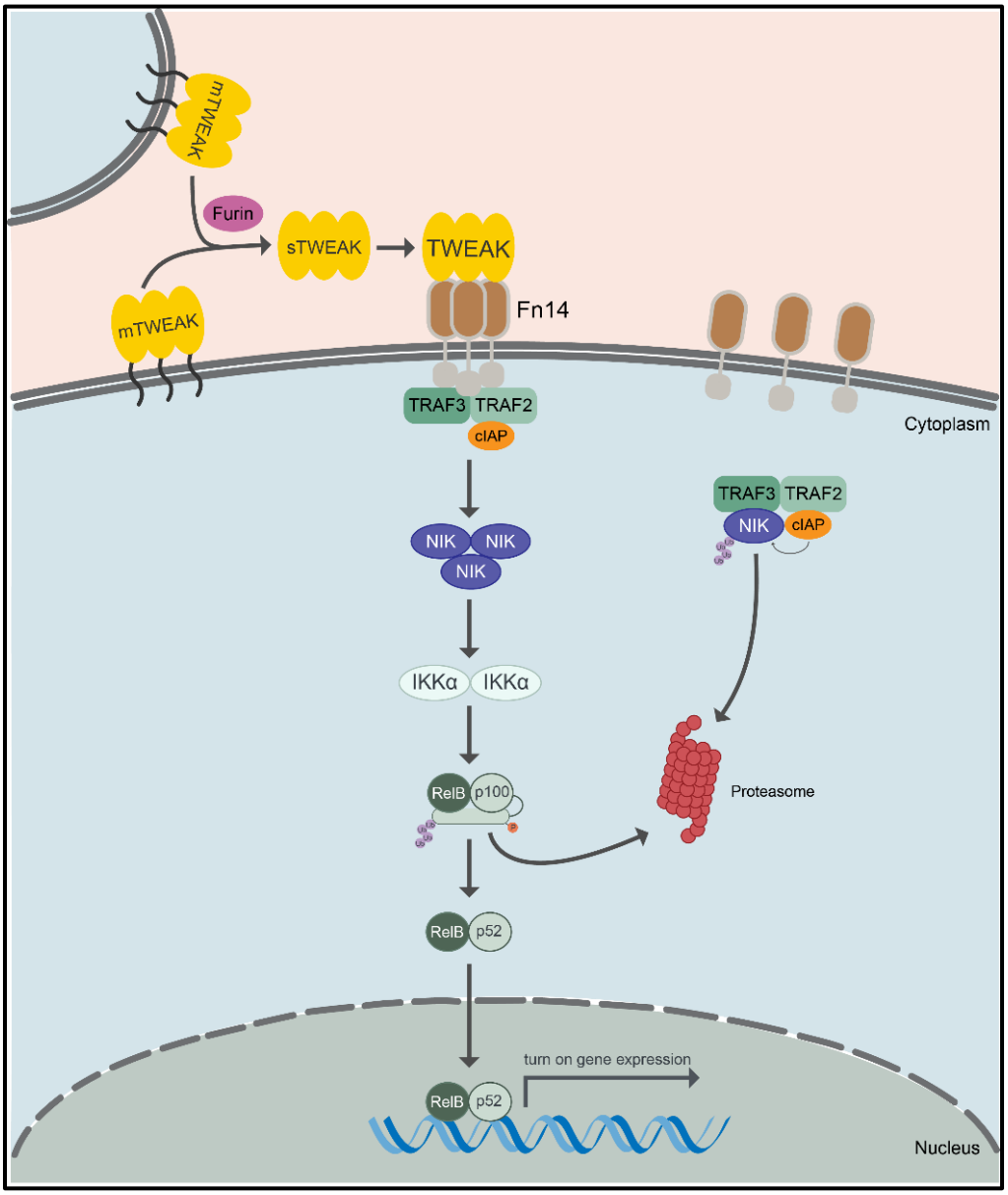

Figure 4 *- TWEAK/Fn14 signaling through non-canonical NF-κB*

TWEAK binding to Fn14 results in TRAF2/3/cIAP binding to the intracellular domain, which can stimulate multiple signaling pathways including NF-κB, ERK1/2, and PI3K/AKT.[79,87–92] In addition to different pathways, different TRAFs can activate the separate branches of the NF-κB pathway. TRAF 2, 5, and 6 are involved in canonical signaling, which occurs through various

receptors and with other receptor associated proteins such as TRADD, RIP1, TIRAP, TRAM, and others.[93]

TRAF2 and 3 are involved in non-canonical signaling.[94] Under unstimulated conditions, the TRAF2/3 heterodimer binds to both cIAP1/2 and NIK, bringing them together and promoting K48 polyubiquitination of NIK which is responsible for its persistent degradation. Ligand binding to TNFRSF members, such as TWEAK binding to Fn14, recruits TRAF2/TRAF3/cIAP to the receptor cytoplasmic tail, sequestering the complex and allowing accumulation of NIK. NIK accumulation leads to activation of IKKα and phosphorylation of p100, leading to its partial proteasomal processing into p52 and allowing the RelB:p52 dimer to translocate to the nucleus.

Function

TWEAK is a multifunctional protein, and its function is highly dependent on context. For example: in Eph4 cells, low concentration TWEAK treatment results in proliferation while high concentrations cause apoptosis. It can regulate proliferation, invasion/migration, survival, differentiation, cell death, angiogenesis, or inflammation.[81,95–99] The primary function of TWEAK/Fn14 is tissue remodeling and wound healing in response to acute injury. Signaling is often regulated by the expression of the receptor Fn14, which has low basal levels of expression but is transiently upregulated in response to injury.[81] However, Fn14 expression can be sustained in chronically diseased tissue, including many cancers, and is generally associated with poor prognosis. Additionally, high levels of Fn14 can result in TWEAK-independent Fn14 activation.[100] Under acute injury conditions, TWEAK/Fn14 plays a protective role and encourages muscle growth. Despite this, high levels of TWEAK are generally associated with negative phenotypes and outcomes in chronic disease.[101]

Aside from injury response, TWEAK is heavily involved in regulating skeletal muscle mass and metabolism and plays a role in several steps of myogenesis.[102] In endothelial cells, TWEAK acts as a growth and migration factor, but not its typical role as a survival factor.[103]

Although its name includes the phrase 'weak inducer of apoptosis', TWEAK/Fn14 only actually induces apoptosis under very specific circumstances. Fn14 is a TRAF-interacting TNF receptor and does not include a death domain typically found in the TNF receptors which cause cell death. When TWEAK/Fn14 induces apoptosis, it does so weakly and indirectly, often through the production of TNFα which activates the death receptor TNFR1.[104,105] In addition to causing apoptosis itself, TWEAK also sensitizes many cells to TNF-induced cell death. This has been observed widely, including in ovarian cancer and in our own work.[104,106,107] This TWEAK-induced sensitization seems to be specific to TNFR1 and is not observed with other TNFSF death domain receptors. TNFR1 typically recruits TRAF2-cIAP1/2 complexes upon stimulation. It is only when this complex is absent that TNFR1 signaling shifts to TRADD/RIPK1 recruitment and thus caspase-8 mediated apoptosis.[108] Fn14 stimulation recruits TRAF2-cIAP1/2, depleting the pool available to TNFR1 and thus sensitizing the cell to TNFR1 apoptosis.[105,106] Interestingly, this same sequestration is also responsible for allowing NIK accumulation, leading to alternative NF-κB signaling.

TWEAK/Fn14 in Cancer

TWEAK overexpression is found in many cancers, including liver[109], colorectal[110], esophageal[111], kidney[112], bladder, pancreatic, ovarian, and prostate, and neuroblastoma. The receptor Fn14 overexpression is found in pancreatic[111] and gastrointestinal[111] cancers, among others. Fn14 is found in the above cancers with known TWEAK overexpression, as well as glioma, breast cancer, lung cancer, and melanoma.[113]

The role of TWEAK in ovarian cancer has not been thoroughly investigated. However, some work has been done by the OB/GYN department at Renji hospital in Shanghai, China. They consistently make use of the HO-8910PM cell line, which is a highly metastatic human ovarian cancer cell line established from ascites of a patient with malignant papillary serous adenocarcinoma.

They first demonstrated that TWEAK is a protein of interest in the context of ovarian cancer.[114] They showed that TWEAK activates the NF-κB pathway. This was demonstrated by western blot of p65 translocation to the nucleus as well as IκBα degradation in whole cell lysates. They did not investigate activation of non-canonical NF-κB signaling. They also showed that TWEAK stimulation caused an increase of VEGF production, which is crucial for primary tumor growth and metastasis. The authors went on to show that TWEAK stimulation had no effect on proliferation in their cell lines, consistent with our own work.

Further work investigated TWEAK/Fn14 signaling in primary patient samples. They found that TWEAK/Fn14 is found at high levels in malignant ovarian tumors, but not in borderline/benign tumors or in normal ovarian tissue.[107] This was determined by IHC of primary tumors, but this correlation was not corrected by subtype. They also found that neither TWEAK nor TNFα had any effect on proliferation, consistent with their previous results, but that the two in combination reduced proliferation. Furthermore, TWEAK treatment increased MCP-1 production, suggesting a possible anti-tumor effect through macrophage recruitment.

More recent work follows the role of TWEAK-stimulated macrophages (TMs) on ovarian cancer, rather than the effects of TWEAK directly on cancer cells.[115] Specifically, they demonstrated that TMs create exosomes which contain miR-7 and are internalized by EOC cells, resulting in reduced metastasis. miR-7 was also shown to be upregulated in macrophages,

exosomes, and EOC upon TWEAK treatment. A previous study had demonstrated that miR-7 inhibits metastasis through the AKT/ERK1/2 pathway.[116,117] EOC treatment with exosomes from TMs showed reduced expression of EGFR as well as reduced phosphorylation of AKT and ERK1/2. AntagomiR-7 was used to demonstrate miR-7 dependence of these effects. This work is interesting as it reveals completely different pathways than we study through which TWEAK is affecting ovarian cancer.

TWEAK/Fn14 Therapeutics

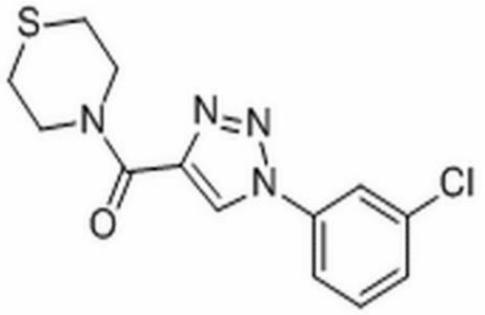

Figure 5 *– Structure of L524-0366*

Attempts have been made to block TWEAK/Fn14 signaling as an approach to treating several diseases. One of the products of this research is L524-0366, a commercially available Fn14 antagonist.[118] It has a K_D of 7.12 μM with Fn14. It is not approved for human use but is used in cells and mice to block TWEAK signaling and was used in the xenograft mouse model in this study.

In addition to L524-0366, several antibodies have been made to block TWEAK/Fn14 signaling. The first is RG7212, a fully humanized IgG1κ monoclonal antibody. It binds directly to soluble TWEAK, reducing free and total TWEAK in the system. Phase I clinical trials boasted

excellent tolerability and favorable pharmacokinetics, yet no further trials have been performed on the antibody since 2015.[119]

BIIB036 and PDL192 are anti-Fn14, blocking the receptor instead of capturing the ligand. BIIB036 is a humanized IgG1 anti-Fn14 agonistic antibody. It inhibits tumor growth and provides enhanced efficacy of standard chemotherapy in xenograft models. It also maintains surprising efficacy after ending dosing and has been proposed as a for use with CAR-T cell targeting. Despite these promising results, no work has been published since 2013.[120–122] PDL192 (Enavatuzumab) is an anti-Fn14 humanized IgG1 recombinant monoclonal antibody. Phase one trials showed too high toxicity at the given dose and schedule, though the authors suggest a more frequent, lower dose may be worth pursuing. [123–125]

18D1, 5B6, and 4G5 are a series of mouse-human cross-reactive llama-derived recombinant Fn14-specific antibodies. These antibodies are novel in that they contain an Fc domain which was absent from previous Fn14 targeting antibodies.[126] Of the three, 18D1 showed the most promise and further development of this antibody is being pursued.[127] An interesting result coming from study of 18D1 is that Fn14 blockade effects are efficient in variants with or without an active Fc domain, so Fn14 blockade is anti-tumor and anti-metastatic with or without antibody-dependent cell-mediated cytotoxicity (ADCC).[126] This is encouraging for our work as inhibition of the pathway is achieved through small molecule inhibition, not antibodies.

2. Materials and Methods

Fn14 Inhibitor

Fn14 Antagonist L524-0366 was purchased from Millipore Sigma/Calbiochem. The inhibitor was reconstituted at 25 mM in DMSO, aliquoted, and stored at -20°C.

This inhibitor has low solubility in water. Stocks were prepared in DMSO and precipitation was visible immediately after addition of the inhibitor to culture media, especially at higher concentrations. The concentration used for experimentation, determined from literature, was 25 µM. At this concentration some amount of precipitation could always be observed. However, the inhibitor was able to reverse TWEAK-induced activation of non-canonical NF-κB as seen by nuclear localization of RelB and processing and nuclear localization of p100 to p52.

General Culture Conditions

OVCAR8 and CAOV4 cells were obtained and authenticated from NCI-Frederick DCTD tumor/cell line repository. OV90 was obtained and authenticated by ATCC. De-identified ascites specimen VBCF004 was collected as pathological waste from post-treatment ovarian cancer patients and was determined to be outside the federal regulations for protection of human subjects [45 CFR 46 (OHSRP #12727 and #12797)]. Viable tumor cells and non-cell fractions from ascites were purified using Ficoll separation.

All adherent (2D) cultures were maintained in standard media (RPMI for OVCAR8, OV90, and CAOV4. DMEM:F12 for ACI23). Media was supplemented with 10% FBS and 5 mL 10,000 U/mL Pen/Strep. When using inducible CRISPR-Cas9 cell lines, tet-free FBS was substituted for standard FBS.

Unless otherwise indicated, spheroid (3D) cultures were maintained in stem cell media prepared with DMEM:F12 and supplemented with 1% KnockOut serum replacement, 0.4% BSA, and 0.1% insulin-transferrin-selenium (ITS) and filtered through 0.2 µm filter. Media was supplemented with epidermal growth factor (EGF) and basic fibroblast growth factor (FGF) every 2-3 days for a final concentration of 20 ng/mL and 10 ng/mL respectively. 3D cultures were cultured in ultra-low-attachment tissue culture flasks.

Luciferase Assay

The NF-κB Luciferase Cignal Lenti Reporter Assay was purchased from Qiagen, transduced per the manufacturer's protocol at MOI of 50, selected with 2µg/ml puromycin, and expanded to generate stably expressing reporter cell lines.

50 µL of cells were plated in a 96 well plate at a density of 1500, 3000, or 6000 cells/well for OVCAR8, OV90, ACI23 respectively. Cell density at plating was chosen to have ~80% confluence at the time the endpoint. Cells were allowed to adhere and grow overnight. The following day, a separate 96 well drug plate was prepared containing 55 µL of the 2x drug in growth media at 2x concentration in row A. A 5-fold serial dilution was performed from rows B through H with mixing by pipetting. 50 µL drug solution per well was transferred from the drug plate to the cell plate and the cell plate was returned to the incubator. The plate was allowed to incubate 24 hours then analyzed using the Promega ONE-Glo EX Luciferase Assay System per manufacturer instructions. Luminescence was read on a SpectraMax iD3 plate reader.

ONE-Glo EX Buffer, ONE-Glo EX Substrate, and the plate to be analyzed must all acclimated to room temperature before analysis. The buffer is stored frozen and must be removed from the freezer several hours ahead of time to give it sufficient time to thaw. The substrate and plate can be acclimated for ~10 min. The luciferase buffer was poured into the substrate and

reconstituted by inversion. 100 µL reagent was then transferred to each well of the cell plate. Plate was shaken for 2 min at 300 rpm and then incubated at room temperature for 5 min. Luminescence was read on a SpectraMax iD3 plate reader.

CellTiter-Glo Cell Viability Assay

Cells were seeded in 50 µL/well into 96-well, opaque white, clear-bottom plates at either 1000 cells/well (OVCAR8 and CAOV4) or 2000 cells/well (OV90) and allowed to rest overnight. The following day 50 µL of 2x TWEAK or TNFα in growth media was added to final concentrations of 100 ng/mL or 10 ng/mL respectively. The plates were returned to the incubator and allowed to grow for 72 hours. Viability was assessed with CellTiter-Glo 2.0 reagent (Promega, Madison, WI) according to manufacturer's instructions. Briefly, reagent was allowed to acclimate to room temperature then 100 µL was added to each well. Plate was shaken on an orbital shaker for 2 min then incubated at room temperature for 10 min. Luminescence was read on a SpectraMax iD3 plate reader.

TransAM & Western Blot Lysate Preparation

Cells were plated in 12 mL growth media at 900,000 cells/well (OVCAR8 and CAOV4) or 150,000 cells/well (OV90) in 10 cm tissue culture dishes and allowed to rest overnight before treating. 3 µL stock TWEAK (100 µg/mL) was added to a final concentration of 25 ng/mL either 2 hr. or 24 hr. prior to cell collection.

To prepare lysates, the plates were washed with PBS and cells were collected using a cell scraper and pelleted by centrifugation at 1200 rpm for 4 min. Nuclear and cytoplasmic fractions were separated using Active Motif Nuclear Extract Kit per manufacturer instructions (Cat. No.

40010). Separation of fractions was validated by western blot for Lamin A/C as a nuclear marker and α-tubulin as the cytoplasmic marker. Pierce Rapid Gold BCA Protein Assay Kit was used for protein quantitation.

Western Blots

SDS-PAGE was performed using NuPAGE 4-12% Bis-Tris gels with MOPS-SDS running buffer. Proteins were transferred to PVDF membrane at constant 200 mA for 16 hours at 4°C. The membrane was blocked with 5% dry milk in TBST for 1 hr. at room temperature, then incubated overnight at 4°C with primary antibodies from Cell Signaling Technology (Danvers, MA) or Millipore Sigma (Burlington, MA) at a 1:1000 dilution. Secondary antibody was incubated at 1:2000 dilution in 5% milk in TBST for 1 hr. at room temperature. Bands were visualized using SuperSignal West Pico PLUS or SuperSignal West Femto chemiluminescent substrate and imaged on the iBright CL1000 Imaging System. Densitometry was performed using Invitrogen iBright Analysis Software (ThermoFisher Scientific, Waltham, MA).

TransAM

The TransAM® NF-κB Activation Assay was purchased from Active Motif (Cat. No. 43296). The assay was performed per manufacturer's instructions using nuclear lysates described above.

RT-qPCR

RNA was isolated using the NucleoSpin RNA Plus kit (Macherey-Nagel) per manufacturer’s protocol. Concentrations were determined using a SpectraMax QuickDrop. RNA

was converted to cDNA using the High-Capacity cDNA Reverse Transcription kit per manufacturer's protocol.

qPCR was performed using Taqman Fast Advanced Master Mix and Taqman probes (ThermoFisher Scientific). Results were analyzed using the delta-delta Ct method with GAPDH as the endogenous control. Experiments were run using a QuantStudio 3 instrument and analyzed using QuantStudio Design and Analysis software.

Proliferation – Ki67 Flow Cytometry

Cells were plated in 12 mL growth media at 175,000 cells/well (OVCAR8 and CAOV4) or 400,000 cells/well (OV90) in 10 cm tissue culture dishes and allowed to rest overnight before treating. The following day the cells were treated with 12 µL stock TWEAK (100 µg/mL) to a final concentration of 100 ng/mL and allowed to incubate for 72 hours. At the end of incubation, the cells were collected in a single cell suspension using CellStripper. Cells were pelleted by centrifugation and fixed by resuspending in 1% formaldehyde for 15 min at room temperature. Cells were then washed with excess PBS and permeabilized in 0.3% Triton X-100 for 5 min at room temperature.

The cells were stained with primary antibody (Ki-67 (8D5) Mouse mAb #9449, Cell Signaling) diluted 1:1000 for 1 hour at room temperature, washed with PBS, and then stained with secondary antibody (Goat anti-Mouse, Alexa Fluor 488, Invitrogen (A11029)) diluted 1:1000 for 30 min at room temperature protected from light. Cells were washed with PBS then resuspended in FACS buffer. Ki67 was detected and quantified by flow cytometry.

Spheroid Assay

Cells were plated at 100-500 cells/well in ultralow attachment, flat bottom 96-well plates in 100 µL growth medium. The growth medium was either stem cell media (SCM) as described

above, or regular 2D growth media, depending on the experiment. After 4–7 days in culture the cells were stained with Hoechst 34580 for >1 hr. and imaged at 10x magnification using the ImageXpress Pico. Spheroids ranging in size from 30–600 µm were counted and analyzed using the CellReporterXpress software. Spheroid efficiency is defined as (# of spheroids)/(# of cells per well).

The spheroid assays were primarily performed in 2D media. Pilot experiments showed that the cell lines produced a large number of spheroids in 3D media and any changes due to treatment were difficult to detect. Switching to 2D media for these experiments increased the sensitivity of the assay.

Caspase Assay

200 µL/well of OVCAR8, CAOV4, and OV90 cells were plated in an opaque black, clear bottom, tissue culture treated 96 well plate at 1000, 1000, and 2000 cells/well respectively. Cells were plated and allowed to rest overnight before addition of the cytokines and carboplatin.

Cells were treated with either vehicle, TWEAK (25 ng/mL final), or carboplatin. IC50 for carboplatin was determined previously by other members of the lab: 100 µM for OVCAR8 and CAOV4 and 250 µM for OV90. The plates were allowed to incubate for 72 hours at 37°C.

At the end of incubation, 21x Hoechst was prepared by diluting 1.68 µL 10 ug/mL Hoechst 34580 in 800 µL RPMI. 10 µL of this solution was added to each well and the plate was returned to the incubator for 30 min. The caspase assay was then performed according to manufacturer specifications. Briefly, 7.5 µL Caspase Reagent was diluted 1:1000 in PBS with 5% FBS to prepare the Working Caspase Reagent. Media was aspirated from the wells and 100 µL Working Caspase Reagent was added to each well. The plate was returned to the incubator for 30 minutes. The plate

was then imaged on the Pico plate imager using the Apoptosis Detection method. Hoechst/DAPI channel was used to identify cells and FITC channel was used to identify apoptotic cells.

Animal Experiments

All animal studies were approved by the SDSU Animal Care and Use Committee (protocol approval numbers 18-04-006H and 21-05-003H). For subcutaneous xenografts, 50,000 - 500,000 OV90 cells in 1:1 Matrigel in PBS were subcutaneously injected into the left flank of 8-week-old female athymic Nu/Nu mice. Mice were weighed and tumors measured twice weekly. Once tumors reached 150mm^3, mice were treated with either vehicle or carboplatin (50mg/kg) delivered via intraperitoneal (IP) injection once per week for three weeks. Mice were sacrificed in two groups: on average 5 days (group 1) or 12 days (group 2) after the third dose of carboplatin to evaluate progressive changes.

For IP xenografts, 4x10^6 CAOV4 cells in 500µl PBS were injected into 8 week-old female athymic Nu/Nu mice. Mice were weighed and monitored for clinical signs twice weekly. 7 days post injection, mice were randomly assigned to either group 1: vehicle, group 2: carboplatin (50mg/kg) IP once per week for three weeks, group 3: carboplatin (as administered in group 2) combined with FN14 inhibitor (9mg/kg) in 5% DMSO/95% Corn oil delivered by IP every other day for three weeks, or group 4: carboplatin (as administered in group 2) followed by FN14 inhibitor (as administered in group 3) for 6 weeks or until humane endpoints. Tumor burden for mice was assessed after necropsy with collection of peritoneal wall, spleen, liver, omentum, spleen, mesentery, ovaries, and diaphragm.

Statistical Analysis

Statistics were generated using Prism 9.3.1 with data acquired from at least three independent biological replicates. Results are presented as mean +/- SEM. Significance was

calculated using either student's t-test for comparisons of two means or ANOVA for comparisons of three or more means with a post-hoc test to identify differences between groups as described in figure legends. Differences between means are considered statistically significant at the 95% level ($p < 0.05$). Statistics were completed as described here or as otherwise noted in the figure legends.

TUNEL Assay

2500-4000 cells were seeded into black 96-well, clear-bottom plates and incubated overnight prior to treatment with either vehicle, TWEAK, or Carboplatin and allowed to incubate for 6 hours. EdUTP incorporation was assessed with the Click-iT Plus TUNEL Alexa Fluor 488 assay per manufacturer's instructions. Hoechst 33342 and EdUTP incorporation were imaged on the Molecular Devices ImageXpress Pico plate imager and analyzed with CellReporterXpress software. Percent EdUTP incorporation was quantified using automated imaging analysis with CellProfiler for counting and scoring.

CRISPR Line Production

Knockout clonal cell lines for RelB were derived per the manufacturer's protocol for Horizon's Edit-R Inducible Lentiviral Cas9 Nuclease with Edit-R Lentiviral sgRNA (Table S2). 10µg/ml blasticidin and 2µg/ml puromycin was used to select for cells with the integrated Cas9 nuclease and sgRNA guides followed by induction of genomic editing with 3µg/ml doxycycline for 7 days. Serially diluted clonal lines were expanded and screened for the loss of RelB by western blot.

Pulse Chase Assay

Cells were plated at 500-3000 cells per well in a 96-well, black well, clear-bottom plate and allowed to rest overnight. For the pulse, cells were grown for at least two divisions in 0.5-1μM EdU prior to the chase, in which cells were removed from EdU and allowed to divide in the presence of either TWEAK or vehicle for 60-72 hours. EdU incorporation was assessed with the Click-iT Plus EdU Alexa Fluor 647 assay and F-actin was also assessed using Phalloidin-Alexa Fluor 488, both used per manufacturer's instructions. Hoechst 33342 and EdU incorporation or F-actin staining were imaged on the Molecular Devices ImageXpress Pico plate imager and analyzed with CellReporterXpress software (Table S2).

siRNA Transfections

Cells were plated the day before to achieve a confluency of around 60% for transfection. 30nM pools of 4 siRNAs targeting either *FN14* or a non-targeting control were transfected using Lipofectamine RNAiMAX per manufacturer's instructions (Table S2). Cells were incubated for 24 hours before being collected for downstream experiments. Cells were replated and cultured for an additional 48 hours for validation of Fn14 silencing.

CD117 Sorting

CAOV4 cells were seeded for 6 days in Ultra Low-Attachment T-75cm^2 flasks with stem cell media (DMEM/F12, 1% Knock-out serum replacement, 0.4% BSA, 0.1% Insulin-Transferrin-Selenium-X (ITS), 1% 10,000 U/ml Pen/Strep and supplemented every 2-3 days with 20ng/ml EGF and 10ng/ml FGF). After 6 days, cells were collected and prepared into single cell suspensions using CellStripper Dissociation Reagent and needle dissociation using 25-gauge needle. Cells were stained for CD117 or propidium iodide (PI), sorted for CD117- and CD117+ cells using BD FACSMelody™ Cell Sorter, and then plated for 24 hours prior to treatment with

either vehicle or TWEAK (Table S2). After 72 hours of treatment, cells were harvested and immediately processed for downstream qRT-PCR.

Enzyme-Linked Immunosorbent Assay (ELISA)

The concentration of cytokines IL-6 and TWEAK (Table S2) was assessed using DuoSet sandwich ELISA per manufacturer's instruction using non-cell fractions from ascites samples and tumor tissue samples which were flash frozen immediately following collection. For the tissue, 1-3mg sections were dissected, weighed, and protein was dissociated on gentleMACS M tubes in RIPA lysis buffer. Samples were prepared and analyzed per manufacturer's instructions.

IHC/IF

For IHC, tumors were resected, fixed in 10% neutral buffered formalin, and stored in 70% ethanol before processing. Tumors were embedded in paraffin and sectioned at 5μm. Antigen retrieval was performed in citrate buffer and quenched with hydrogen peroxide. Slides were incubated with primary antibodies overnight followed by an HRP-linked secondary and processed using DAB (Table S2). Four randomly selected images per slide were acquired with an Olympus BX51 with CellSens Standard software. A digital quantification of DAB staining was performed using ImageJ with a FIJI deconvolution package as described previously[21].

For IF, tumors were fixed, embedded and antigen retrieval was done as above. Slides were blocked with 1% goat serum in PBS and then incubated with RelB-FITC primary antibody overnight (Table S2). Secondary antibody was incubated for 1 hour at room temperature (Table S2). Slides were mounted with Fluoroshield antifade medium with DAPI and four randomly selected images per slide were acquired within 1-3 days with an Olympus BX63 with CellSens Standard software. Nuclear and cytosolic digital quantification of IF staining was performed using

automated imaging analysis with CellProfiler[128] and modelled with image set BBC014v1[129]. Nuclear:Cytosolic ratio was calculated as described previously[130].

3. Results

3.1 Identifying TWEAK

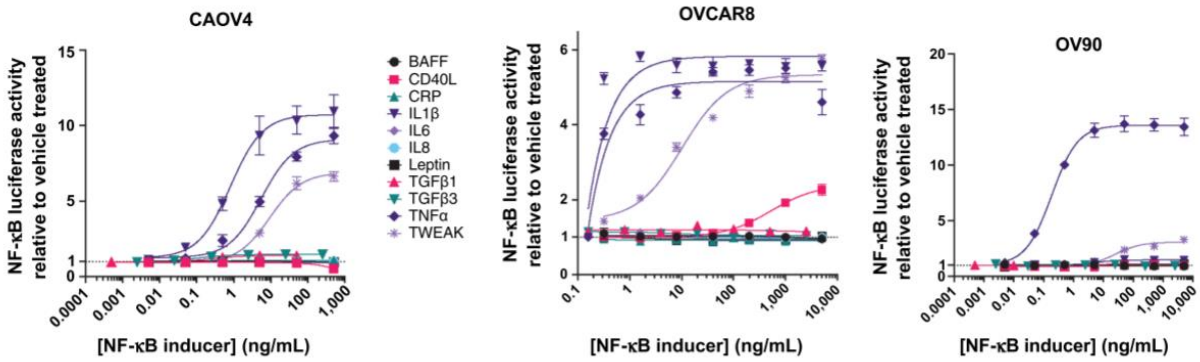

Figure 6 *– NF-κB Luciferase assay showing NF-κB activity in response to different cytokines. n=3*

Because of the previous finding that the CSC phenotype is supported by non-canonical NF-κB signaling, we sought RelB activators which had been previously reported in HGSOC. We started with a panel of 11 cytokines: BAFF, CD40L, CRP, IL-1β, IL-6, IL-8, Leptin, TGF-β1, TGF-β3, TNFα, and TWEAK. These cytokines were chosen because they are known activators of NF-κB which are either produced by macrophages or otherwise known to be present in the ovarian TME. We screened these cytokines against three cell lines: tumor-derived OVCAR8, metastatic site-derived CAOV4, and ascites-derived OV90, each cell lines transduced with NF-κB luciferase reporter. The luciferase reporter shows activation of the NF-κB pathway but does not distinguish between canonical and non-canonical signaling. Of the 11 cytokines, only four, BAFF, CD40L, TNFα, and TWEAK, showed responses at reasonable concentrations. TWEAK had a response in all three cell lines at physiological concentrations, so was the cytokine we continued with for future experiments (**Figure 6**). TNFα also strongly induces NF-κB activity but is a known canonical

activator which has been previously studied in ovarian cancer.[131–133] Because TWEAK is a non-canonical activator and is understudied in the disease, we followed up with TWEAK.

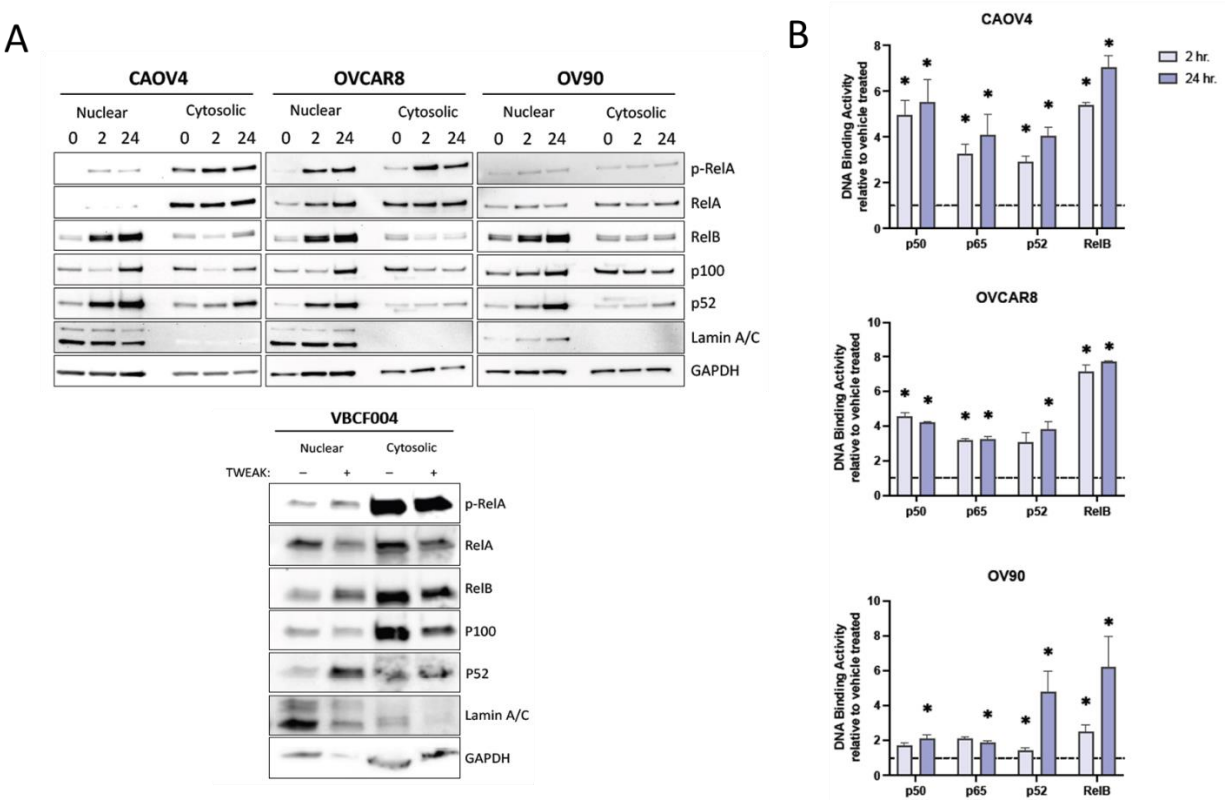

Figure 7 *– TWEAK activates non-canonical NF-κB in HGSOC cell lines. (A, Top) Nuclear and cytosolic western blots of HGSOC cell lines after 25 ng/mL TWEAK stimulation for 2 or 24 hr. Representative of n=2 (A, Bottom) Western Blots of NF-κB proteins from patient ascites-derived HGSOC cells upon 100 ng/mL TWEAK stimulation. (B) NF-κB TransAM assay showing DNA binding of NF-κB proteins with TWEAK stimulation for 2 or 24 hr. Data shown relative to vehicle. One-way ANOVA with Dunnet's post-hoc (n=3).*

While the luciferase assay was able to demonstrate that TWEAK activates NF-κB, it is not specific to either the canonical or non-canonical branch of the pathway. To determine which branch of the NF-κB TWEAK activates, we treated four cell lines, CAOV4, OVCAR8, OV90, and VBCF004, with TWEAK for 2 or 24 hours. These time points were chosen because the canonical NF-κB pathway turns on quickly in response to stimuli while the non-canonical pathway takes more time to activate, so separate time points are necessary to enable detection of both pathways.

The treated cells were separated into nuclear and cytosolic fractions and blotted for NF-κB pathway members. We observed activation of the non-canonical pathway, as indicated by nuclear localization of RelB as well as processing of p100 to p52 alongside its nuclear localization. We also observed canonical pathway activation, as demonstrated by the phosphorylation and nuclear localization of RelA. Although both pathways show activation by TWEAK, the effect is stronger for the non-canonical pathway (**Figure 7A**).

This data is further supported by the NF-κB Trans-AM assay. This is a colorimetric DNA binding assay derived from ELISA assays. The advantage of the assay is that it is more quantitative than western blots, and it demonstrates that the NF-κB members in the lysate are active and capable of binding NF-κB binding sites. The assay showed that both canonical (p50 and p65) and non-canonical NF-κB (p52 and RelB) are activated by TWEAK in three cell lines, but like with the western blots, non-canonical was more strongly activated (**Figure 7B**).

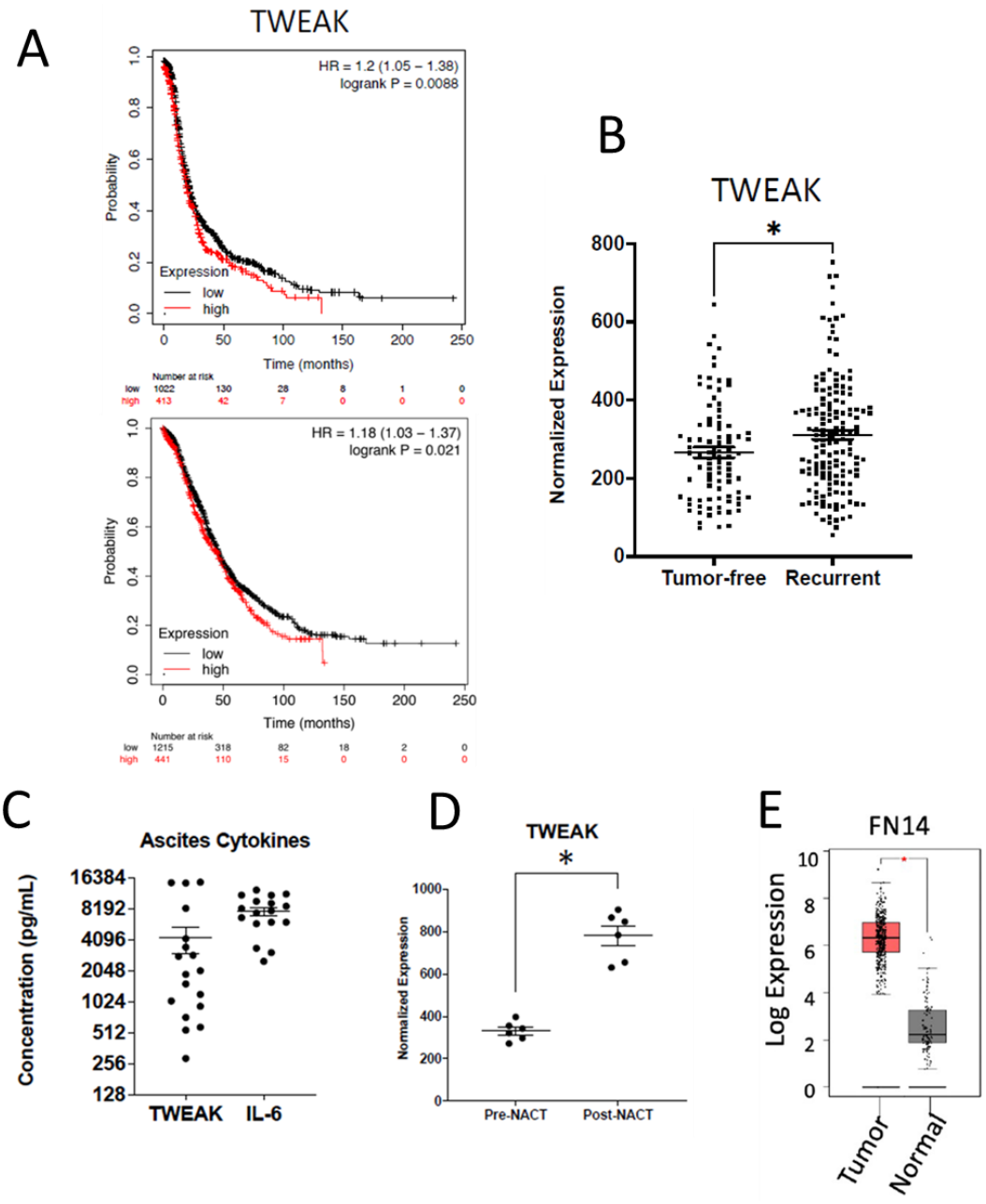

Figure 8 *– TWEAK clinical information. (A) Kaplan-Meier plots showing progression free survival (PFS, top) and Overall Survival (bottom) of ovarian cancer patients with high or low expression of TWEAK in their tumors. (B) TCGA analysis of TWEAK expression in tumor-free and recurrent (<5 years) tumors. (C) TWEAK and IL-6 protein levels in non-cellular ascites. (D) TWEAK gene expression pre- and post-neoadjuvant chemotherapy. Paired t-test (n=6). (E) Gepia2 analysis of Fn14 expression in matched ovarian epithelium and ovarian tumors.*

Because TWEAK was a cytokine of interest after the luciferase screen, we searched publicly available clinical data seeking existing translational relevance. Analysis of public data sets, including TCGA and others, showed that high TWEAK levels in tumors are significantly associated with decreased Overall Survival and Progression Free Survival (**Figure 8A**). Additionally, TWEAK is elevated in patients whose tumors end up being recurrent compared to those who remain tumor free for 5 years (**Figure 8B**). TWEAK is also found at high levels in the ascites of ovarian cancer patients (**Figure 8C**) as well as being increased in tumors post chemotherapy (**Figure 8D**). mRNA for the TWEAK receptor Fn14 is also enhanced in ovarian cancer tumors relative to normal ovary epithelial tissue (**Figure 8E**).

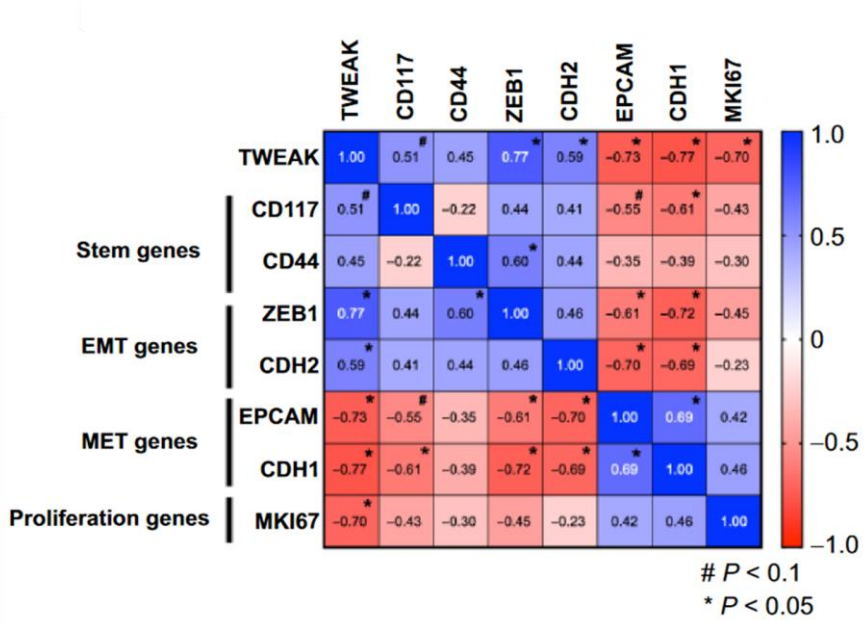

Figure 9 *- Pearson correlation of select genes to TWEAK expression for all collected samples (pre- and post-NACT; n=6).*

In addition to being a poor prognostic indicator, clinical data also reveal that TWEAK mRNA positively correlates with the CSC marker CD117, as well as the EMT markers ZEB1 and CDH2. It also negatively correlates with the MET markers EPCAM and CDH1 and the proliferation marker MKI67 (Ki-67) (**Figure 9**). Taken together these demonstrate that TWEAK

is elevated in HGSOC, correlates with stem and EMT genes, and portray TWEAK as a negative prognostic indicator.

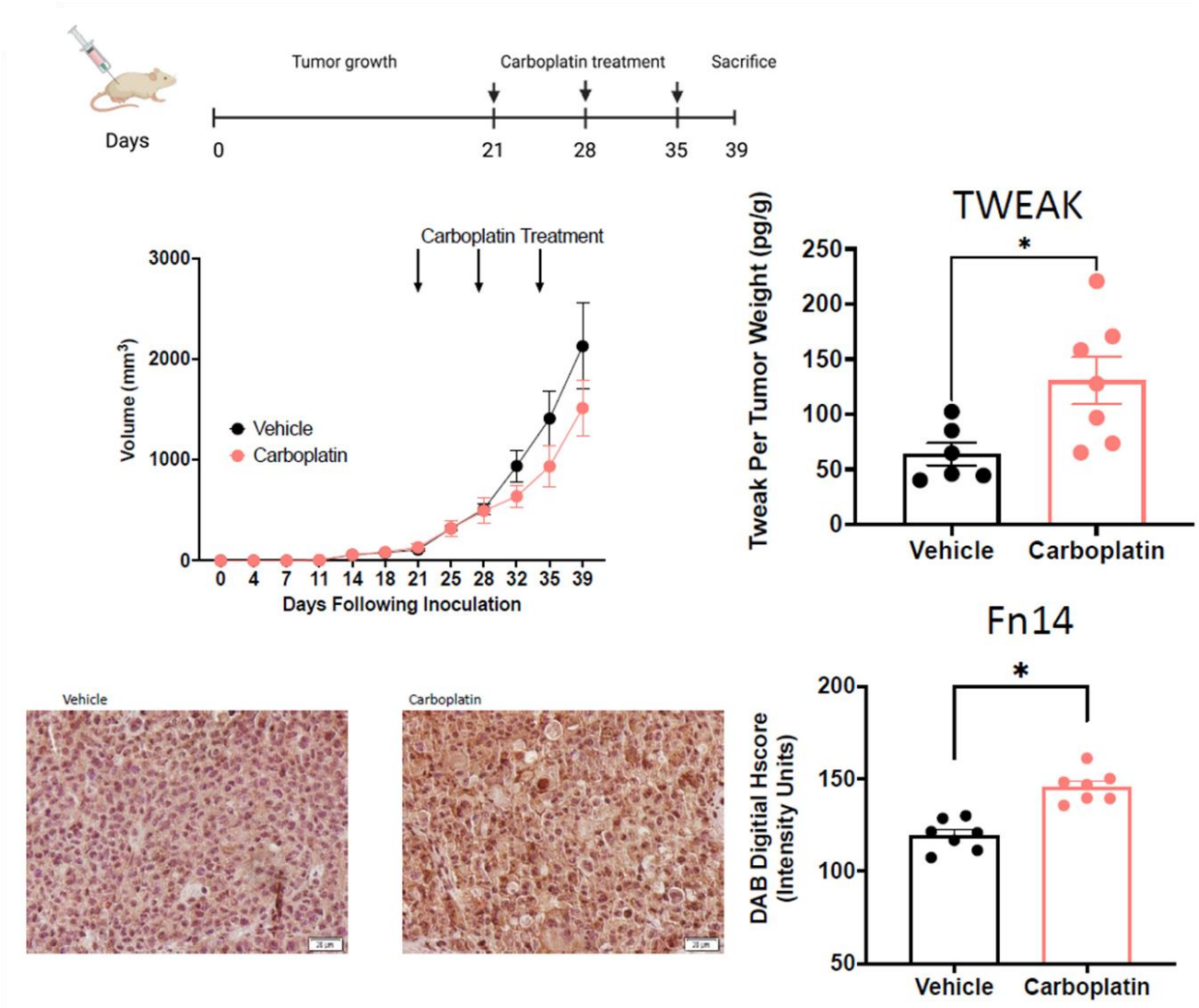

Figure 10 *– OV90 Mouse Study – short endpoints. Subcutaneous tumors were generated in nude mice using OV90 cells. Tumors were allowed to grow for 21 days followed by 3cycles of carboplatin (50mg/kg) or vehicle and resected 5 days after the final carboplatin treatment. Experimental design created with BioRender.com (top). Tumor volume was measured twice weekly (center, left). TWEAK concentration per tumor weight measured using ELISA (center, right). Student's t-test (n=14). Fixed tumor fractions were histologically stained for Fn14. Representative images (bottom, left) and Fn14 digital Hscore quantification using ImageJ (bottom, right). Student's t-test (n=14). Data represent mean and SEM. * p<0.05.*

Because of its primary role in tissue repair, which is dysregulated in cancer, as well as its elevated expression post chemotherapy, we reasoned that TWEAK should be elevated in chemotherapy treated tumors. To investigate this, mice were given subcutaneous OV90 tumors and then subjected to three rounds of chemotherapy. Tumors were harvested 5 days after the last round of chemotherapy and TWEAK concentration was measured by ELISA. We found that TWEAK concentration was significantly higher in chemotherapy-treated tumors than in tumors receiving vehicle. The TWEAK receptor Fn14 was also increased in chemo treated tumors relative to vehicle treated control, as shown histologically by DAB staining. (**Figure 10**). These data support that TWEAK is present in the ovarian cancer TME and is elevated post-NACT.

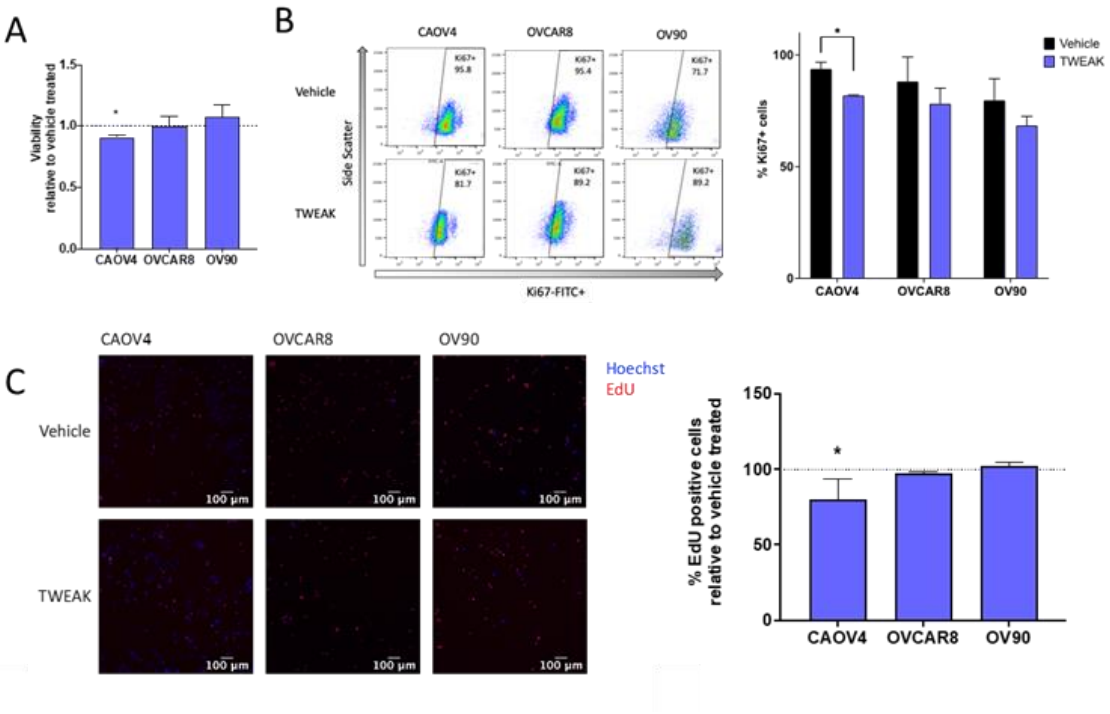

Figure 11 *- TWEAK has minimal effect on proliferation of ovarian cancer cells. (A) Viability of HGSOC cells treated with TWEAK (100ng/ml) for 72 hours relative to vehicle control. Unpaired t-test for vehicle versus TWEAK treated. (B) Ki-67 flow cytometry for HGSOC cells treated with TWEAK (100ng/ml) for 72 hours relative to vehicle control (n=3). Representative gates (left) and quantification of mean plus SD (right). Unpaired t-test. (C) EdU (5µM) proliferation assay for HGSOC cells treated with TWEAK (100ng/ml) for 72 hours relative to vehicle control. Representative gating (left) and percent EdU+ cells (right). Unpaired t-test (n=6).*

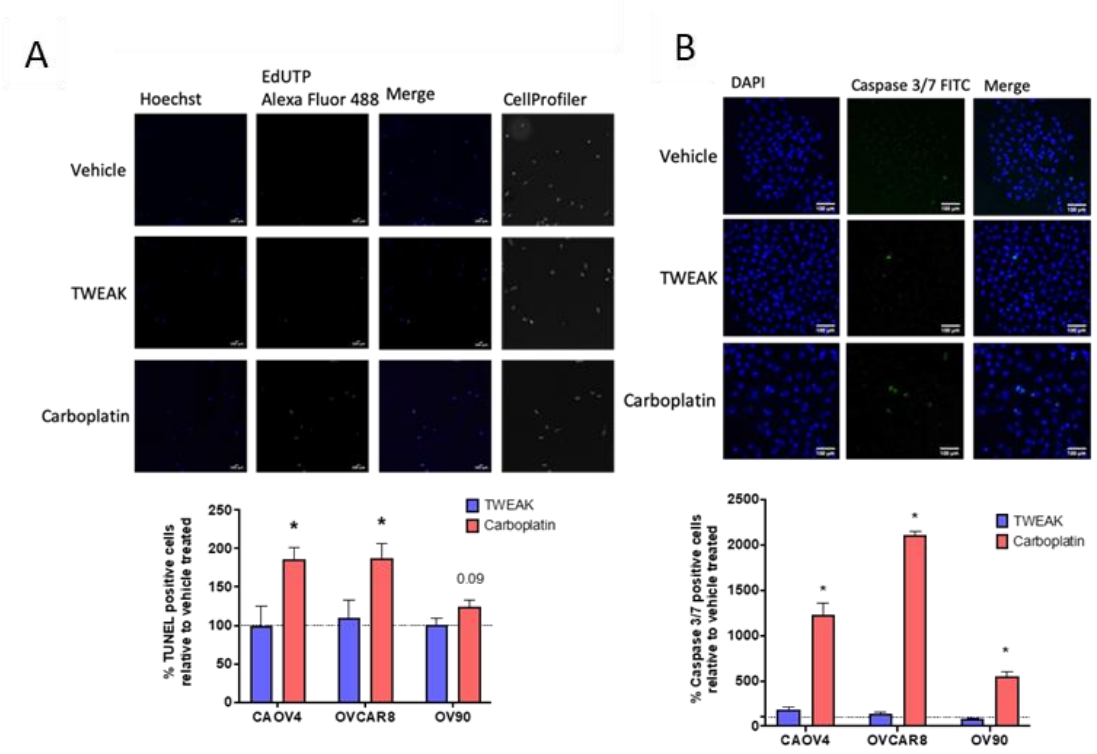

Figure 12 *- TWEAK has no effect on apoptosis of ovarian cancer cells. . (A) TUNEL assay of HGSOC cells treated with TWEAK (100ng/ml) or carboplatin (100µM for CAOV4 and OVCAR8 or 250µM for OV90) for 6 hours. Representative images (top) and quantification (bottom). One-way ANOVA with Tukey's post-hoc test (n=2). * indicates significance of carboplatin to vehicle and carboplatin to TWEAK treatment. (B) Caspase-3/7 assay of HGSOC cells treated with TWEAK (25ng/ml) or carboplatin (100µM for CAOV4 and OVCAR8 or 250µMfor OV90) for 72 hours (n=3). Representative images (top) and quantification (bottom). One-way ANOVA with Tukey's post-hoc test. * indicates significance of carboplatin to vehicle and carboplatin to TWEAK treatment. Data represent mean and SEM. * p<0.05.*

We next performed several experiments to understand the effect TWEAK stimulation has on cancer cells. Treating ovarian cancer cells with exogenous TWEAK for 72 hours had only minimal effect on viability measured by Celltiter GLO (**Figure 11A**) or proliferation measured by Ki67 flow cytometry and EdU incorporation (**Figure 11B-C**). Only the CAOV4 cell line showed a small decrease in proliferation. Additionally, there was no effect on apoptosis when treated with TWEAK for 72 hours when measured by TUNEL assay (**Figure 12A**) or Caspase 3/7 activity (**Figure 12B**). Carboplatin treatment significantly induces apoptosis in these cells. Given these findings, as well as the correlation with CSC markers and the ability to stimulate non-canonical NF-κB signaling, we hypothesize that TWEAK may contribute to CSC phenotypes in HGSOC.

3.2 TWEAK promotes a CSC phenotype in ovarian cancer.

CSC gene expression

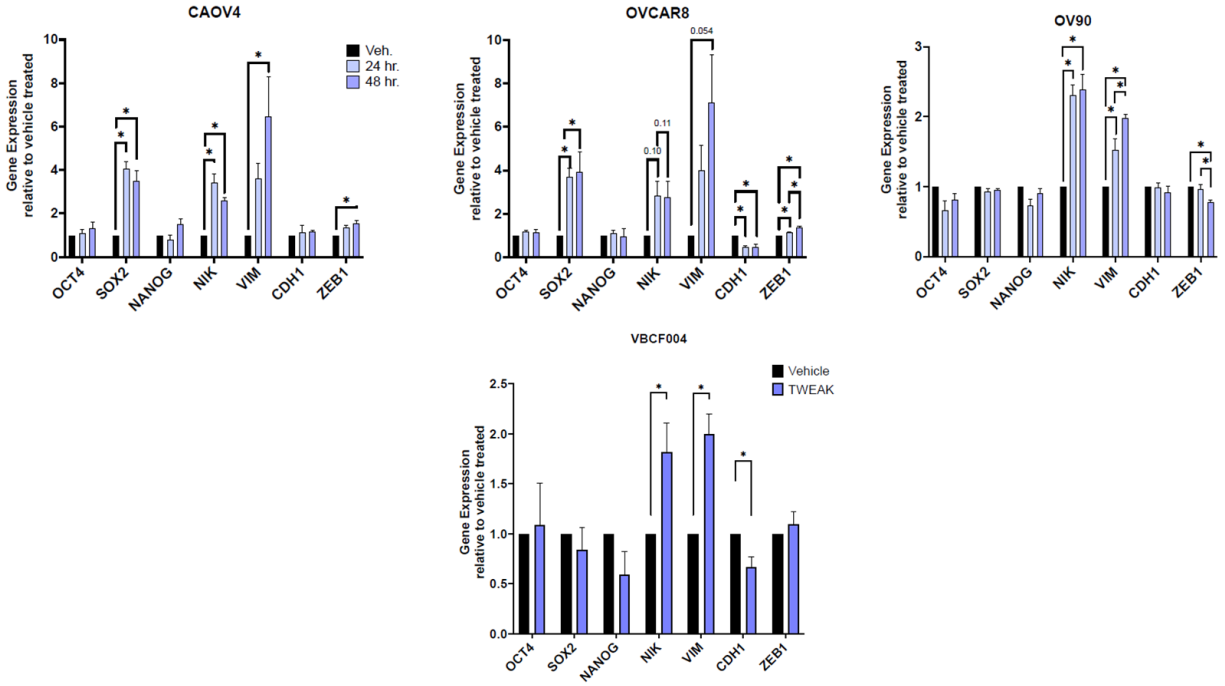

Figure 13 *– CSC Gene Expression. (Top) qRT-PCR for stemness and EMT genes in three cell lines treated with TWEAK (100 ng/mL) for 24 or 48 hours. One-way ANOVA with Tukey's post-hoc test (n=3) (bottom) qRT-PCR for stemness and EMT genes in an ascites-derived cell line treated with TWEAK (100 ng/mL) for 48 hours. Student's t-test (n=3)*

CSCs have stem-like features and gene activations. To begin testing our hypothesis that TWEAK promotes a CSC-like phenotype, we looked at relevant stemness and EMT genes. Long-term renewal and asymmetric division are defining qualities of CSCs, and these processes have been previously shown to be dependent on stem-cell transcription factors and some EMT genes.[30,35] Because of this, and because we saw correlation between TWEAK expression and these genes, we monitored the expression of the stem cell transcription factors *OCT4*, *SOX2*, and *NANOG* and the EMT/MET markers *VIM*, *CDH1*, and *ZEB1*. The cells were treated with TWEAK for 24 or 48 hours then mRNA was assessed by RT-qPCR. We found that *SOX2* was significantly

upregulated in CAOV4 and OVCAR8, but not in OV90 or the patient ascites-derived cell line VBCF004 (**Figure 13**). TWEAK had no effect on either *OCT4* or *NANOG* in any lines tested, which is not surprising considering that *SOX2* is a marker for ovarian cancer CSCs while *OCT4* and *NANOG* are not.[21] The mesenchymal marker Vimentin (*VIM*) was induced significantly by TWEAK in all lines tested. The EMT-TF *ZEB1* was significantly increased in CAOV4 and OVCAR8, and the epithelial marker *CDH1* decreased in OVCAR8 and VBCF004 (**Figure 13**). All together these indicate that TWEAK promotes progression through the EMT in our cell lines.

In addition to CSC and EMT gene expression, we also looked at phenotypes associated with CSCs such as spheroid formation and asymmetric division. Spheroid formation demonstrates resistance to anoikis, which is a type of programmed cell death which occurs when anchorage-dependent cells detach from the basement membrane, as well as the cell's ability to form new heterogeneous spheroids from low cell numbers. This heterogeneity requires asymmetric division. Together these model a CSCs ability survive the initial chemotherapy, survive in the body in low numbers, and then generate new heterogeneous tumors. This process has been previously shown is at least partially dependent on NF-κB signaling[76]. We also looked at F-Actin staining, which is a marker for stem cell differentiation.

Spheroid Formation and Asymmetric Division

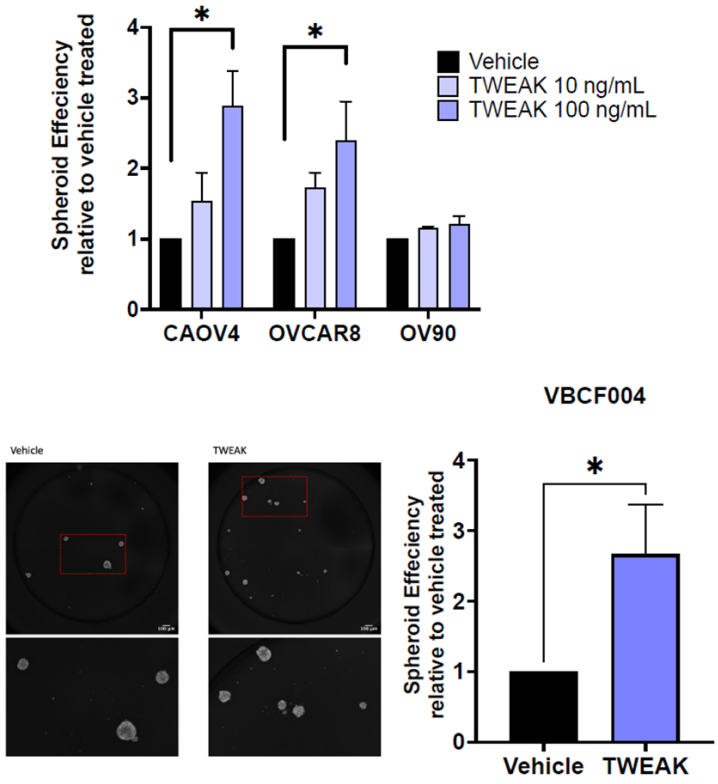

Figure 14 *– Spheroid Formation Assay. (Top) Spheroid formation efficiency of HGSOC cell lines treated with 10 or 100 ng/mL TWEAK for 6 days. One-way ANOVA with Dunnett's post-hoc test (n=4). (Bottom) Spheroid formation efficiency of ascites-derived cell line VBCF004. (left) Representative images and (right) quantification. Student's T-test (n=3)*

Asymmetric division is a process where a cell undergoing division maintains its own phenotype while producing a daughter cell with a different phenotype. This is a known feature of stem cells, including CSCs.[134–136] One feature of asymmetric division is non-random segregation of chromosomes. During normal cell mitosis, the homologous chromosomes are divided randomly among the daughter cells. However, during asymmetric division the chromosomes are divided non-randomly and the parent cell retains the original chromosomes while the daughter cell receives the copies. This serves the purpose of reducing the mutation rate in the stem cells because any errors made during chromosome duplication will be passed on to the daughter cell.[137]

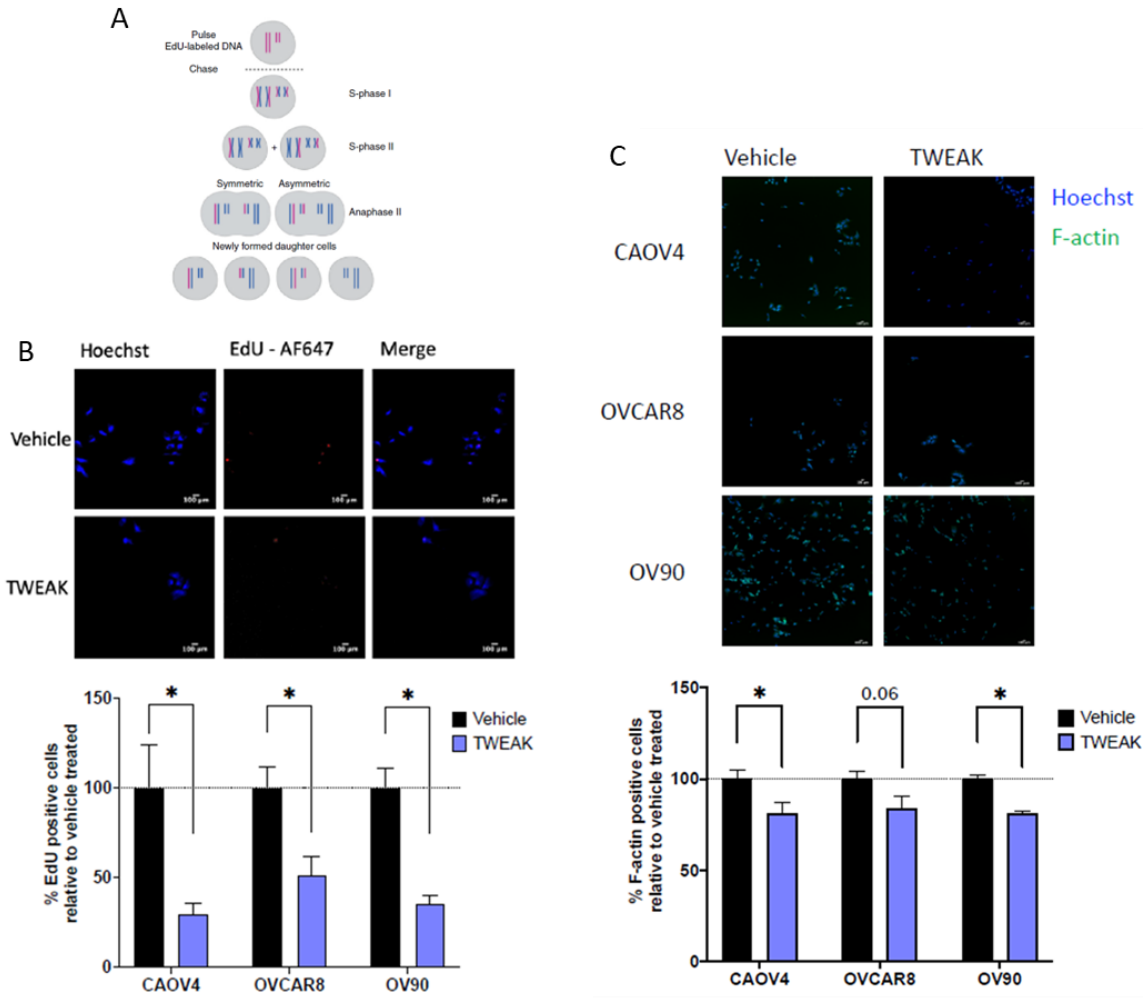

Figure 15 *– EdU incorporation pulse-chase assay and F-actin staining. (A) Schematic diagram of the pulse-chase EdU incorporation assay. (B) Representative images. (bottom) quantification. Student's t-test (n=6). (C) F-actin staining of HGSOC cell lines treated with 100 ng/mL TWEAK for 72 hours. (top) representative images and (bottom) quantification. Student's t-test (n=6).*

To investigate whether HGSOC cell lines treated with TWEAK have increased asymmetric cell division, we used a pulse-chase EdU incorporation pulse-chase assay (**Figure 15A**). TWEAK treatment significantly reduced the number of cells containing EdU, supporting an increase of stemness (**Figure 15B**).

As another phenotype for stemness, we looked at the amount of F-actin in our cells. F-actin staining has been shown to increase when stem cells are differentiated.[138,139] with or without

treatment with TWEAKThere was a decrease in F-actin staining in cells treated with TWEAK (100 ng/mL) for 72 hours relative to those treated with vehicle (**Figure 15C**). This is consistent with a decrease in differentiation and therefore a more stem-like phenotype.

Taken together these data indicate that TWEAK induces expression of stemness and/or EMT genes and promotes spheroid formation and asymmetric division in multiple ovarian cancer cell lines.

3.3 TWEAK and carboplatin together enrich for CSCs both by promoting CSCs and eliminating non-CSCs

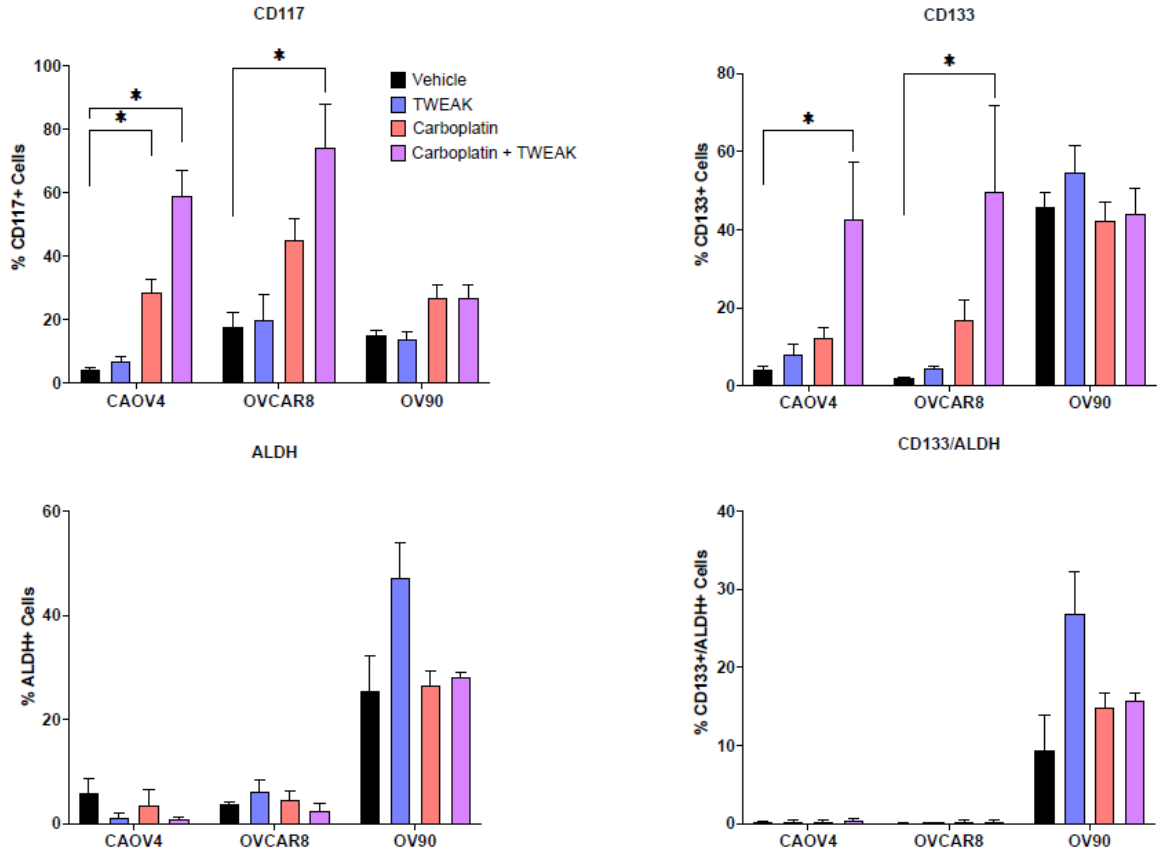

Figure 16 *– Stem cell marker flow cytometry. HGSOC cells treated with vehicle, TWEAK (100ng/ml), carboplatin (125 µM), or TWEAK and carboplatin for 72 hours. Percent positive cells representing mean plus SD. One-way ANOVA, Dunnett's post-hoc test (n=3).*

We next sought to investigate established markers for CSCs in ovarian cancer, whether they are present in our cell lines, and whether they are enhanced with TWEAK treatment. Because the CSC phenotype is chemoresistant and because we are interested in the post-chemotherapeutic niche, we also looked at how TWEAK affected our cells in the presence of carboplatin. CD117, CD133, and ALDH are currently established markers for ovarian CSCs.[19–24] TWEAK treatment alone did not significantly upregulate any of these markers. However, there was an enrichment of $CD117^+$ and/or $CD133^+$ cells in CAOV4 and OVCAR8 with carboplatin treatment. This

enrichment was amplified by TWEAK and carboplatin co-treatment. (**Figure 16**). OV90 cells with TWEAK treatment are enriched for $CD133^{+}ALDH^{+}$ double positive cell, in agreement with previous findings.[21] The inability to enrich ALDH activity in CAOV4 and OVCAR8 is not surprising, as it has been previously demonstrated that CSCs in these cell lines do not express sufficient $CD133^{+}$/ALDH+.[21,140]

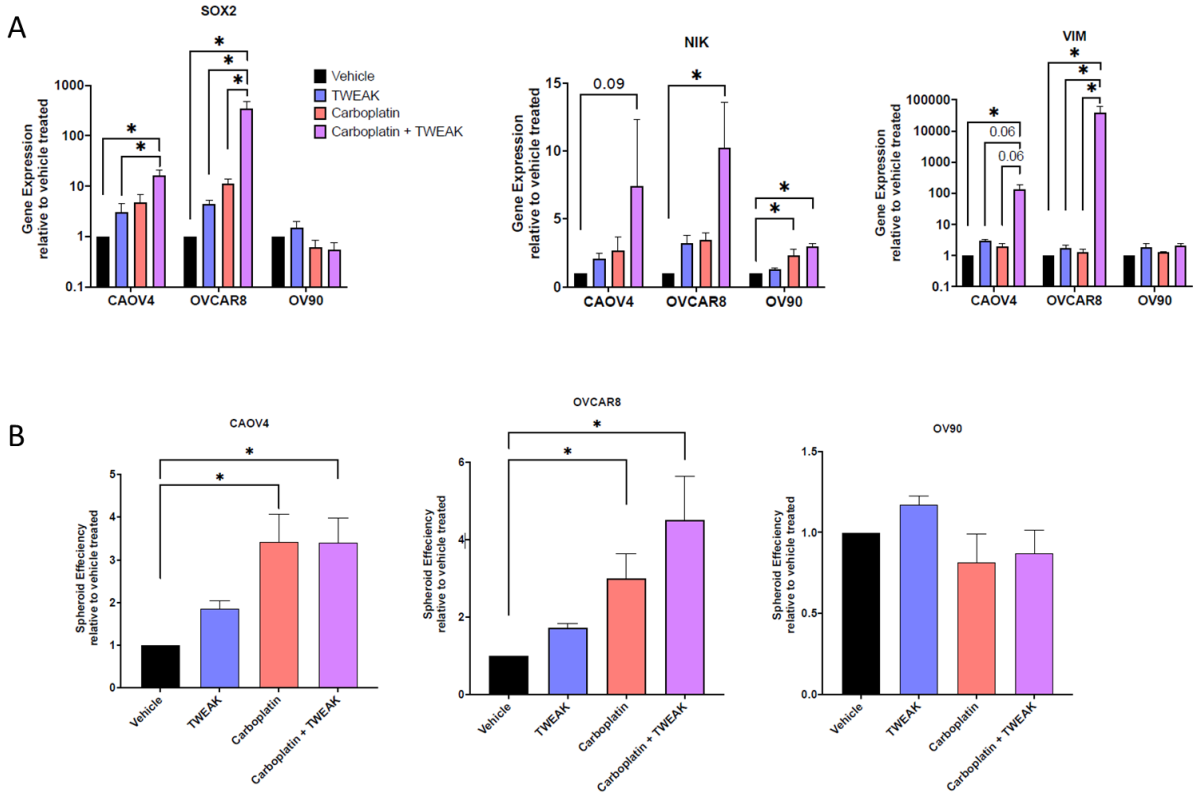

Figure 17 *– TWEAK and Carboplatin enrich stemness markers in HGSOC (A) cells with vehicle, TWEAK (100ng/ml), carboplatin (125 µM), or TWEAK and carboplatin for 72 hours represented relative to vehicle. One-way ANOVA, Tukey's post-hoc test (n=3). (B) Spheroid efficiency of HGSOC cells treated with vehicle, TWEAK (100ng/ml), carboplatin (125 M), or TWEAK and carboplatin for 4 days represented relative to vehicle. One-way ANOVA, Dunnett's post-hoc test (n=4).*

Because of the interesting result that combination of chemotherapy and TWEAK enriched most strongly for CSC markers, we next looked to see if the previously observed gene enrichments and phenotypes would be affected by similar treatment. We looked at three gene expression targets: *SOX2*, *NIK*, and *VIM*. In CAOV4 and OVCAR8, combination treatment with both

TWEAK and carboplatin resulted in a strong response for all three genes (**Figure 17A**). This is similar to what was observed with CD117 and CD133 above. Similarly, TWEAK or carboplatin both increase spheroid formation independently in CAOV4 and OVCAR8 and have an even stronger response when treatments are combined (**Figure 17B**). OV90 do not respond to TWEAK and carboplatin in the same way as the other two cell lines, likely because it contains a relatively low level of Fn14 expression (**Figure 20**-**Figure 21**). Together these data indicate that TWEAK is either promoting novel CSC formation during chemotherapy or promoting the carboplatin-induced elimination of non-CSCs, or both. The end result either way is the enrichment of CSCs after chemotherapy.

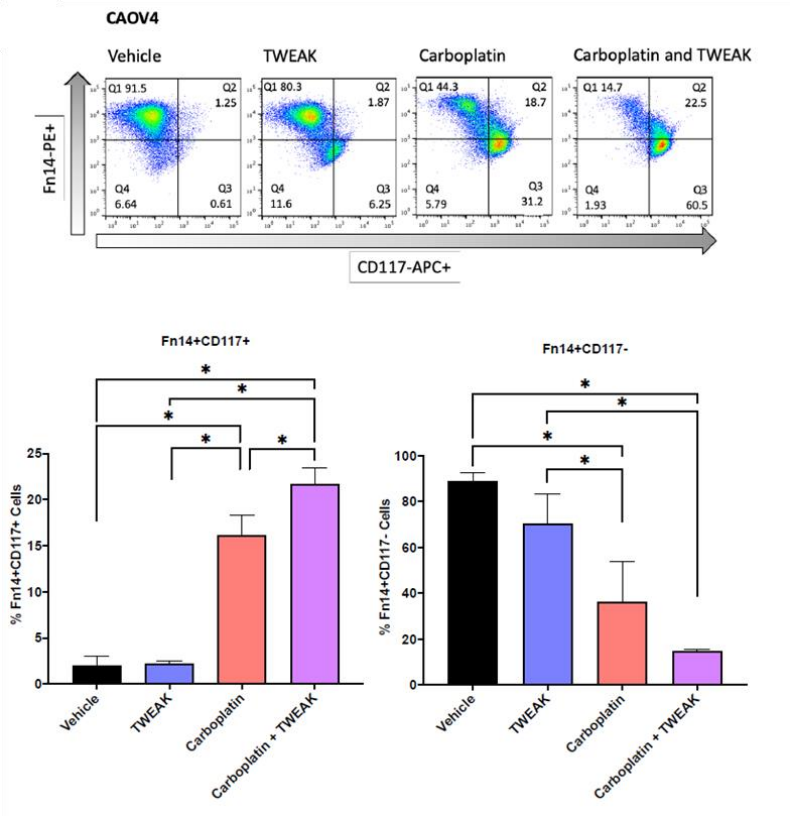

Figure 18 *– TWEAK and carboplatin in combination enrich CD117⁺ . Flow cytometry analysis of CD117 expression on Fn14+ cells treated with vehicle, TWEAK (100ng/ml), carboplatin (125 µM), or TWEAK and carboplatin for 72 hours. Representative gating (left) and percent positive cells representing mean plus SD (right). One-way ANOVA, Tukey's post-hoc test (n=3).*

In order to further study this phenomenon, we looked at TWEAK-sensitive cells ($Fn14^+$) and then compared the effects of treatment on the relative abundance of CD117. Initially only ~2% of the cells are $CD117^+$, but >92% $Fn14^+$, which shows that Fn14 expression is not specific to either CSCs or non-CSCs. Treatment with carboplatin or combination therapy enriched $Fn14^+CD117^+$ while reducing $Fn14^+CD117^-$ (**Figure 18**). These results suggest that TWEAK has different effects on CSCs and non-CSCs. To corroborate these findings, we sorted CAOV4 cells by CD117 then treated each population with TWEAK for 72 hours. *FN14*, *NIK*, *SOX2*, and *VIM* are all increased upon TWEAK treatment in $CD117^-$ sorted cells. However, these elevated levels are comparable to basal $CD117^+$ levels. Furthermore, all four genes showed the strongest increases in the TWEAK-treated $CD117^+$ cells.

In order to validate CD117 as a CSC marker, we sorted by CD117 and then looked at growth rates and spheroid efficiency in the separate populations. We see that $CD117^+$ cells appear quiescent, growing significantly slower than their $CD117^-$ counterparts (**Figure 19A**) and that $CD117^+$ spheroids are less sensitive to chemotherapy than $CD117^-$ spheroids (**Figure 19B**). In order to further test this induced chemoresistance, we sorted for $CD117^+$ cells, then subjected the cells to TWEAK and carboplatin treatment, but varied the order of treatment: TWEAK was added either before, concurrently with, or after carboplatin treatment. We found that the group that received TWEAK pre-treatment had significantly increased viability after chemotherapy relative to the chemotherapy-only control (**Figure 19D**).

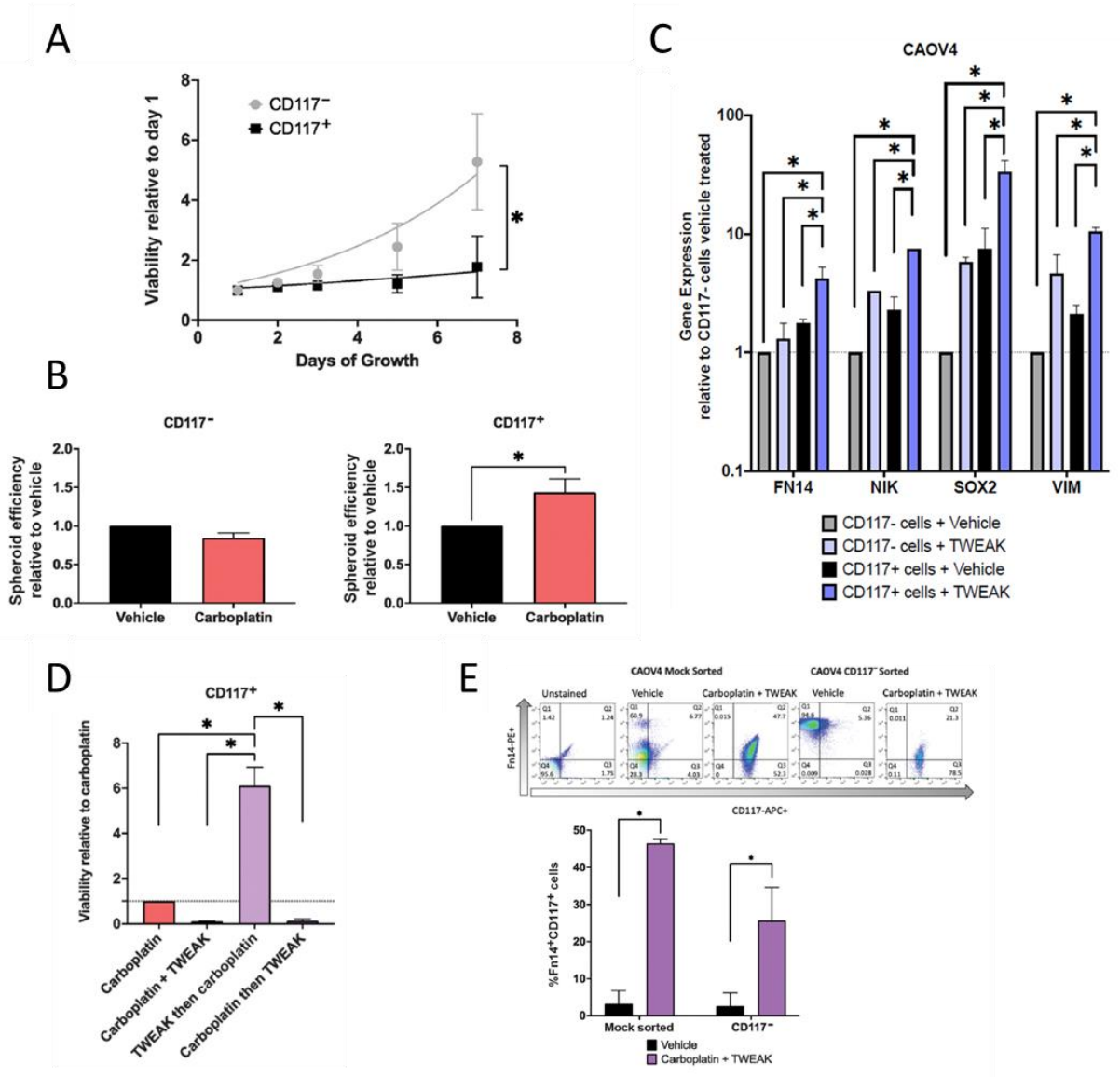

Figure 19 *– Differential behavior of CD117⁺ and CD117⁻ populations (A)Viability of sorted OV90 CD117⁺ or CD117⁻ cells grown for 8 days normal media Two-way repeated-measures ANOVA, Sidak post hoc test (n ¼ 4). (B) Spheroid efficiency of OV90 CD117⁺ or CD117⁻ cells treated with carboplatin (90 mmol/L) for 4 days represented relative to vehicle. Unpaired t test (n ¼ 4). (C) qRT-PCR of select genes for sorted CD117+ or CD117- cells treated with vehicle or TWEAK (100ng/ml) for 72 hours. One-way ANOVA, Tukey's post-hoc test (n=4). (D) Viability of CD117⁺ sorted CAOV4 cells treated with either carboplatin (125 mmol/L), carboplatin and TWEAK (100 ng/mL), TWEAK then carboplatin, and carboplatin then TWEAK for 120 hours. One-way ANOVA, Tukey post hoc test (n¼3). (E) Flow cytometry analysis of CD117 and Fn14 expression CAOV4 cells mock sorted or CD117⁻ sorted cells treated with vehicle or TWEAK (100 ng/mL) and carboplatin (30 mmol/L) for two cycles of 7 days, where initial treatment is for 24 hours with subsequent 2-fold dilution with media. Representative gating (top) and percent Fn14⁺CD117⁺ cells representing mean plus SD.Two-way ANOVA, Sidak post hoc test (n ¼ 4 mock, 5 CD117⁻ sorted). Data represent mean and SEM. *, P < 0.05.*

3.4 TWEAK receptor Fn14 is required for TWEAK mediated CSC features.

TWEAK acts through its receptor Fn14 which is overexpressed in spheroid conditions, after chemotherapy, and is elevated in ovarian tumors. We therefore sought to verify that the TWEAK-induced CSC phenotypes observed previously are Fn14-dependent by impeding the signaling pathway at this receptor. This was accomplished through siRNA and small molecule inhibition.

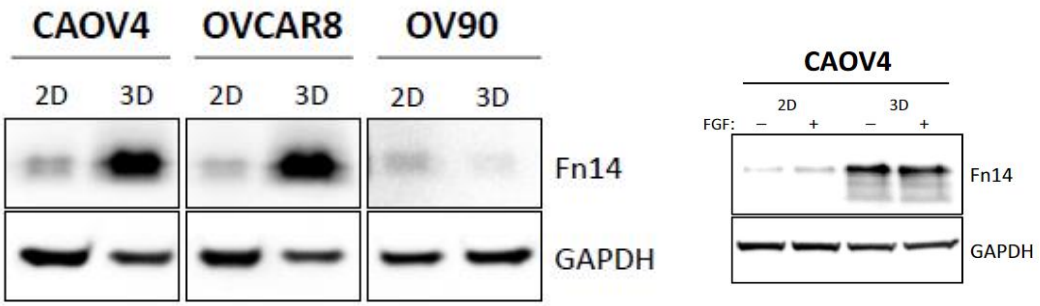

***Figure 20** – Fn14 expression in 2D vs 3D. (Left) Western blot for Fn14 from cells grown in standard adherent conditions or in spheroid conditions. (Right) CAOV4 cells grown in 2D or 3D conditions, with or without FGF.*

To begin, we grew the three cell lines in 2D and 3D conditions and blotted for Fn14. We observed that Fn14 was upregulated in 3D conditions in CAOV4 and OVCAR8 but not OV90 (**Figure 20, left**). Additionally, Fn14 expression is known to be induced by FGF, which is present in our spheroid growth media.[97] We were therefore concerned that the Fn14 expression observed was only due to the media. To rule this out so we grew CAOV4s in 2D and 3D conditions, with or without exogenous FGF, and blotted for Fn14. We observed no change in Fn14 expression in either 2D or 3D conditions when FGF was added. (**Figure 20, right**).

Knockback of Fn14 by siRNA caused significant reduction in Fn14 expression in all three cell lines. Additionally, non-canonical NF-κB activity was significantly reduced with Fn14

knockback, which is seen by reduced RelB expression and p100 processing to p52 (**Figure 21A-B**).

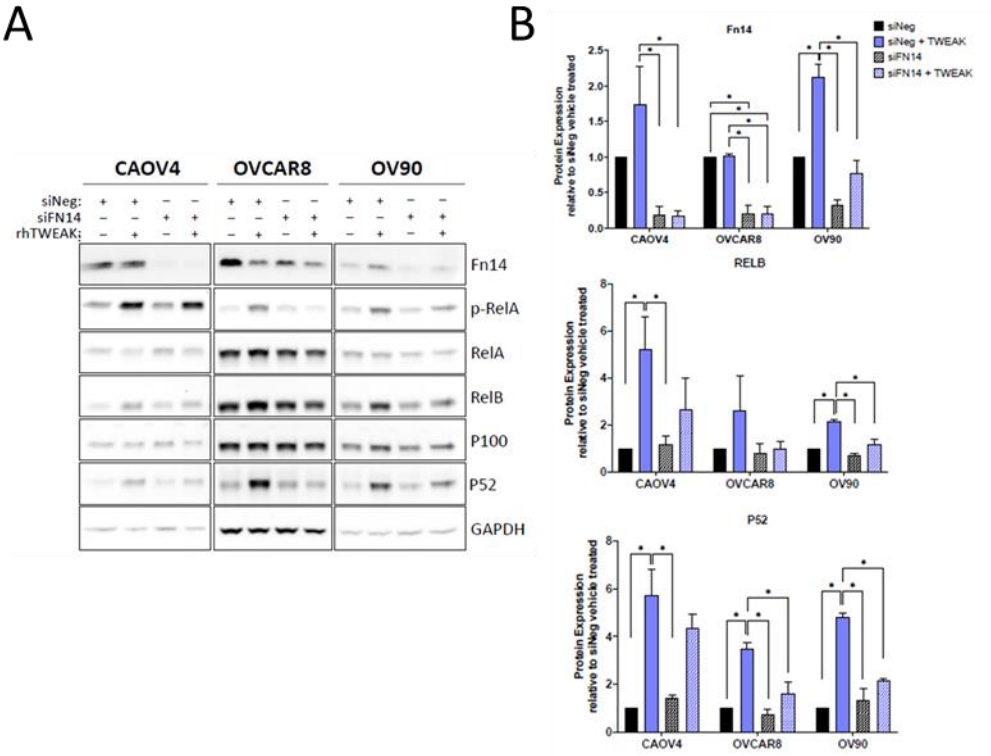

Figure 21 *– Validation of siFn14. (A) Western blot of Fn14 and NF-κB proteins in siNeg or siFN14 HGSOC cells treated with vehicle or TWEAK (100ng/ml) for 72 hours. (B) Quantification of band intensities. One-way ANOVA, Tukey's post-hoc test (n=3)*

Additionally, inhibition by small molecule inhibitor L524-0366 ablated TWEAK-induced NF-κB activity (**Figure 22A-B**). Fn14 knockback also significantly reduced spheroid efficiency as well as gene expression of *SOX2* and *NIK* (**Figure 22C-D**), which links TWEAK/Fn14 with the TWEAK-induced CSC phenotype.

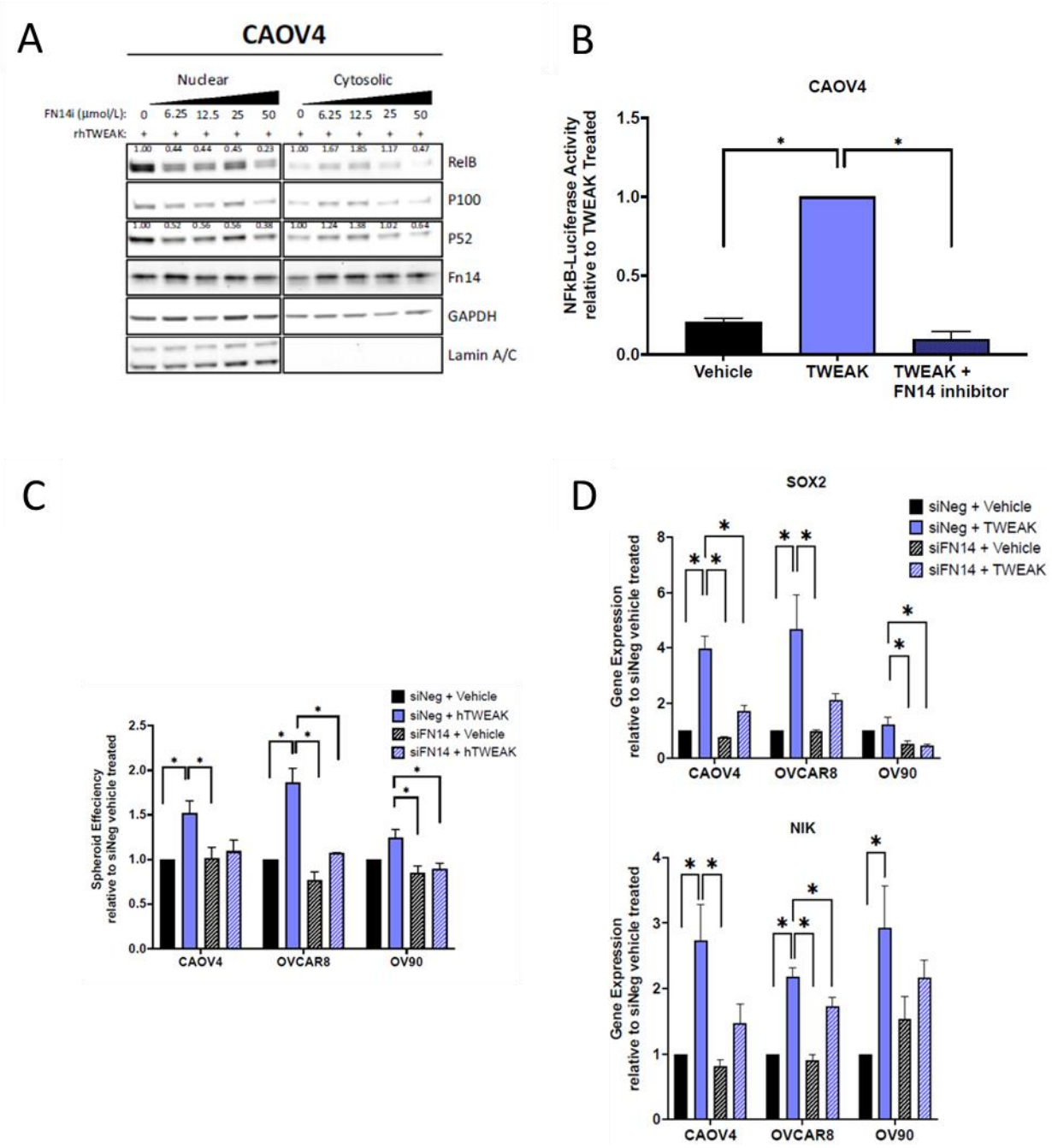

Figure 22 *-Fn14 mediates TWEAK activity (A) Nuclear and cytosolic western blots for indicated proteins in CAOV4 cells treated with TWEAK (100 ng/mL), or TWEAK plus FN14 inhibitor (L542-0366, 6.25–50 mmol/L). Quantification values normalized to Lamin A/C for nuclear fraction and GAPDH for a cytosolic fraction.. (B) Luciferase reporter assay showing NF-kB activity is lost in response to TWEAK (100 ng/mL) plus FN14i (L542-0366, 50 mmol/L) inCAOV4 cells (n=4). (C) Spheroid efficiency of siNeg or siFN14 HGSOC cells treated with vehicle or TWEAK (100ng/ml) for 4 days, represented relative to vehicle. One-way ANOVA, Tukey's post-hoc test (n=4). (D) qRT-PCR for SOX2 or NIK in siNeg or siFN14 HGSOC cells treated with TWEAK (100ng/ml) for 48 hours, relative to vehicle. One-way ANOVA, Tukey's post-hoc test (n=3).*

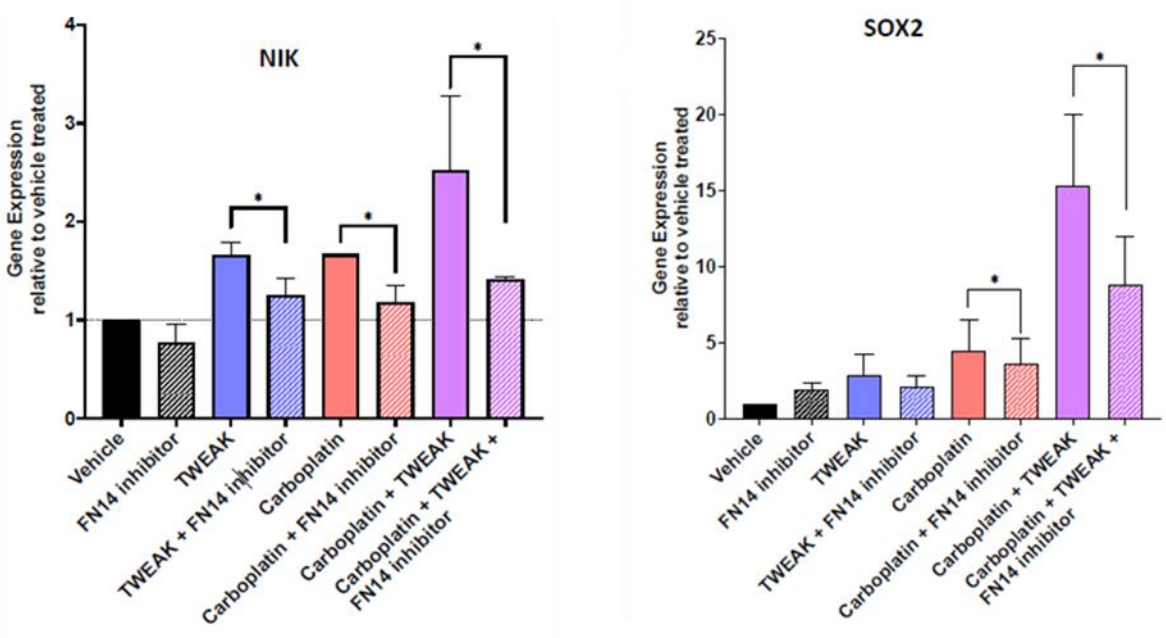

Figure 23 *– Fn14i qRT-PCR for EMT genes. qRT-PCR for SOX2 or NIK in CAOV4 cells treated with FN14 inhibitor (L542-0366, 50 M) for 72hrs in combination with vehicle, TWEAK (100ng/ml), carboplatin (125 µM), or TWEAK and carboplatin conditions. Student's t-test for condition versus condition plus FN14 inhibitor (n=3). Data represent mean and SEM. * p<0.05.*

We next used qPCR to look at gene expressions of *NIK* and *SOX2* under our TWEAK and carboplatin treatment regime with or without Fn14 inhibition. In the series with no inhibitor, we see the expected trend of TWEAK and chemo separately inducing gene expression, while both treatments together have the strongest response. In all TWEAK and/or carboplatin stimulated conditions, the inhibitor reduces TWEAK-induced expression of both *NIK* and *SOX2*, including in samples which only received carboplatin but not exogenous TWEAK (**Figure 23**).

3.5 RelB mediates TWEAK-induced CSC features.

In addition to Fn14 dependency, we also wanted to confirm non-canonical NF-κB dependence for TWEAK-induced CSC features, as well as for carboplatin-mediated CSC enrichment. RelB has been previously shown to be upregulated both in 3D conditions and with carboplatin treatment.[76] Additionally, experiments in this study reveal that TWEAK is a stronger inducer of non-canonical NF-κB than carboplatin (**Figure 24**). We therefore sought to investigate the role of TWEAK/Fn14/RelB in a post-chemotherapy relapse environment.

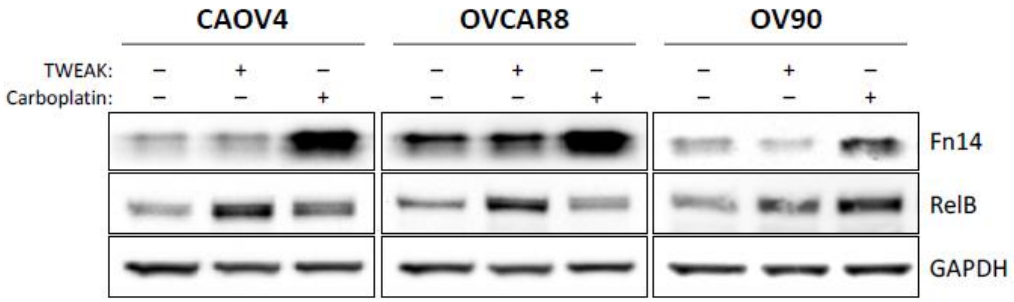

Figure 24 *– Carbo Treated Western Blots. Western blot for Fn14 and RelB from cells treated with vehicle, TWEAK, or Carboplatin for 72 hours.*

For this experiment, mouse xenograft tumors which had been treated with three rounds of carboplatin were resected 12 days after cessation of therapy (**Figure 25A**). This is a similar experimental setup as shown in **Figure 10** except the tumors were allowed to recover for 12 days instead of 5 to better asses delayed effects chemotherapy and better model a relapse environment. As would be expected, carboplatin treated tumors grew at a slower rate than vehicle treated (**Figure 25B**). There was also a significant increase in TWEAK expression in the tumors, as well as an increase in $CD117^{+}$ cells as well as RelB nuclear localization (**Figure 25C-E**). Together these confirm the induction of TWEAK/RelB signaling in a post-chemotherapy environment.

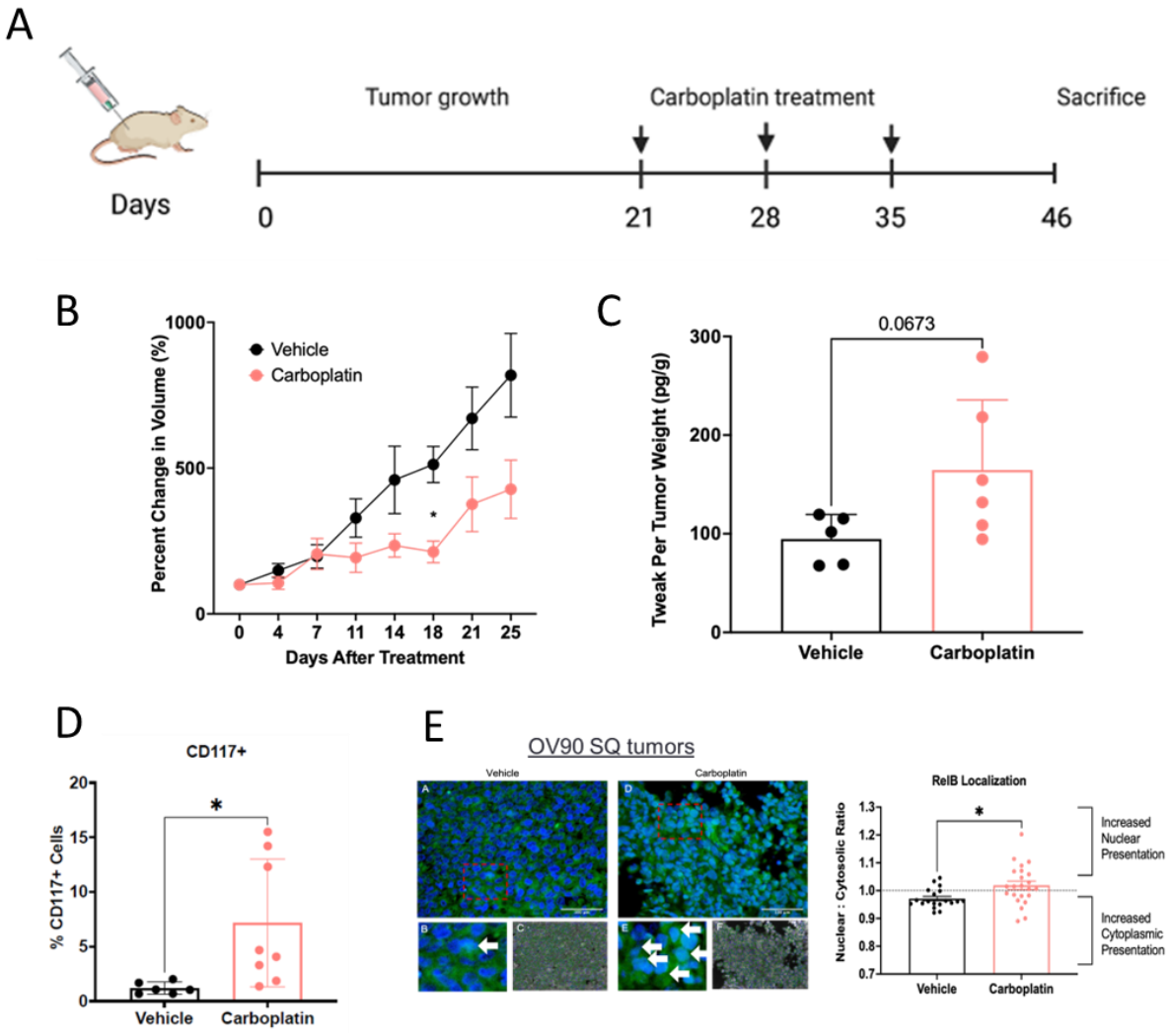

Figure 25 *– OV90 Mouse Study – long endpoints. Subcutaneous tumors were generated in nude mice using OV90 cells. Tumors were allowed to grow for 21 days followed by 3 cycles of carboplatin (50mg/kg) or vehicle and resected 12 days after the final carboplatin treatment. (A) Experimental design created with BioRender.com. (B) Tumor volume was measured twice weekly. Two-way ANOVA, Tukey's post-hoc test (n=6). (C) TWEAK concentration per tumor weight measured using ELISA. Student's t-test (n=6). (D) Flow cytometry analysis of CD117 expression. Student's t-test (n=8).(E) Fixed tumor fractions were histologically stained for nuclei (DAPI) and RelB. Representative images (left) and nuclear relative to cytosolic RelB was quantified per field using Cellprofiler (right). Student's t-test (n=3).*

In order to establish the RelB dependence of TWEAK-induced CSC effects, we used CRISPR-mediated RelB knockout cell lines. The cell lines were validated by western blot and confirmed to lack RelB (**Figure 26A**). TWEAK stimulation still activates other aspects of NF-κB signaling such as phosphorylation of RelA and processing of p100 to p52, but the non-canonical pathway is inoperative without RelB. We then treated the knockout cells with TWEAK and saw that they lost TWEAK-inducible expression of *SOX2, VIM,* and *ZEB1* (**Figure 26B)**. There was also a recovery in the TWEAK-induced downregulation of *CDH1*, though this did not reach significance. The knockout cells also show a loss in spheroid forming ability, and an increase in EDU incorporation (which indicates less stemness) (**Figure 26C)**. Additionally, enrichment of $Fn14^{+}CD117^{+}$ double positive cells with either carboplatin alone or TWEAK and carboplatin together is greatly reduced in the knockout lines (**Figure 26E)**. Similarly, the $Fn14^{+}CD117^{-}$ population was enriched in the TWEAK and carboplatin condition with RelB lost. These data demonstrate that EMT/MET genes, stem cell marker genes, CSC phenotypes, chemoresistance of CSCs, and chemosensitivity of non-CSCs, all rely at least in part on RelB for the observed TWEAK-induced changes.

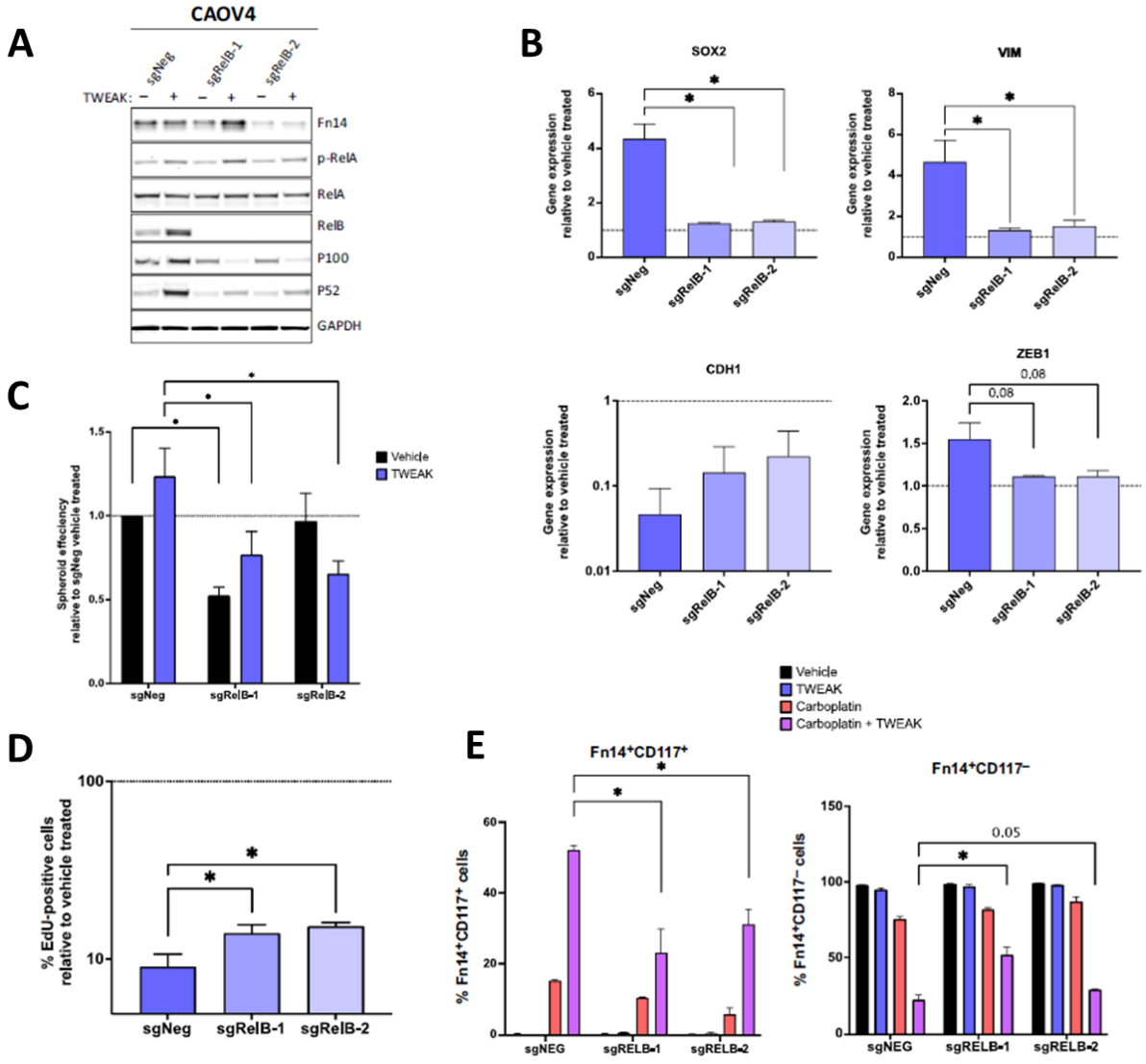

Figure 26 *– RelB KO Line Experiments. (A) Western blot of NF-κB proteins in CAOV4-RelB knockout (KO) lines with TWEAK treatment (100ng/ml) for 48 hours.(B) RelB KO gene expression. qRT-PCR for select genes in CAOV4-RelB KO lines treated with TWEAK (100ng/ml) for 48 hours, relative to vehicle. One-way ANOVA, Tukey's post-hoc test (n=3). (C) Spheroid efficiency of CAOV4-RelB KO lines treated with TWEAK (100ng/ml) for 7 days, relative to vehicle. Twoway ANOVA, Tukey's post-hoc test (n=6). (D) EdU incorporation pulse-chase assay of CAOV4-RelB KO lines treated with TWEAK (100ng/ml) for 60 hours, relative to vehicle. One-way ANOVA, Tukey's post-hoc test (n=6).(E) RelB KO Flow Cytometry. Flow cytometry of CD117 expression on Fn14+ CAOV4-RelB KO lines treated with TWEAK (100ng/ml), carboplatin (125 μM), or TWEAK and carboplatin for 72 hours, represented relative to vehicle as mean plus SD. Oneway ANOVA, Tukey's post-hoc test (n=3). Data represent mean and SEM. * p<0.05.*

3.6 Small molecule inhibition of Fn14 significantly slows ovarian cancer relapse.

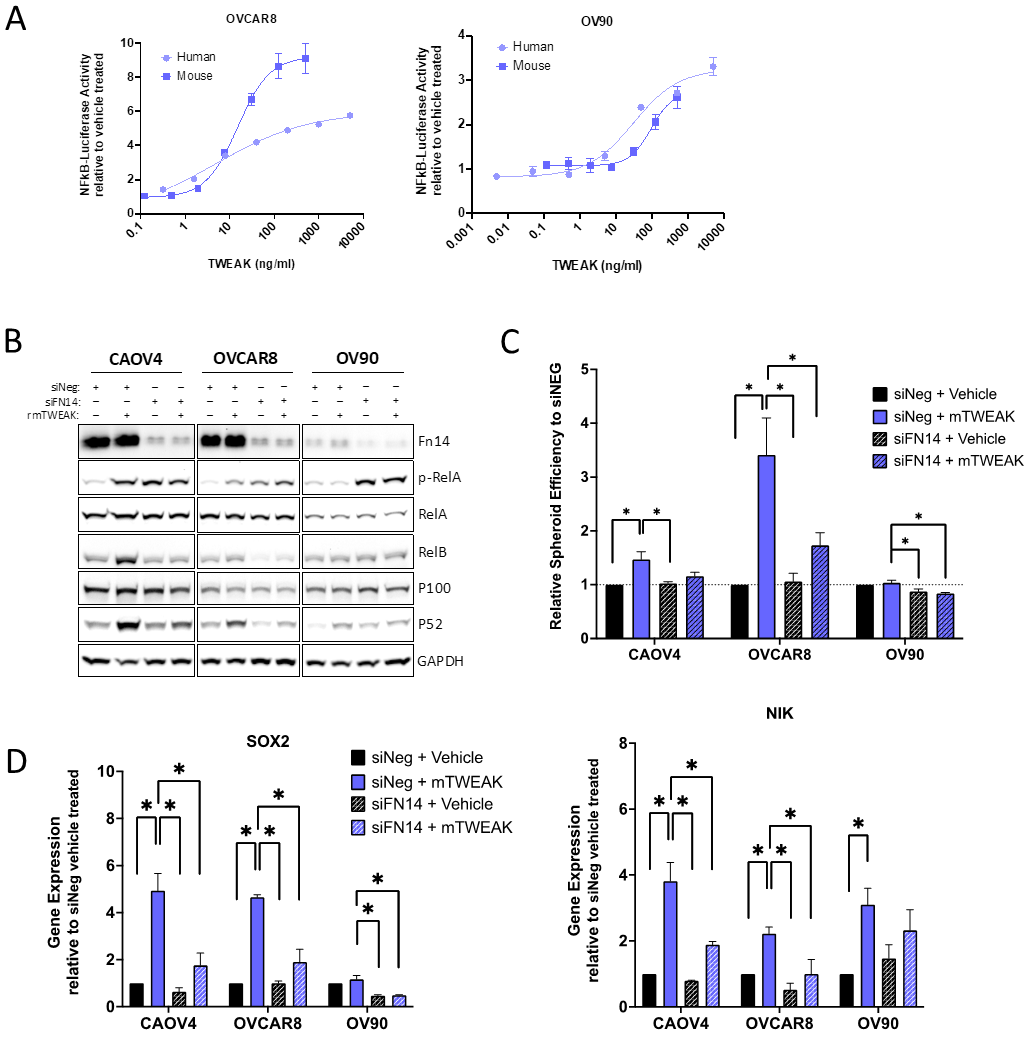

Figure 27 *- Mouse TWEAK activates NF-κB pathway in human ovarian cancer cells. (A) Luciferase reporter assay showing NF-κB activity in response to human or mouse TWEAK (n=3). (B) Western blot of Fn14 and NF-κB proteins in siNeg or siFN14 HGSOC cells treated with vehicle or mouse TWEAK (100ng/ml) for 72 hours (n=3) (C) Spheroid efficiency of siNeg or siFN14 HGSOC cells treated with vehicle or mouse TWEAK (100ng/ml) for 4 days, represented relative to vehicle. One-way ANOVA, Tukey's post-hoc test (n=3). (D) qRT-PCR for select stemness genes of siNeg or siFN14 HGSOC cells treated with vehicle or mouse TWEAK (100ng/ml) for 48 hours, represented relative to vehicle. One-way ANOVA, Tukey's post-hoc test (n=3). Data represent mean and SEM. * p<0.05.*

We next wanted to test our findings in a mouse model. However, TWEAK is most likely secreted by stromal cells so we first needed to verify that TWEAK produced in mice would react with the human Fn14 on our cancer cells. Murine and human TWEAK are very similar structurally, having 93% identity in the receptor binding domain, so it is reasonable that they should cross

react.[77] We verified murine TWEAK's ability to stimulate human Fn14 by NF-κB luciferase (**Figure 27A**), western blot for NF-κB members (**Figure 27B**), spheroid efficiency (**Figure 27C**), and induction of *SOX2* and *NIK* (**Figure 27D**). We also confirmed that these effects are dependent on human Fn14 by siRNA knockdown (**Figure 27A-D**).

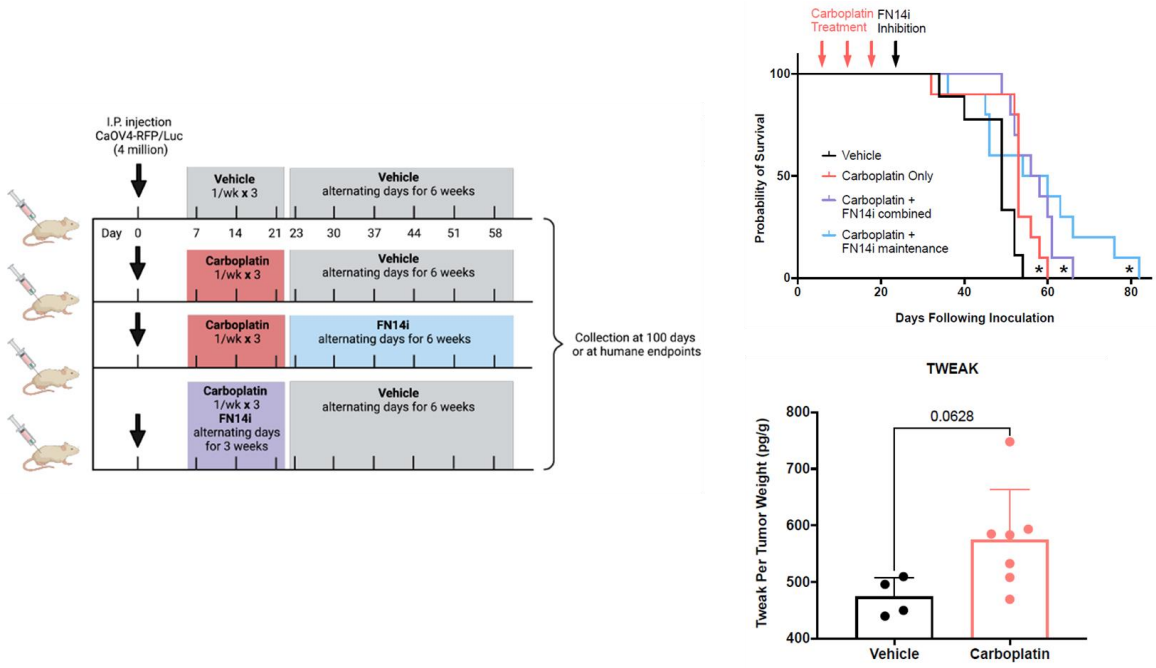

Figure 28 *– Fn14i IP Mouse Study (Left) Experimental design created with BioRender.com. (Right) Kaplan-Meier survival of intraperitoneal xenograft tumors with CAOV4 cells treated with either vehicle, carboplatin (50mg/kg), carboplatin and FN14i (L542-0366, 9mg/kg) combined, or carboplatin followed by FN14i maintenance. Log-rank test (n=10). (Right bottom) TWEAK concentration per tumor weight. Student's t-test (n=4 vehicle, n=7 treatment).*

Because of the observation that TWEAK works in concert with chemotherapy, and because TWEAK appears to be highest after chemotherapy, we inhibited TWEAK/Fn14 signaling both in combination with chemotherapy and as a maintenance therapy after the completion of 3 rounds of carboplatin treatment in an i.p. mouse model (**Figure 28**, left). We found that administering Fn14 inhibitor L542-0366 in combination with carboplatin significantly increased overall survival. However, Fn14 inhibition as maintenance therapy had the longest overall survival of any of the groups (**Figure 28**, top right). We also observed that chemotherapy treated tumors had increased expression of TWEAK, which is consistent with our xenograft results (**Figure 28**, bottom right).

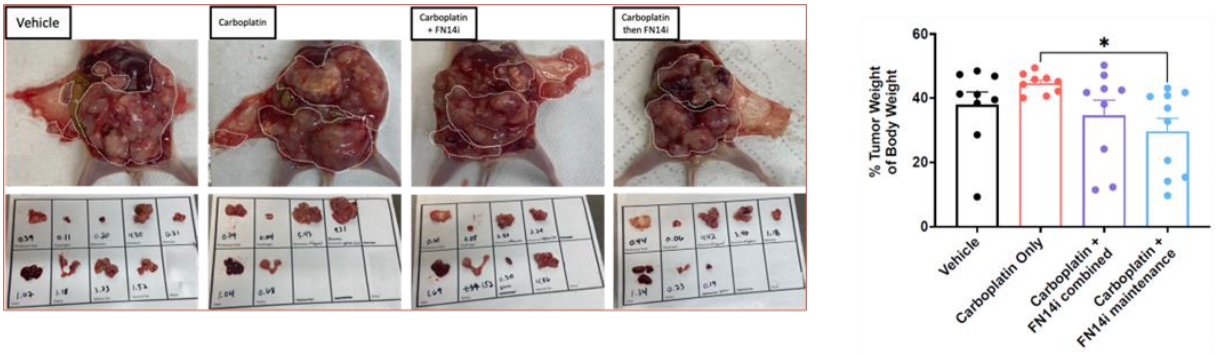

Figure 29 *– Fn14i IP Mouse Study Tumor Weight (Left) Representative images of tumors from different treatment groups at necropsy. (Right) Tumors were resected and weighed relative to body weight. One-way ANOVA, Tukey's post-hoc test.*

Tumor weights for mice receiving inhibitor as maintenance were significantly lower than those that received carboplatin alone (**Figure 29** bottom). IHC analysis by DAB staining showed that there was no significant difference in RelB levels between any of the groups (**Figure 30A**). However, further analysis using automated image analysis showed reduced nuclear localization of RelB in L542-0366 treated groups relative to carboplatin alone (**Figure 30B**). Taken together these data indicate that inhibiting TWEAK/Fn14 following chemotherapy provides survival benefits. Our *in vitro* work suggests that TWEAK may be conferring a chemoresistant, CSC-like phenotype to the cells through non-canonical NF-κB signaling. Future studies could aim to reduce recurrence of relapse in ovarian cancer through regulation of TWEAK in the ovarian TME.

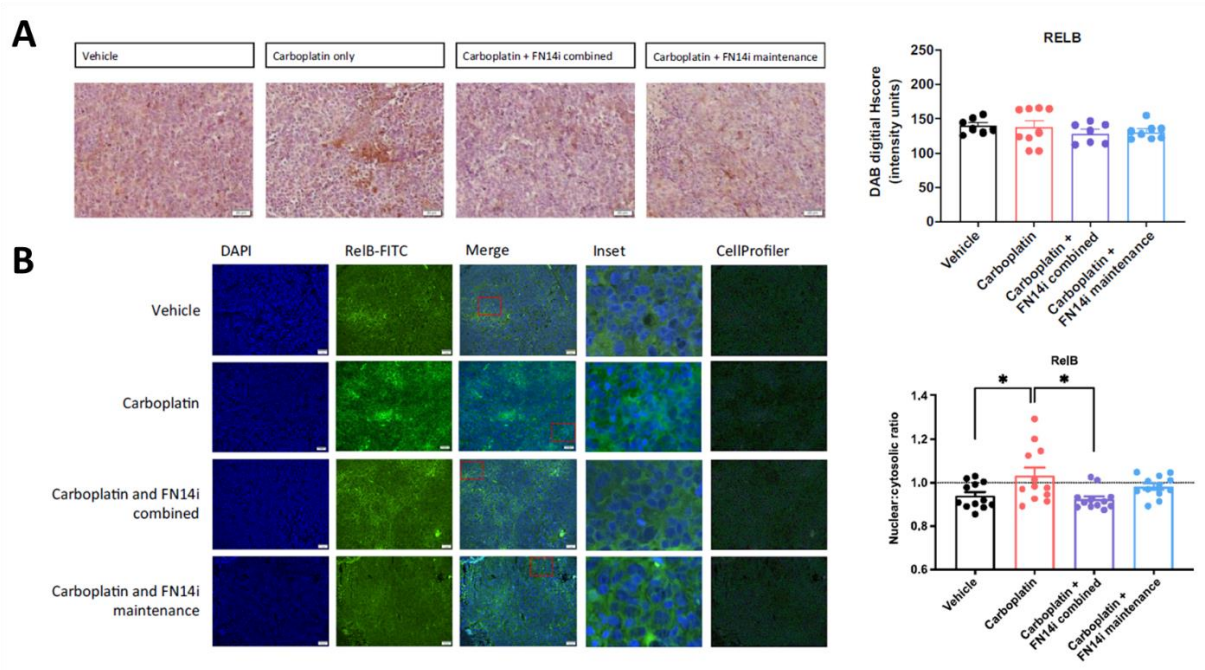

Figure 30 *– Fn14i Mouse Study IHC. Fixed tumor fractions were histologically stained for nuclei (DAPI) and RelB. Representative images (top) and nuclear relative to cytosolic RelB was quantified per field using Cellprofiler (bottom). One-way ANOVA, Tukey's post-hoc test (n=3). Data represent mean and SEM. * p<0.05.*

4. Discussion

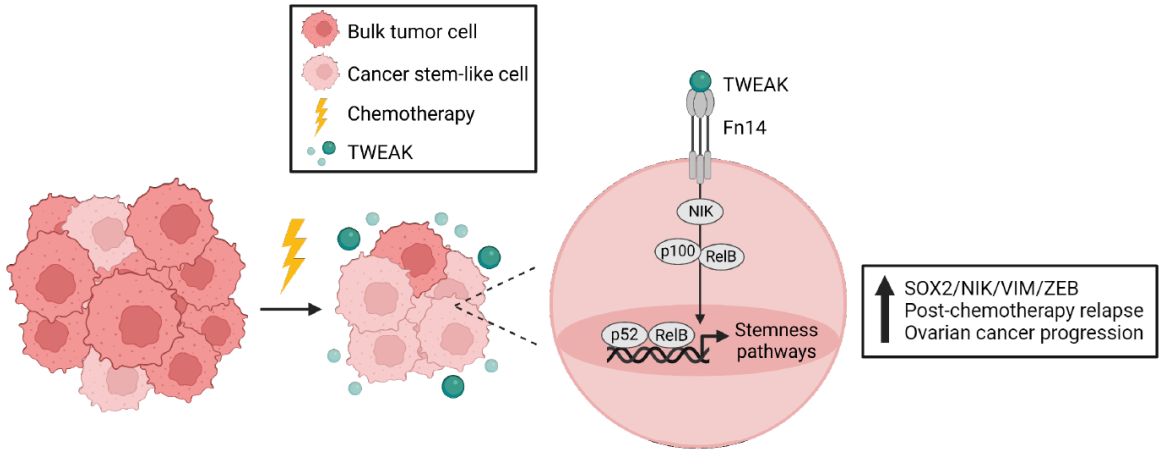

Figure 31 *– Graphical Abstract. TWEAK/Fn14/RelB signaling supports post-chemotherapy ovarian cancer progression. Created with BioRender.com*

Ovarian tumors are heterogeneous, and the tumor microenvironment (TME) adds to this heterogeneity. Cancer microenvironments include cancer cells, which are themselves heterogeneous, as well as macrophages, fibroblasts, T cells (CD4+, CD8+, and regulatory), and myeloid-derived suppressor cells. Each of these cells is secreting its own set of cytokines and chemokines which affect the overall tumor state.[35] The tumors themselves contain a heterogeneous population, including bulk proliferative cells as well as non-proliferative stem-like cells. These stem-like cells are proposed to be critical in relapse and have been shown previously to be supported by non-canonical NF-κB signaling.[76] It is unclear, however, what induces NF-kB activation in tumors and because of this, we sought to find what components of the TME are responsible for non-canonical NF-κB signaling and therefore could be supporting relapse by promoting a CSC phenotype.

The different pathways of NF-κB can have distinctly different effects on the same tissue. Work from our lab has shown that canonical signaling promotes proliferative phenotypes, while

non-canonical signaling supports CSC phenotypes.[76] In other studies, TWEAK-induced canonical signaling promotes myoblast proliferation and inhibits myogenesis in skeletal muscle tissue, while non-canonical signaling simultaneously promotes myogenesis.[96] Within HGSOC, canonical NF-κB signaling through TWEAK treatment increases VEGF production and enhances migration and invasion.[114] This study was conducted in bulk tumor cells and did not investigate CSCs. In this study we focus on the non-canonical pathway, but there is much room to explore effects specific to canonical signaling as well. Additionally, TWEAK/Fn14 signaling is not restricted to NF-κB, but also signals through ERK, JNK, and PI3K/AKT pathways, which are implicated in many cancers.[79,89,99] Although these have not all been demonstrated in HGSOC, they are all potential routes for further investigation into TWEAK's effects on HGSOC and its role in promoting heterogeneous phenotypes. TWEAK can also work less directly through recruitment of macrophages and modulation of their signaling profiles.[115]

TWEAK is a multifunctional protein which is found at low levels basally in most tissues. TWEAK has many roles which are dependent on cell type and concentration, but its main function is in tissue remodeling and wound healing following acute injury where it promotes muscle survival and repair.[86] It has one primary signaling receptor, Fn14, but also interacts with CD163, primarily as a scavenger receptor. Like TWEAK, Fn14 is basally expressed at low levels. Both TWEAK and Fn14 are upregulated strongly after acute injury or in chronic disease such as cancer, rheumatoid arthritis, and cardiovascular disease.[81,97,141] In this study we found that TWEAK and Fn14 are both upregulated in tumors following chemotherapy, both *in vivo* and *in vitro*. Because TWEAK/Fn14 has been shown to have protective roles under acute injury, it is possible that chemotherapy is activating TWEAK/Fn14 and hijacking it's normal role in wound healing to support the tumor. TWEAK's function in tissue remodeling, which is key for tumor formation

and growth, particularly post-chemotherapy, could be advantageous for activating stem-like cells needed for cancer progression.

CD117 is a marker for CSCs in ovarian cancer.[21,142] Because of this we studied the differential effects of TWEAK on $CD117^+$ (CSCs) and $CD117^-$ (bulk tumor) cells. The relative portion of $CD117^-$ cells decreased when treated with TWEAK and carboplatin, implying that TWEAK is sensitizing bulk tumor cells to chemotherapy-mediated death. This agrees with previous observations that TWEAK can sensitize cells to apoptosis.[114,143] In $CD117^+$ cells, the relative fraction increases with TWEAK and carboplatin treatment. Additionally, the $CD117^+$ population also showed significant increases in stemness genes after chemotherapy, which would provide increased resistance to chemotherapy as well as contribute to relapse. Together these data suggest that TWEAK is promoting chemoresistance in $CD117^+$ CSCs, and conversely promoting chemosensitivity in CD117- bulk tumor cells. Current studies are focused on understanding the differences in expression of TNFR receptors and associated TRAFs in chemoresistant versus chemosensitive ovarian cancer cells which might explain their different responses to TWEAK signaling.

Fn14 overexpression has previously been shown to sensitize HGSOC to chemotherapy, though the specific role of TWEAK or CSCs was not investigated.[143] It is interesting to note that this effect was only observed in a cell line with p53-R248Q mutation and not in p53-wt SKOV3 cells. It was originally argued that the effect is dependent on this specific mutation. However, none of the three cell lines used in this study bear this mutation, yet the effect is seen in two of them. All three cell lines bear mutant p53, but not R248Q, indicating that the effect is either independent of p53 mutation or the mechanism depends on general p53 dysfunction and not a specific mutation. The lack of effect on OV90s may be explained by their low Fn14 expression. Given that p53

dysfunction is observed in 95% of HGSOC cases and not as frequently in other subtypes, these studies suggest that the effect of TWEAK signaling may be specific to HGSOC, however additional studies in p53 wt cells would need to be performed.

Given that TWEAK and Fn14 are upregulated after chemotherapy and that CSC features are enhanced, we propose that the TWEAK/Fn14/RelB signaling axis contributes to CSC development, thereby enhancing relapse potential in ovarian cancer (**Figure 31**). In a HGSOC IP model mouse, we showed that TWEAK inhibition as maintenance therapy after carboplatin treatment significantly increases survival. Our *in vitro* work suggests that these effects are supported by non-canonical NF-κB signaling through RelB, but it is also possible that other pathways are at work, including ERK, JNK, and PI3K/AKT as described above. Future studies will focus on characterizing what downstream signaling pathways are activated by TWEAK and what phenotypes these different cascades support. Moreover, the effects of classical NF-kB activation by TWEAK should be explored, especially since classical NF-kB activity tends to promote proliferation in ovarian cancer cells. This could be another mechanism by which TWEAK promotes chemosensitivity. My work, as well as studies published by others, suggests that TWEAK might regulate cell fate in the face of chemotherapy. Understanding the mechanisms behind this will be crucial for predicting patient responses and developing new therapies to prevent recurrence.

Acknowledgments

Chapter 1 includes material as it appears in Molecular Cancer Research 2023. My coauthors are Mikella Robinson, Samuel F. Gilbert, Omar Lujano-Olazaba, Jennifer A. Waters, Emily Kogan, Candyd Lace R. Velasquez, Denay Stevenson, Luisjesus S. Cruz, Logan J. Alexander, Jacqueline Lara, Emily M. Mu, Jared Rafael Camillo, Benjamin G. Bitler, Tom Huxford, and Carrie D. House. The dissertation/thesis author was the primary investigator and author of this paper.

Supplementary Information

***Table 1**- Cell Line Information*

	High Grade Serous (HGS)			
Cell Lines	**CAOV4**	**OVCAR8**	**OV90**	**VBCF004**
Domcke Designation[1]	Likely HGSOC	Possibly HGSOC	Possibly HGSOC	Not included
Histology[2,3]	Adeno-carcinoma	Adeno-carcinoma G3	Adeno-carcinoma	Adeno-carcinoma
Cell Line Source	ATCC: HTB-76	NCI-DTP: OVCAR-8	ATCC: CRL-11732	NIH-DTP
Maintenance Media (Gibco)	RPMI	RPMI	RPMI	DMEM/F12
Patient Source	45Y Female Metastatic Fallopian Tube Site	64Y Female Primary Site	64Y Female Ascites-derived	Ascites-derived
Prior Therapy	Unknown	Multi-chemo	None	Multi-chemo
TP53	Mutant	p.Y126 - splice (Hm)	p.S215R (Hm)	Unknown
Dutil Ancestry[4]	European	European	European	Unknown
RRID	CVCL_0202	CVCL_1629	CVCL_3768	Derived in house

Table 2 *– Reagent Information*

Reagent (in order of appearance in methods)	Company and Order Information
RPMI 1540 Media	Gibco 11875135
DMEM/F12 Media	Gibco 11320033
Molecules	rh-TWEAK (R&D Systems 1090-TW-025) rm-TWEAK (R&D Systems 1237-TW-025) BAFF (Miltenyi 130-093-807) CD40L (Miltenyi 130-096-712) CRP (R7D Systems 1707-CR) IL-1β (Miltenyi 130-095-374) IL-6 (Miltenyi 130-093-929) IL-8 (Miltenyi 130-122-353) Leptin (R&D Systems 398-LP) TGF-b1 (Miltenyi 130-095-067) TGF-b3 (Miltenyi 130-094-007) TNF-alpha (R&D Systems 210-TA) Carboplatin (*in vitro*, R&D Systems 2626) Carboplatin (*in vivo*, 50mg/5ml in PBS, Veterinarian Source Pharmacy) FN14 inhibitor L524-0366 (Millipore 509374)
Cignal Lenti Reporter Assay	Qiagen (CLS-013L-1)
Polybrene	Millipore Sigma TR-1003-G
ONE-Glo EX Luciferase Assay	Promega E6110
SoftMax Pro Software	Molecular Devices Version 7.1.0
SpectraMax iD3 plate reader	Molecular Devices
TransAM NF-kB Activation Assay	Active Motif 43296
Nuclear Extract Kit	Active Motif 40010
Pierce Rapid Gold BCA Protein Assay Kit	ThermoFisher Sci A53225
Pierce Detergent Compatible Bradford Assay Kit	ThermoFisher Sci 23246
Primary Western Blot Antibodies	FN14 (Cell Signaling CST-4403), RRID: AB_10693941 RELB (Cell Signaling CST-4922), RRID: AB_2179173 RELA (Cell Signaling CST-8242), RRID: AB_10859369 P-RELA (Cell Signaling CST-3033), RRID: AB_331284 p100/p52 (Millipore 05-361), RRID: AB_309692 LAMIN A/C (Santa Cruz sc-7292), RRID: AB_627875 GAPDH (Millipore MAB374), RRID: AB_2107445
Secondary Western Blot Antibody	Anti-mouse IgG, HRP-linked (Cell Signaling CST-7076), RRID: AB_330924 Anti-rabbit IgG, HRP-linked (Cell Signaling CST-7074), RRID: AB_2099233
Melody cell sorter and Chorus Software	Becton Dickinson BDFACS
FlowJo	Becton Dickinson FlowJo Version 10.8.1
SuperSignal West Pico PLUS	ThermoFisher Sci 34580
SuperSignal West Femto	ThermoFisher Sci 34094
CellTiter-Glo luminescent reagent 2.0	Promega G9242
CellStripper	Corning 25-056-CI

Table 2 *– Reagent Information continued*

Reagent (in order of appearance in methods)	Company and Order Information
Flow Antibodies	Ki-67 - unconj (1:1000, Cell Signaling 9449), RRID: AB_2797703 Goat anti-mouse Alexa Fluor 488 (1:1000, Invitrogen A11029), RRID: AB_2534088 CD113 - PE (1:100, MACS 130-111-085), RRID: AB_2654885 FN14 – PE (1:11, MACS 130-123-395), RRID: AB_2656763 CD117-APC 1:100 (1:100, MACS 130-111-671), RRID: AB_2654578 PI (Propidium iodide, 1:500, ThermoFisher Sci P1304MP)
ALDH Activity Assay	AldeFluor Stem Cell Technologies 01700
Caspase Assay	Invitrogen CellEvent Caspase-3/7 Green Detection Reagent C10423
EDU Click-it Assay Alexa Fluor 647	ThermoFisher Sci C10419
Hoechst	ThermoFisher Scientific Hoechst 33342
ImageXpress	Molecular Devices ImageXpress Pico
CellReporterXpress Software	Molecular Devices Version 2.1.5156
Click-iT TUNEL Assay Alexa Fluor 488	ThermoFisher Sci C10617
ULA flat bottom 96-well plates	Corning 3474
NucleoSpin RNA Plus kit	Macherey-Nagel 740984.50
Direct-zol RNA Miniprep Plus Kit	Zymo Research R2071
SpectraMax QuickDrop	Molecular Devices
High-Capacity cDNA Reverse Transcription Kit	ThermoFisher Scientific 4368814
QuantStudio 3 machine and Design software	ThermoFisher Scientific Version 1.5.1
Taqman Probes from ThermoFisher Scientific	OCT4 Assay ID: Hs04260367_gH SOX2 Assay ID: Hs01053049_s1 NANOG Assay ID: Hs02387400_g1 GAPDH Assay ID: Hs99999905_m1 CD117 Assay ID: Hs00174029_m1 NIK Assay ID: Hs01089753_m1 FN14 Assay ID: Hs00171993_m1 VIM Assay ID: Hs00185584_m1 CDH1 Assay ID: Hs01023894_m1 ZEB1 Assay ID: Hs01566408_m1
CD117 Microbead Kit, human	Miltenyi Biotec 130-091-332
QuadroMACS Separator Kits	Miltenyi Biotec 130-091-051
FN14 siRNA	Horizon Discovery On-Targetplus Human TNFRSFS12A siRNA - SMARTpool L-010661-00-0005
CRISPR	Lentiviral hEF1aBlast-Cas9 Nuclease Particles (Horizon VCAS11227) RelB sgRNA Lentiviral Particles (Horizon Cat. VSGH10143-246635034, VSGH10143-246635035, VSGH10143-246635037) Non-targeting Control sgRNA Lentiviral Particles (Horizon VSGC10215, VSGC10216, VSGC10217)
iBRIGHT software	ThermoFisher Sci Version 3.1.2
KnockOut™ Serum Replacement	Gibco 10828028

Table 2 *– Reagent Information continued*

Reagent (in order of appearance in methods)	Company and Order Information
Insulin-transferrin-selenium (ITS-G)	Gibco 41400045
ULA T-75s	Corning 3814
IHC Antibodies	RelB (1:800, Cell Signaling, 10544), RRID: AB_2797727 Fn14 (1:250, Cell Signaling 4403), RRID: AB_10693941 HRP-linked polymer (Cell Signaling, 8114S), RRID: AB_10544930
DAB kit	Vector Laboratories SK-4100
Matrigel	Corning Matrigel 354263 Lot number 8260015
IL-6 DuoSet ELISA	R&D Systems DY206
TWEAK DuoSet ELISA	R&D Systems DY1090
GentleMACS M Tubes	Miltenyi Biotec 130-093-236
RIPA lysis buffer	ThermoFisher Sci 89900
IF Antibodies	F-actin (Phalloidin-Alexa Fluor 488, 1:1000, ThermoFischer Sci A12379) RelB (1:800, Cell Signaling, 10544), RRID: AB_2797727 Goat anti-rabbit FITC (1:100, ThermoFisher Sci A32731), AB_2633280
Fluoroshield Mounting Medium with DAPI	Abcam 104139
Prism	GraphPad Prism Version 8.4.3

Table 3 *- Public databases used in this study*

Public Database	Genes	Group	Notes	Reference
Cancer Cell Line Encyclopedia (CCLE)[1,2]	TWEAK (TNFSF12); FN14 (TNFRSF12A)	Ovarian Cancer Cell Lines	Reconstructed in excel by unique ID	https://www.cbioportal.org/
Kaplan-Meier Plotter[3]	TWEAK (TNFSF12)	Ovarian cancer	No modifications	https://kmplot.com/analysis
Genotype-Tissue Expression Project (GTEx)[4]	TWEAK (TNFSF12); FN14 (TNFRSF12A)	Normal tissue	Reconstructed in excel by unique ID	https://gtexportal.org/home/
The Cancer Genome Atlas (TCGA)	TWEAK (TNFSF12)	Ovarian Serous Cystadenocarcinoma	Reconstructed in excel by unique ID. Z-scores associated with survival outcomes at 5 years	https://www.cbioportal.org/
curatedOvarianData Forest plots[5]	TWEAK (TNFSF12); FN14 (TNFRSF12A)	Ovarian cancer	No modifications	http://bioconductor.org/packages/release/data/experiment/html/curatedOvarianData.html
Gene Expression Profiling Interactive Analysis, version 2 (GEPIA2)[6]	FN14 (TNFRSF12A)	Ovarian and normal tissue	No modifications	http://gepia2.cancer-pku.cn
Jordan et al[7]	TWEAK (TNFSF12); other selected genes	Pre- vs Post-NACT	Reconstructed in excel by gene	Accessed with permission
Javallana et al[8]	TWEAK (TNFSF12)	Pre- vs Post-NACT	Reconstructed in excel by gene	The data analyzed in this study were obtained from PMC at doi:10.1158/0008-5472.CAN-21-1467.

Chapter 2: Inhibition of IκBζ, a Nuclear IκB

1. Introduction

Prior to working in the House lab I spent a few years working on a project in the Structural Biochemistry Laboratory led by Dr. Huxford that was focused on the understudied and significantly less well understood nuclear IκB protein known as IκBζ.[59,64,144] The aim of the project was to exploit a recently completed high resolution x-ray crystallographic model for the interaction of IκBζ with the NF-κB p50 homodimer to design and develop a simple fluorescence-based assay for monitoring the binding status of IκBζ. The long-term goal was miniaturization and parallelization of the assay so that it could be used in high throughput fashion to screen against libraries of compounds for their ability to disrupt the interaction. Although the work did not result in the development of an assay with properties amenable to screening for potential inhibitors, the project was successful in detecting IκBζ binding to NF-κB homodimer in solution via fluorescence.

1.1 IκBζ

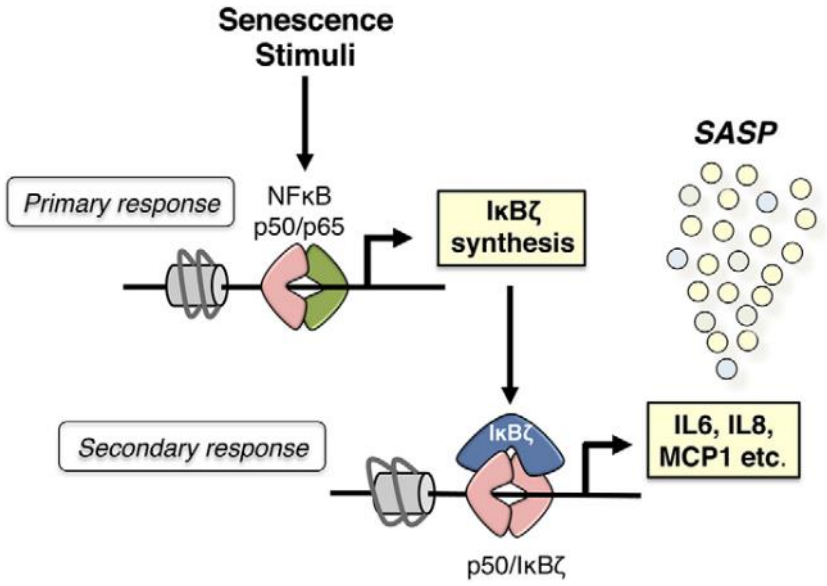

Figure 32 *– Schematic Diagram of delayed-response gene activation by IκBζ.*[145]

The NF-κB family contains eight IκB proteins, which collectively exert regulatory control over NF-κB. These were described previously in the Introduction section to Chapter 1 of this dissertation (**Figure 2**). IκBζ is one of three proteins, with Bcl-3 and IκBNS, that are classified as "Nuclear IκB" proteins. They are classified as such because, in contrast to classical IκB inhibitor proteins, upon NF-κB-dependent expression in response to LPS or Interleukin-1 stimulation of cells IκBζ accumulates within the cell nucleus. IκBζ also shows a binding profile that is distinct from classical IκB proteins. Whereas classical IκB binds preferentially to RelA and RelB NF-κB subunits, IκBζ selectively binds to NF-κB p50. Moreover, genetic ablation of IκBζ was observed to eliminate the ability of cells to elevate expression levels of a select subset of NF-κB-dependent genes in response to some inducers of canonical NF-κB signaling.[146,147]

At present, IκBζ is known to act as a context-dependent regulator of NF-κB: it represses expression of some NF-κB-dependent genes and activates others[58–62]. IκBζ is typically absent from resting cells but is itself a primary transcript of NF-κB induction through TLR-4 or the IL-1R receptors. The role of IκBζ has been defined primarily by its involvement in the transcription of pro-inflammatory cytokines including CCL2, IL-6, IL-17, IFNγ, and others.[61,63–66] In the right context however, it demonstrates strong anti-inflammatory effects, most significantly through the production of IL-10 and M2 macrophage polarization.[67] In addition to cytokine production, IκBζ is also a key regulator for H3K4 trimethylation and a regulator for the chromatin remodeling factor Brg1.[68–70] Furthermore, IκBζ has been implicated in several diseases including gliomas, psoriasis, dust mite allergies, and broader inflammatory diseases.[71–73,147,148] For these reasons, IκBζ is a protein of interest for further study as well as a potential therapeutic target.

X-ray crystallographic analysis of the C-terminal ankyrin repeat-containing domain of IκBζ in complex with the dimerization domain of NF-κB p50 homodimer revealed that IκBζ employs a closely similar strategy as classical IκB proteins in binding to NF-κB. Differences in amino acid positions at key locations – most notably the first ankyrin repeat of IκBζ and the nuclear localization signal-containing (NLS) polypeptide from p50 – was shown to contribute significantly to specificity and affinity of the complex (**Figure 32**). Therefore, we hypothesized that small molecules that could compete for and disrupt this relatively small portion of the protein-protein interaction might serve as inhibitors for greater investigation into IκBζ biological function and, potentially, as therapeutic lead compounds.

1.2 FRET

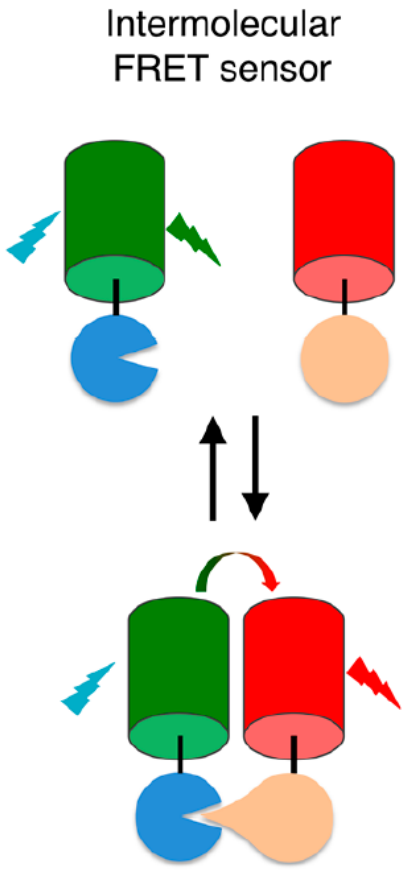

Figure 33 *- A basic FRET model. Unbound, the donor fluorophore emits at its own natural emission wavelength (green). Binding of the proteins brings the fluorophores into proximity, inducing FRET and causing emission in the acceptor fluorophore emission wavelength (red). From Bajar et. al.*[149]

Förster resonance energy transfer (FRET) is a phenomenon whereby excitation energy from a donor fluorophore can be transferred to an acceptor fluorophore. The result is a quenching of donor fluorescence and increase of acceptor fluorescence. This effect only occurs if the two fluorophores are very close to one another, typically within less than 10 nm. FRET can be used to monitor binding events between two compounds by placing an appropriate donor fluorophore on one of the compounds and an acceptor on the other. Energy transfer will be observed only when the compounds are bound to one another in complex.

1.3 Description of the Project

The goal of the project was to develop an assay to detect disruption of the IκBζ:NF-κB p50 interaction for investigation into the cellular role and mechanism of IκBζ. IκBζ is known to regulate NF-κB transcription, influence macrophage polarization, and is necessary for TH17 differentiation. Most of this is accomplished through interaction with p50 containing dimers.[61] IκBζ has primarily been studied through knockout/knockdown and transfection/overexpression techniques. These methods are informative, but complete elimination of a protein can have far-ranging and unexpected effects. Inhibition rather than elimination of IκBζ would be a useful for clarifying the role of IκBζ and this assay would be an invaluable tool in screening potential inhibitors.

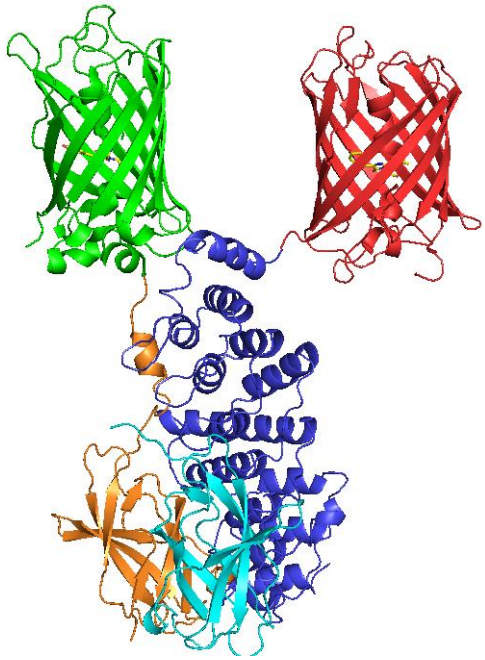

Figure 34 *– Cartoon showing the approximate arrangement of p50-GFP (orange and green), p65dd (light blue), and mCherry-IκBζ (red and dark blue) in complex.*

The first aim of the project was the development of a FRET-based assay for reporting the binding of IκBζ to the NF-κB p50 homodimer. Fluorescently labeled constructs of IκBζ and NF-

κB p50 were cloned which would FRET when bound. Inhibition by unlabeled proteins or by small molecule inhibitors cause loss of FRET, giving a quick and simple assay for the interaction. GFP was cloned to the n-terminal end of p50 while the mCherry was cloned to the c-terminal end of IκBζ. This arrangement allowed the fluorescent domains to be in near enough to one another when bound to engage in FRET (**Figure 34**). Because the proteins need to be close together to FRET but not so close that they stearically hinder binding of the complex, we created four variants of mCherry-IκBζ with varied linker lengths to optimize the distance between chromophores.

The second aim was to design a peptide-based inhibitor for the IκBζ:NF-κB p50 interaction. Since the NLS is a major interaction surface between p50 and IκBζ, a small peptide was designed which matched the NLS sequence. Additionally, a peptide was designed wherein two glutamines were replaced with tryptophans and then 'stapled' together with a small molecule to mimic the single alpha helical turn in the NLS.

2. Materials and Methods

2.1 Plasmid Preparation

Recombinant plasmid preparation

mCherry-IκBζ(404-718), p50-GFP, and p65dd plasmids were provided by previous members of the lab. mCherry-IκBζ variants were subcloned into pHis8 vector using BamHI and NotI restriction sites in frame with an N-terminal hexahistadine tag. The original vector containing mCherry-IκBζ(404-718) was digested with BamHI and NotI to remove the IκBζ region. Inserts were created by PCR using full length human IκBζ in pCDNA3 as a template with the primers described in **Table 4**. Inserts were digested with BamHI and NotI, then ligated into the above vector. Ligated DNA was transformed into XL1-Blue competent cells then miniprepped to obtain final plasmids.

Table 4 *- Oligonucleotides used in this study.*

Primer Name	Direction	Sequence
GGG-hIkBz(417-x)BamHI	Forward	5'-GAA GCT GGA TCC GGC GGC GGC CTT TTT CAG TGG CAG GTG-3'
GGG-hIkBz(421-x)BamHI	Forward	5'-GAA GCT GGA TCC GGC GGC GGC CAG GTG GAG CAG GAA GAA AG-3'
GGG-hIkBz(430-x)BamHI	Forward	5'-GAA GCT GGA TCC GGC GGC GGC GCA AAT ATT TCC CAA GAC-3'
GGG-hIkBz(437-x)BamHI	Forward	5'-GAA GCT GGA TCC GGC GGC GGC TTT CTT TCA AAG GAT GCA G-3'
hIkBz(x-718)NotI	Reverse	5'-ACT ACC GCG GCC GCC TAA TAC GGT GGA GCT CTC-3'

Digestion

Plasmid DNA or PCR amplicons were digested with BamHI-HF and/or NotI-HF for 3 hours at 37°C. Resulting DNA was run on an agarose gel and purified using QIAquick Gel Extraction Kit and stored at -20°C.

2.2 Expression and Purification

Transformation

1 µL plasmid DNA added to 50 µL XL1-Blue or BL21(DE3) competent cells and incubated on ice for 30 minutes. Cells were then heat shocked at 42°C in a water bath for 45 s, then chilled on ice for 2 min. 500 mL SOC was added then the tube was shaken at 37°C for 50 min. 20 µL of the suspension was plated onto pre-warmed LB-KAN or LB-AMP plates and incubated overnight. Isolated colonies were picked for miniprep or protein expression, described below. Unused plates were wrapped in parafilm and stored at 4°C for up to a week.

Miniprep

***Table 5**- Miniprep Solutions*

Reagent Name	Contents
Solution I	50 mM glucose, 25 mM Tris-HCl pH 8.0, 10 mM EDTA pH 8.0, 100 µg/mL RNAse (fresh)
Solution II	0.2 N NaOH, 1% SDS
Solution III	3 M KOAc, 2 M HOAc

Isolated colonies from transformation were picked and placed in 50 mL LB-KAN or LB-AMP starter cultures and shaken for ~3-8 hr. 1.6 mL each of starter culture was transferred to Eppendorf tubes and centrifuged at 13500 RPM for 30 s to pellet the cells. Supernatant was removed with vacuum aspiration. 0.3 mL cold Solution I was added to each tube and the pellet was resuspended by vortex. 0.3 mL room temperature Solution II was added carefully, and the tubes were inverted slowly 10 times. 0.3 mL cold Solution III was added to each tube and tubes were inverted until no more precipitate forms, approximately 10x. Tubes were centrifuged at 13200 RCF for 10 min at 4°C. Supernatant was transferred to fresh tubes containing 0.8 mL isopropyl alcohol. Tubes were incubated for >10 min at -20°C. DNA was pelleted by

centrifugation at 13200 RCF for 10 min at room temperature, then supernatant was removed by aspiration. DNA was washed with 0.5 mL 70% EtOH with several inversion. DNA was pelleted by centrifugation at 13200 RCF for 5 min at room temperature, then supernatant was removed by aspiration. Tubes were air-dried inverted on a paper towel for 5 min. DNA was resuspended at 150 µL TE buffer and stored at -20°C.

Expression

Individual isolated colonies from transformation plates were picked and placed in 50 mL LB-KAN or LB-AMP starter cultures and shaken for ~3 hr. Starter cultures poured into 2 L pre-warmed LB-AMP or LB-KAN cultures and shaken at 37°C until OD600 is ~0.1, approximately 3 hr., then moved to room temperature with aggressive stirring. Cultures were induced at OD600 of ~0.2 with IPTG to a final concentration of 0.1 mM and allowed to stir overnight. The next morning, cultures were centrifuged at 4000 RMP for 10 min and supernatant poured off. Pellets were either purified immediately or stored at -20°C.

Purification

***Table 6**- Purification Solutions*

Reagent Name	Contents
1X Lysis Buffer	25 mM Tris-HCl pH 8.0, 150 mM NaCl, 5 mM Imidazole
Wash Buffer	25 mM Tris-HCl pH 8.0, 150 mM NaCl, 25 mM Imidazole
Elute Buffer	25 mM Tris-HCl pH 8.0, 150 mM NaCl, 250 mM Imidazole
SEC Buffer	25 mM Tris-HCl pH 7.5, 50 mM NaCl, 1 mM DTT

Cell pellets were resuspended in 50 mL 1x lysis buffer with fresh protease inhibitor added per manufacturer instructions. Cells were lysed by microfluidizer then centrifuged at 12000 RMP for 50 min. The supernatant was then filtered through a 0.8 µm syringe-tip filter. The clarified lysate was then purified by nickel-sepharose fast flow as follows:

~1-1.5 mL Ni-Sepharose FF pipetted into an empty column then washed with 10 column volumes (CV) MilliQ water. Column was equilibrated with 10 CV 1x Lysis Buffer with protease inhibitor. Clarified lysate was then loaded onto the column, then washed with 10 CV wash buffer. Protein was eluted using 10 CV Elute Buffer and collected in 1 mL fractions. Fractions with protein were identified with a combination of visual inspection (in the case of fluorescent proteins), Bradford Assay, and Western Blot. Fractions containing protein of interest were combined and filtered through a 0.2 µm syringe-tip filter, then loaded onto an equilibrated Superdex 200 16/60 SEC column. Fractions containing protein were analyzed by Western Blot. Fractions with pure protein of interest were pooled, and optionally concentrated using Amicon Ultra-4 10K centrifugal concentrator. Purified protein solution was then aliquoted, snap frozen with liquid nitrogen, and stored at -80°C.

2.3 Plate Reader Assays

Comparison of Variants

All wells being tested were filled with 100 µL 25 mM Tris-HCl pH 7.5, 50 mM NaCl. 100 µL of mCherry-IκBζ variant was added to the first well in the column and mixed well. A serial dilution was created by transferring 100 µL from the first well to the second well then mixing, and so on through column 12. 100 µL 0.1 µM p50-GFP was added to each well. Fluorescence was recorded with an excitation wavelength of 422 nm and emission spectrum collected from 480 nm – 660 nm using a Tecan Infinite M200 plate reader.

Peptide Test

All wells except blanks were filled with to final concentrations of 0.2 µM mCherry-IκBζ(421-718), 0.05 µM p50-GFP, and either 35 µM unlabeled p50dd or 175 µM peptide inhibitor. Fluorescence was recorded with an excitation wavelength of 422 nm and emission spectrum collected from 480 nm – 660 nm using a Tecan Infinite M200 plate reader. Peptides used for the test are listed in **Table 7**.

***Table 7**- Peptide Inhibitors of IκBζ*

Name	Sequence
p50 NLS (354-368)	KDKEEVQRKRQKLMP
Inhibitor Peptide	KDKEEVQRKRQKLMP
Scrambled Inhibitor	Unknown
Trp-substituted (linear)	KDKEEVWRKRWKLMP
Trp-substituted (stapled)	KDKEEVWRKRWKLMP

3. Results and Discussion

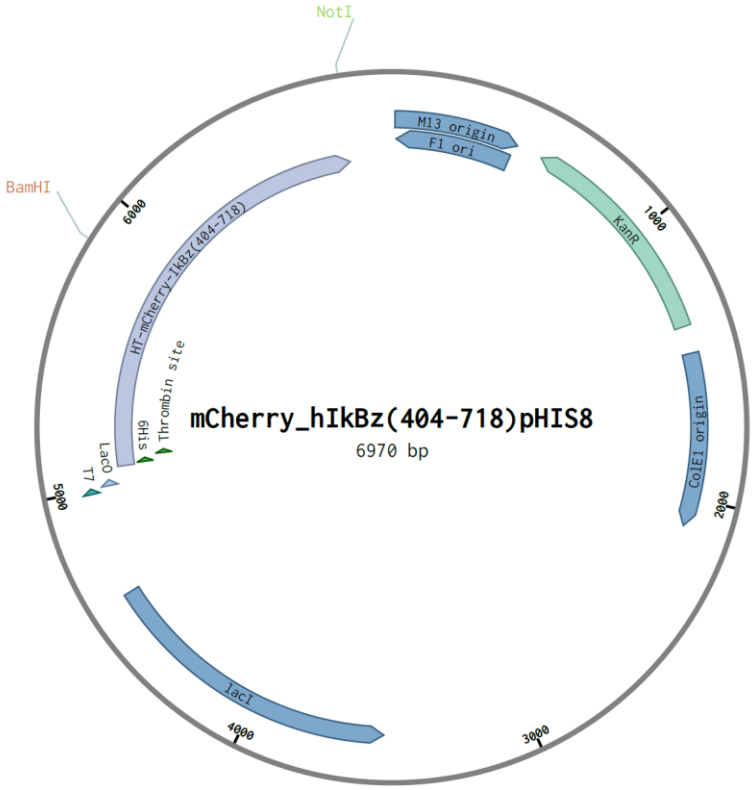

Figure 35 *– Plasmid Map for mCherry-hIkBz(404-718)*

3.1 Cloning and Protein Purification

The p50-GFP/p65dd/mCherry-IκBζ(404-718) complex was the original design for the system. However, it showed only weak signs of FRET (data not shown). Because FRET requires very short distances between chromophores, we were concerned that the fluorophores were too far apart and therefore experimented with different linker lengths between IκBζ and mCherry in order to bring the fluorescent proteins closer together. The original mCherry-hIκBζ(404-718) was taken as the longest linker length. The IκBζ portion of this plasmid was cut out using BamHI and NotI and replaced with four versions of IκBζ with fewer amino acids on the N-terminal disordered region. The new inserts that were cloned in are IκBζ AAs 417-718, 421-718, 430-718, and 437-

718. Ultimately the 430-718 and 437-718 variants would prove difficult to express and purify and were not used.

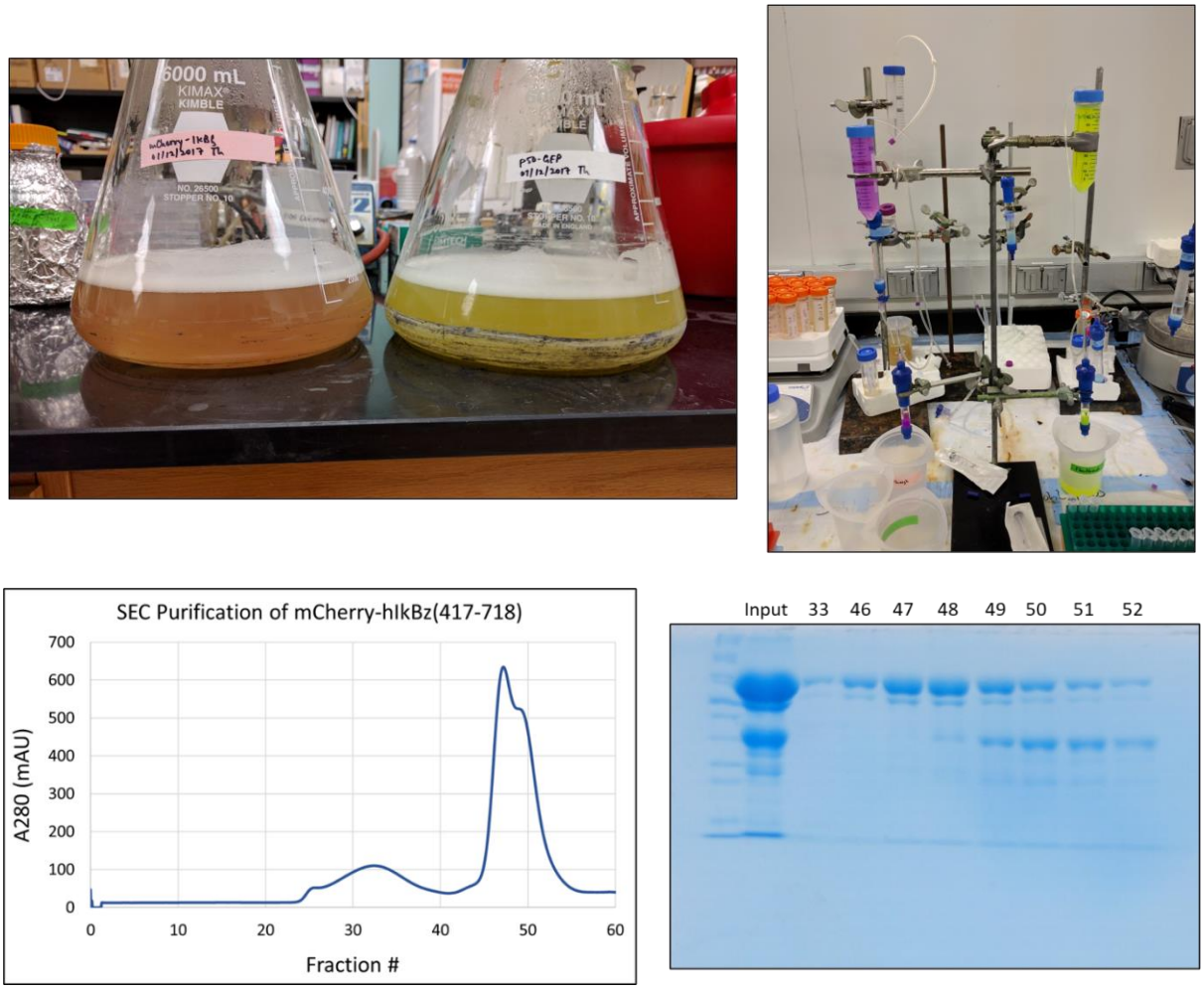

Figure 36 *– Expression and Purification of fluorescent proteins expressed in E. coli. (Top left) Fluorescent proteins being expressed in culture. (Top right) Ni-Sepharose purification. (Bottom left) Sample SEC chromatogram and (Bottom right) it's accompanying SDS-PAGE gel.*

The new vectors for our three variants of interest – mCherry-IκBζ(404-718), mCherry-IκBζ(417-718), and mCherry-IκBζ(421-718) – were transformed and expressed in BL21(DE3) cells. Expression was robust and fluorescence was easily visible to the naked eye (**Figure 36**, top). SEC purification revealed significant decomposition, but the final products were able to be purified (**Figure 36**, bottom). This decomposition was consistent between variants and expression lots. It

is possible that the proteins continue to decompose after purification as we did not test for ongoing degradation.

3.2 FRET Experiments

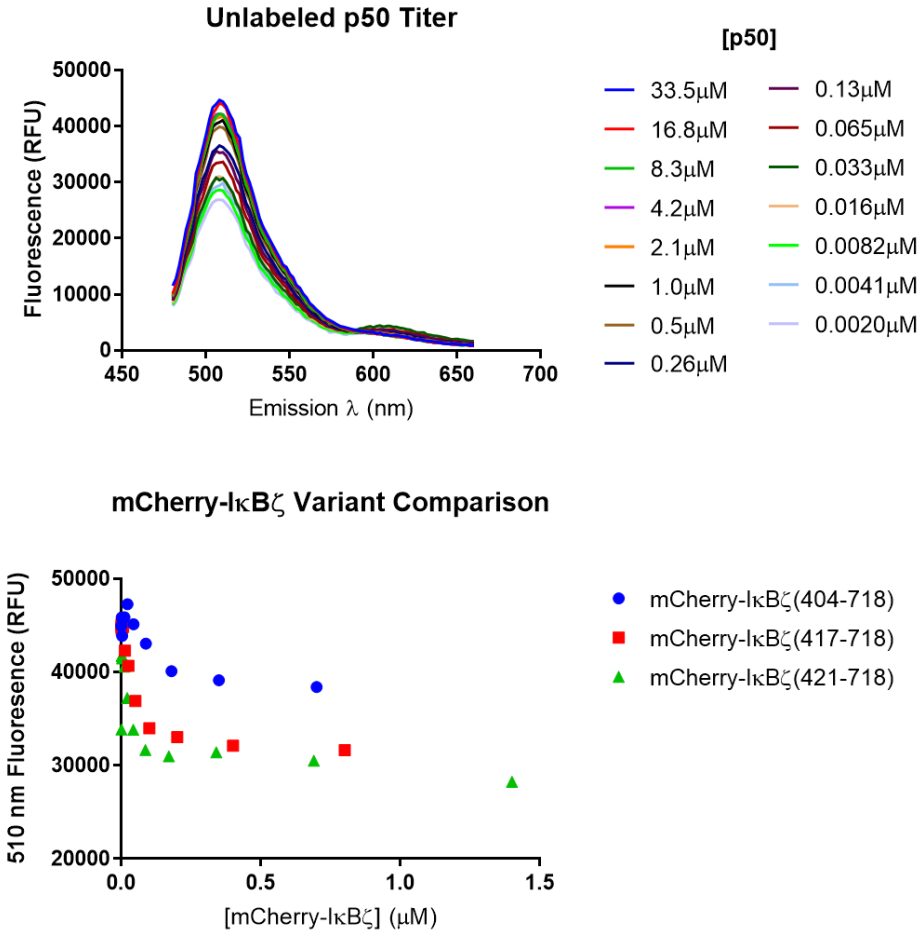

Figure 37 *– Validation of FRET between p50-GFP and mCherry-IκBζ. (Top) Titration of unlabeled p50 into p50-GFP/mCherry-IκBζ. (Bottom) Titration of mCherry-IκBζ variants into p50-GFP.*

In order to test whether FRET was occurring between our proteins, we titrated unlabeled p50dd into a p50-GFP/mCherry-IκBζ complex. The unlabeled protein should compete out p50-GFP thus removing the FRET. Loss of FRET was observed in a dose-dependent manner, both through quenching of GFP at 509 nm as well as emission of mCherry at 610 nm. Notably, the

quenching of p50 gave a stronger signal than the emission of mCherry (**Figure 37**, top). The quenching of GFP at 510 nM was therefore used as the primary measure of FRET occurrence.

After observing that FRET was taking place, we tested to see which of our variants had the strongest effect. We therefore titrated varying amounts of mCherry-IκBζ variants into p50-GFP. We observed a dose-dependent quenching of GFP in all three tested variants, though the effect was stronger in mCherry-IκBζ(417-718) and mCherry-IκBζ(421-718) (**Figure 37**, bottom).

3.3 Peptide Inhibitors

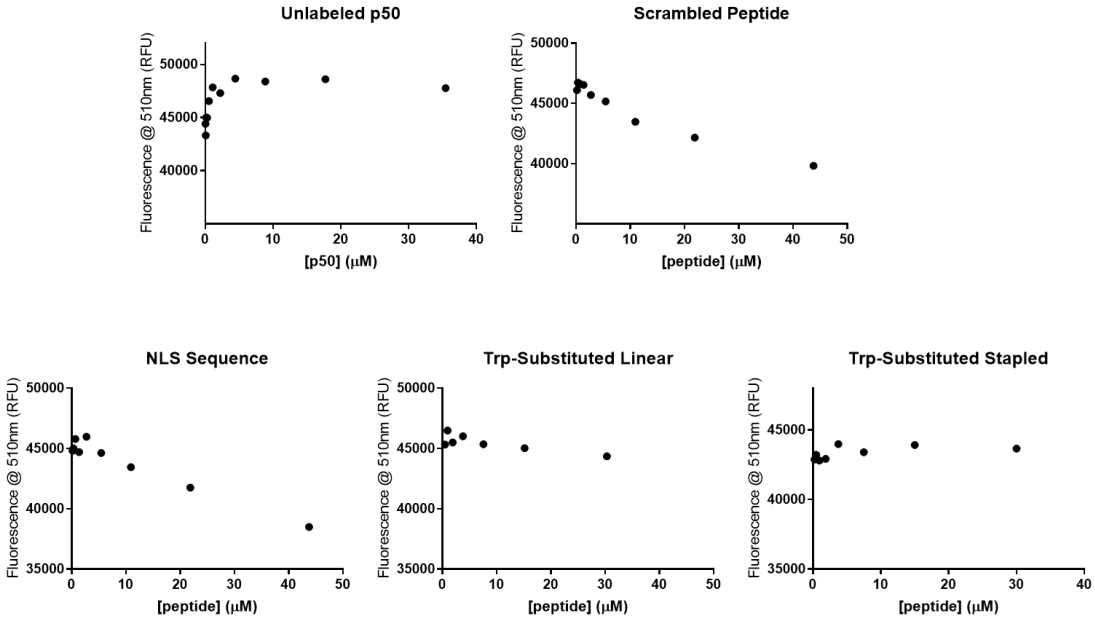

Figure 38 *- Peptide inhibitor tests.*

The nuclear localization sequence (NLS) of p50 is a major contact point for the binding of IκB proteins and p50. Reasoning that disruption of this interface may interfere with complex formation, a peptide with the NLS sequence was used as a potential inhibitor of IκBζ. Additionally, a non-natural peptide was made in which two of the residues had been stapled in order to stabilize the natural alpha helical turn in the NLS. Unfortunately, none of the peptide inhibitors showed an

ability to disrupt complex formation, even at high concentrations (**Figure 38**). It was at this point that the project was set aside.

4. Future of the Project

Interest in unraveling the functional consequences and chemical mechanisms of selective NF-κB-dependent gene expression by IκBζ remains high. Research work is currently under way to adapt the FRET-based assay to a dual fluorescence reporter microtiter plate-based assay. To this end, new versions of IκBζ have been engineered that express the mScarlet protein, which has a greater fluorescence yield than mCherry and, consequently, will generate a signal at lower concentration. Additionally, the fusion protein is engineered to contain a N-terminal reactive cysteine residue, which can easily be coupled via conjugation to biotin. The biotinylated mScarlet-IκBζ fusion protein will then be applied to streptavidin coated plates. After this, the p50-GFP protein will be added and, after washing away unbound proteins, fluorescent signals for both IκBζ and p50 will be measured by fluorimetry.

To test for disruptors of IκBζ:NF-κB complex formation, unlabeled NF-κB p50 homodimer dimerization domain will be titrated in excess until the p50-GFP signal is removed in the wash. Then screening will commence with peptides derived from p50, with small molecules designed to mimic the p50 binding element, with small molecules derived from in silico screening, and from compound libraries. Compounds that disrupt the interaction in the assay will be tested in cells and ultimately in mice to assess their effect on NF-κB-dependent gene expression in response to inducers that involve IκBζ.

References

1. Siegel, R. L., Miller, K. D. & Jemal, A. Cancer statistics, 2019. *CA Cancer J Clin* **69**, 7–34 (2019).

2. Koshiyama, M., Matsumura, N. & Konishi, I. Subtypes of Ovarian Cancer and Ovarian Cancer Screening. *Diagnostics* **7**, 1–10 (2017).

3. Buys, S. S. *et al.* Ovarian cancer screening in the Prostate, Lung, Colorectal and Ovarian (PLCO) cancer screening trial: Findings from the initial screen of a randomized trial. *Am J Obstet Gynecol* **193**, 1630–1639 (2005).

4. Buys, S. S. *et al.* Effect of screening on ovarian cancer mortality: the Prostate, Lung, Colorectal and Ovarian (PLCO) Cancer Screening Randomized Controlled Trial. *JAMA* **305**, 2295–303 (2011).

5. Torre, L. A. *et al.* Ovarian cancer statistics, 2018. *CA Cancer J Clin* **68**, 284–296 (2018).

6. Vang, R., Shih, I. M. & Kurman, R. J. Ovarian low-grade and high-grade serous carcinoma: Pathogenesis, clinicopathologic and molecular biologic features, and diagnostic problems. *Advances in Anatomic Pathology* vol. 16 267–282 Preprint at https://doi.org/10.1097/PAP.0b013e3181b4fffa (2009).

7. Koshiyama, M., Matsumura, N. & Konishi, I. Recent concepts of ovarian carcinogenesis: type I and type II. *Biomed Res Int* **2014**, 934261 (2014).

8. Tone, A. A. *et al.* Gene Expression Profiles of Luteal Phase Fallopian Tube Epithelium from *BRCA* Mutation Carriers Resemble High-Grade Serous Carcinoma. *Clinical Cancer Research* **14**, 4067–4078 (2008).

9. Norquist, B. M. *et al.* The molecular pathogenesis of hereditary ovarian carcinoma. *Cancer* **116**, 5261–5271 (2010).

10. Perets, R. *et al.* Transformation of the Fallopian Tube Secretory Epithelium Leads to High-Grade Serous Ovarian Cancer in Brca;Tp53;Pten Models. *Cancer Cell* **24**, 751–765 (2013).

11. Dubeau, L. The Cell of Origin of Ovarian Epithelial Tumors and the Ovarian Surface Epithelium Dogma: Does the Emperor Have No Clothes? *Gynecol Oncol* **72**, 437–442 (1999).

12. Lee, Y. *et al.* A candidate precursor to serous carcinoma that originates in the distal fallopian tube. *J Pathol* **211**, 26–35 (2007).

13. Bowtell, D. D. *et al.* Rethinking ovarian cancer II: Reducing mortality from high-grade serous ovarian cancer. *Nat Rev Cancer* **15**, 668–679 (2015).

14. American Cancer Society Medical and Editorial Content Team. Ovarian Cancer Staging. *cancer.org* (2018).

15. Nieman, K. M., Romero, I. L., Van Houten, B. & Lengyel, E. Adipose tissue and adipocytes supports tumorigenesis and metastasis. *Biochim Biophys Acta*. **1831**, 1533–1541 (2013).

16. Matulonis, U. A. *et al.* Ovarian cancer. *Nat Rev Dis Primers* **2**, 16061 (2016).

17. Batlle, E. & Clevers, H. Cancer stem cells revisited. *Nat Med* **23**, 1124–1134 (2017).

18. Burgos-Ojeda, D., Rueda, B. R. & Buckanovich, R. J. Ovarian cancer stem cell markers: Prognostic and therapeutic implications. *Cancer Lett* **322**, 1–7 (2012).

19. Hatina, J. *et al.* Ovarian Cancer Stem Cell Heterogeneity. in *Advances in Experimental Medicine and Biology* vol. 1139 201–221 (Springer New York LLC, 2019).

20. Zhang, S. *et al.* Identification and Characterization of Ovarian Cancer-Initiating Cells from Primary Human Tumors. *Cancer Res* **68**, 4311–4320 (2008).

21. Robinson, M. *et al.* Characterization of SOX2, OCT4 and NANOG in Ovarian Cancer Tumor-Initiating Cells. *Cancers (Basel)* **13**, 262 (2021).

22. Parte, S. C., Batra, S. K. & Kakar, S. S. Characterization of stem cell and cancer stem cell populations in ovary and ovarian tumors. *J Ovarian Res* **11**, 1–16 (2018).

23. Foster, R., Buckanovich, R. J. & Rueda, B. R. Ovarian cancer stem cells: Working towards the root of stemness. *Cancer Lett* **338**, 147–157 (2013).

24. Zhang, S. *et al.* Ovarian cancer stem cells express ROR1, which can be targeted for anti–cancer-stem-cell therapy. *Proceedings of the National Academy of Sciences* **111**, 17266–17271 (2014).

25. Peng, S., Maihle, N. J. & Huang, Y. Pluripotency factors Lin28 and Oct4 identify a sub-population of stem cell-like cells in ovarian cancer. *Oncogene* **29**, 2153–2159 (2010).

26. Lin, Z., Radaeva, M., Cherkasov, A. & Dong, X. Lin28 Regulates Cancer Cell Stemness for Tumour Progression. *Cancers* vol. 14 Preprint at https://doi.org/10.3390/cancers14194640 (2022).

27. Di, J. *et al.* The stem cell markers Oct4A, Nanog and c-Myc are expressed in ascites cells and tumor tissue of ovarian cancer patients. *Cellular Oncology* **36**, 363–374 (2013).

28. Siu, M. K. Y. *et al.* Stem cell transcription factor NANOG controls cell migration and invasion via dysregulation of E-cadherin and FoxJ1 and contributes to adverse clinical outcome in ovarian cancers. *Oncogene* **32**, 3500–3509 (2013).

29. Wen, Y., Hou, Y., Huang, Z., Cai, J. & Wang, Z. SOX2 is required to maintain cancer stem cells in ovarian cancer. *Cancer Sci* **108**, 719–731 (2017).

30. Kong, D., Li, Y., Wang, Z. & Sarkar, F. Cancer Stem Cells and Epithelial-to-Mesenchymal Transition (EMT)-Phenotypic Cells: Are They Cousins or Twins? *Cancers (Basel)* **3**, 716–729 (2011).

31. Loret, N., Denys, H., Tummers, P. & Berx, G. The role of epithelial-to-mesenchymal plasticity in ovarian cancer progression and therapy resistance. *Cancers* vol. 11 Preprint at https://doi.org/10.3390/cancers11060838 (2019).

32. Nelson, W. J. Remodeling Epithelial Cell Organization: Transitions Between Front-Rear and Apical-Basal Polarity. *Cold Spring Harb Perspect Biol* **1**, a000513–a000513 (2009).

33. Akhmetkaliyev, A., Alibrahim, N., Shafiee, D. & Tulchinsky, E. EMT/MET plasticity in cancer and Go-or-Grow decisions in quiescence: the two sides of the same coin? *Mol Cancer* **22**, 90 (2023).

34. Ribatti, D., Tamma, R. & Annese, T. Epithelial-Mesenchymal Transition in Cancer: A Historical Overview. *Transl Oncol* **13**, 100773 (2020).

35. Dongre, A. & Weinberg, R. A. New insights into the mechanisms of epithelial–mesenchymal transition and implications for cancer. *Nature Reviews Molecular Cell Biology* vol. 20 69–84 Preprint at https://doi.org/10.1038/s41580-018-0080-4 (2019).

36. Berr, A. L. *et al.* Vimentin is required for tumor progression and metastasis in a mouse model of non–small cell lung cancer. *Oncogene* **42**, 2074–2087 (2023).

37. Liu, C.-Y., Lin, H.-H., Tang, M.-J. & Wang, Y.-K. Vimentin contributes to epithelial-mesenchymal transition cancer cell mechanics by mediating cytoskeletal organization and focal adhesion maturation. *Oncotarget* **6**, 15966–15983 (2015).

38. Invasive Epithelial Ovarian Cancer Treatment, by Stage. https://www.cancer.org/cancer/ovarian-cancer/treating/by-stage.html.

39. Terraneo, N., Jacob, F., Dubrovska, A. & Grünberg, J. Novel Therapeutic Strategies for Ovarian Cancer Stem Cells. *Front Oncol* **10**, (2020).

40. Herceg, Z. & Wang, Z.-Q. Functions of poly(ADP-ribose) polymerase (PARP) in DNA repair, genomic integrity and cell death. *Mutation Research/Fundamental and Molecular Mechanisms of Mutagenesis* **477**, 97–110 (2001).

41. Morales, J. *et al.* Review of Poly (ADP-ribose) Polymerase (PARP) Mechanisms of Action and Rationale for Targeting in Cancer and Other Diseases. *Crit Rev Eukaryot Gene Expr* **24**, 15–28 (2014).

42. Fong, P. C. *et al.* Inhibition of Poly(ADP-Ribose) Polymerase in Tumors from BRCA Mutation Carriers . *New England Journal of Medicine* **361**, 123–134 (2009).

43. Dal Molin, G. Z., Westin, S. N. & Coleman, R. L. Rucaparib in ovarian cancer: extending the use of PARP inhibitors in the recurrent disease. *Future Oncology* **14**, 3101–3110 (2018).

44. Zheng, F. *et al.* Mechanism and current progress of Poly ADP-ribose polymerase (PARP) inhibitors in the treatment of ovarian cancer. *Biomedicine & Pharmacotherapy* **123**, 109661 (2020).

45. Yang, X., Yao, R. & Wang, H. Update of ALDH as a Potential Biomarker and Therapeutic Target for AML. *BioMed Research International* vol. 2018 Preprint at https://doi.org/10.1155/2018/9192104 (2018).

46. Tang, B. *et al.* Combined treatment of disulfiram with PARP inhibitors suppresses ovarian cancer. *Front Oncol* **13**, (2023).

47. Choi, S. A. *et al.* Disulfiram modulates stemness and metabolism of brain tumor initiating cells in atypical teratoid/rhabdoid tumors. *Neuro Oncol* **17**, 810–821 (2015).

48. Jia, Y. & Huang, T. Overview of Antabuse® (Disulfiram) in Radiation and Cancer Biology. *Cancer Manag Res* **Volume 13**, 4095–4101 (2021).

49. Schilder, R. J. *et al.* Phase II evaluation of imatinib mesylate in the treatment of recurrent or persistent epithelial ovarian or primary peritoneal carcinoma: A gynecologic oncology group study. *Journal of Clinical Oncology* **26**, 3418–3425 (2008).

50. Juretzka, M. *et al.* A phase 2 trial of oral imatinib in patients with epithelial ovarian, fallopian tube, or peritoneal carcinoma in second or greater remission. *Eur J Gynaecol Oncol* **29**, 568–72 (2008).

51. Huxford, T., Hoffmann, A. & Ghosh, G. Understanding the logic of IκB:NF-κB regulation in structural terms. *Curr Top Microbiol Immunol* **349**, 1–24 (2011).

52. Ko, M. S. *et al.* Regulatory subunit NEMO promotes polyubiquitin-dependent induction of NF-κB through a targetable second interaction with upstream activator IKK2. *Journal of Biological Chemistry* **298**, 101864 (2022).

53. Baeuerle, P. A. & Baltimore, D. Activation of DNA-binding activity in an apparently cytoplasmic precursor of the NF-κB transcription factor. *Cell* **53**, 211–217 (1988).

54. Sun, S.-C. Non-canonical NF-κB signaling pathway. *Cell Res* **21**, 71–85 (2011).

55. Xia, L. *et al.* Role of the NFκB-signaling pathway in cancer. *Onco Targets Ther* **11**, 2063–2073 (2018).

56. Taniguchi, K. & Karin, M. NF-κB, inflammation, immunity and cancer: coming of age. *Nat Rev Immunol* **18**, 309–324 (2018).

57. Sarnico, I. *et al.* Chapter 24 NF-KappaB Dimers in the Regulation of Neuronal Survival. in 351–362 (2009). doi:10.1016/S0074-7742(09)85024-1.

58. Yamamoto, M. *et al.* Regulation of Toll/IL-1-receptor-mediated gene expression by the inducible nuclear protein IκBζ. *Nature* **430**, 218–222 (2004).

59. Yamazaki, S., Muta, T. & Takeshige, K. A Novel IκB Protein, IκB-ζ, Induced by Proinflammatory Stimuli, Negatively Regulates Nuclear Factor-κB in the Nuclei. *Journal of Biological Chemistry* **276**, 27657–27662 (2001).

60. Totzke, G. *et al.* A novel member of the IκB family, human IκB-ζ, inhibits transactivation of p65 and its DNA binding. *Journal of Biological Chemistry* **281**, 12645–12654 (2006).

61. Okamoto, K. *et al.* IκBζ regulates TH17 development by cooperating with ROR nuclear receptors. *Nature* **464**, 1381–1385 (2010).

62. Kohda, A., Yamazaki, S. & Sumimoto, H. The nuclear protein IκBζ forms a transcriptionally active complex with nuclear factor-κB (NF-κB) p50 and the Lcn2 promoter via the N- and C-terminal ankyrin repeat motifs. *Journal of Biological Chemistry* **291**, 20739–20752 (2016).

63. Hildebrand, D. G. *et al.* IkBz Is a Transcriptional Key Regulator of CCL2/MCP-1. *The Journal of Immunology* (2013) doi:10.4049/jimmunol.1300089.

64. Kitamura, H., Kanehira, K., Okita, K., Morimatsu, M. & Saito, M. MAIL, a novel nuclear IκB protein that potentiates LPS-induced IL-6 production. *FEBS Lett* **485**, 53–56 (2000).

65. Seshadri, S., Kannan, Y., Mitra, S., Parker-Barnes, J. & Wewers, M. D. MAIL Regulates Human Monocyte IL-6 Production. *The Journal of Immunology* **183**, 5358–5368 (2009).

66. MaruYama, T. *et al.* Control of IFN-γ production and regulatory function by the inducible nuclear protein IκB-ζ in T cells. *J Leukoc Biol* **98**, 385–393 (2015).

67. Hörber, S. *et al.* The atypical inhibitor of NF-κB, IκBζ, controls macrophage interleukin-10 expression. *Journal of Biological Chemistry* **291**, 12851–12961 (2016).

68. Kayama, H. *et al.* Class-specific regulation of pro-inflammatory genes by MyD88 pathways and IκBζ. *Journal of Biological Chemistry* **283**, 12468–12477 (2008).

69. Yamazaki, S. *et al.* Gene-specific requirement of a nuclear protein, IκB-ζ, for promoter association of inflammatory transcription regulators. *Journal of Biological Chemistry* **283**, 32404–32411 (2008).

70. Tartey, S. *et al.* Akirin2 is critical for inducing inflammatory genes by bridging IκB-ζ and the SWI/SNF complex. *EMBO J* **33**, 2332–2348 (2014).

71. Brenenstuhl, H., Armento, A., Braczysnki, A. K., Mitelbron, M. & Nauman, U. IκBζ, an atypical member of the inhibitor of nuclear factor kappa B family, is induced by γ-

irradiation in glioma cells, regulating cytokine secretion and associated with poor prognosis. *Int J Oncol* **47**, 1971–1980 (2015).

72. Tsoi, L. C. *et al.* Enhanced meta-analysis and replication studies identify five new psoriasis susceptibility loci. *Nat Commun* **6**, 7001 (2015).

73. Coto-Segura, P. *et al.* NFKBIZ in Psoriasis: Assessing the association with gene polymorphisms and report of a new transcript variant. *Hum Immunol* **78**, 435–440 (2017).

74. Huynh, Q. K. *et al.* Characterization of the recombinant IKK1/IKK2 heterodimer: Mechanisms regulating kinase activity. *Journal of Biological Chemistry* **275**, 25883–25891 (2000).

75. Antonia, R. J., Hagan, R. S. & Baldwin, A. S. Expanding the View of IKK: New Substrates and New Biology. *Trends Cell Biol* **31**, 166–178 (2021).

76. House, C. D. *et al.* NFκB Promotes Ovarian Tumorigenesis via Classical Pathways That Support Proliferative Cancer Cells and Alternative Pathways That Support ALDH+ Cancer Stem–like Cells. *Cancer Res* **77**, 6927–6940 (2017).

77. Chicheportiche, Y. *et al.* TWEAK, a new secreted ligand in the tumor necrosis factor family that weakly induces apoptosis. *Journal of Biological Chemistry* **272**, 32401–32410 (1997).

78. Marsters, S. A. *et al.* Identification of a ligand for the death-domain-containing receptor Apo3. *Current Biology* **8**, 525–528 (1998).

79. Winkles, J. A. The TWEAK–Fn14 cytokine–receptor axis: discovery, biology and therapeutic targeting. *Nat rev Cancer* **7**, 411–425 (2008).

80. Uhlén, M. *et al.* Tissue-based map of the human proteome. *Science (1979)* **347**, (2015).

81. Burkly, L. C., Michaelson, J. S., Hahm, K., Jakubowski, A. & Zheng, T. S. TWEAKing tissue remodeling by a multifunctional cytokine: Role of TWEAK/Fn14 pathway in health and disease. *Cytokine* vol. 40 1–16 Preprint at https://doi.org/10.1016/j.cyto.2007.09.007 (2007).

82. Brown, S. A. N., Hanscom, H. N., Vu, H., Brew, S. A. & Winkles, J. A. TWEAK binding to the Fn14 cysteine-rich domain depends on charged residues located in both the A1 and D2 modules. *Biochemical Journal* **397**, 297–304 (2006).

83. Wiley, S. R. *et al.* A novel TNF receptor family member binds TWEAK and is implicated in angiogenesis. *Immunity* **15**, 837–846 (2001).

84. Moreno, J. A. *et al.* The CD163-expressing macrophages recognize and internalize TWEAK. Potential consequences in atherosclerosis. *Atherosclerosis* **207**, 103–110 (2009).

85. Bover, L. C. *et al.* A Previously Unrecognized Protein-Protein Interaction between TWEAK and CD163: Potential Biological Implications. *The Journal of Immunology* **178**, 8183–8194 (2007).

86. Ratajczak, W., Atkinson, S. D. & Kelly, C. The TWEAK/Fn14/CD163 axis—implications for metabolic disease. *Rev Endocr Metab Disord* **23**, 449–462 (2022).

87. Donohue, P. J. *et al.* TWEAK Is an Endothelial Cell Growth and Chemotactic Factor That Also Potentiates FGF-2 and VEGF-A Mitogenic Activity. *Arterioscler Thromb Vasc Biol* **23**, 594–600 (2003).

88. Li, H. *et al.* Tumor Necrosis Factor-related Weak Inducer of Apoptosis Augments Matrix Metalloproteinase 9 (MMP-9) Production in Skeletal Muscle through the Activation of Nuclear Factor-κB-inducing Kinase and p38 Mitogen-activated Protein Kinase. *Journal of Biological Chemistry* **284**, 4439–4450 (2009).

89. Kumar, M., Makonchuk, D. Y., Li, H., Mittal, A. & Kumar, A. TNF-Like Weak Inducer of Apoptosis (TWEAK) Activates Proinflammatory Signaling Pathways and Gene Expression through the Activation of TGF-β-Activated Kinase 1. *The Journal of Immunology* **182**, 2439–2448 (2009).

90. Fortin, S. P. *et al.* Tumor Necrosis Factor–Like Weak Inducer of Apoptosis Stimulation of Glioma Cell Survival Is Dependent on Akt2 Function. *Molecular Cancer Research* **7**, 1871–1881 (2009).

91. Winkles, Jeffrey, A. Role of TWEAK and Fn14 in tumor biology. *Frontiers in Bioscience* **12**, 2761 (2007).

92. Poveda, J. *et al.* TWEAK/Fn14 and non-canonical NF-kappaB signaling in kidney disease. *Front Immunol* **4**, 1–7 (2013).

93. Yu, H., Lin, L., Zhang, Z., Zhang, H. & Hu, H. Targeting NF-κB pathway for the therapy of diseases: mechanism and clinical study. *Signal Transduction and Targeted Therapy* vol. 5 Preprint at https://doi.org/10.1038/s41392-020-00312-6 (2020).

94. Yamamoto, M., Gohda, J., Akiyama, T. & Inoue, J. I. TNF receptor-associated factor 6 (TRAF6) plays crucial roles in multiple biological systems through polyubiquitination-mediated NF-κB activation. *Proc Jpn Acad Ser B Phys Biol Sci* **37**, 145–160 (2021).

95. Michaelson, J. S. *et al.* Tweak induces mammary epithelial branching morphogenesis. *Oncogene* **24**, 2613–2624 (2005).

96. Enwere, E. K., LaCasse, E. C., Adam, N. J. & Korneluk, R. G. Role of the TWEAK-Fn14-cIAP1-NF-κB signaling axis in the regulation of myogenesis and muscle homeostasis. *Frontiers in Immunology* vol. 5 Preprint at https://doi.org/10.3389/fimmu.2014.00034 (2014).

97. Burkly, L. C., Michaelson, J. S. & Zheng, T. S. TWEAK/Fn14 pathway: an immunological switch for shaping tissue responses. *Immunol Rev* **244**, 99–114 (2011).

98. Gupta, G. *et al.* Letter to the editor: Activation of TWEAK/Fn14 Signaling Supresses TRAFs/NF-KB Pathway in the Pathogenesis of Cancer. *EXCLI J* **20**, 232–235 (2021).

99. Sanz, A. B. *et al.* Tweak induces proliferation in renal tubular epithelium: A role in uninephrectomy induced renal hyperplasia. *J Cell Mol Med* **13**, 3329–3342 (2009).

100. Brown, S. A. N., Cheng, E., Williams, M. S. & Winkles, J. A. TWEAK-Independent Fn14 Self-Association and NF-κB Activation Is Mediated by the C-Terminal Region of the Fn14 Cytoplasmic Domain. *PLoS One* **8**, e65248 (2013).

101. Burkly, L. C. Tweak/Fn14 axis: the current paradigm of tissue injury-inducible function in the midst of complexities. *Semin Immunol* (2014) doi:10.1016/j.smim.2014.02.006.

102. Tajrishi, M. M., Zheng, T. S., Burkly, L. C. & Kumar, A. The TWEAK-Fn14 pathway: A potent regulator of skeletal muscle biology in health and disease. *Cytokine Growth Factor Rev* **25**, 215–225 (2014).

103. Donohue, P. J. *et al.* TWEAK is an endothelial cell growth and chemotactic factor that also potentiates FGF-2 and VEGF-A mitogenic activity. *Arterioscler Thromb Vasc Biol* **23**, 594–600 (2003).

104. Schneider, P. *et al.* TWEAK can induce cell death via endogenous TNF and TNF receptor 1. *Eur J Immunol* **29**, 1785–1792 (1999).

105. Vince, J. E. *et al.* TWEAK-FN14 signaling induces lysosomal degradation of a cIAP1-TRAF2 complex to sensitize tumor cells to TNFα. *Journal of Cell Biology* **182**, 171–184 (2008).

106. Wicovsky, A. *et al.* TNF-like weak inducer of apoptosis inhibits proinflammatory TNF receptor-1 signaling. *Cell Death Differ* **16**, 1445–1459 (2009).

107. Gu, L. *et al.* Functional Expression of TWEAK and the Receptor Fn14 in Human Malignant Ovarian Tumors: Possible Implication for Ovarian Tumor Intervention. *PLoS One* **8**, 1–8 (2013).

108. Wajant, H. & Siegmund, D. TNFR1 and TNFR2 in the Control of the Life and Death Balance of Macrophages. *Front Cell Dev Biol* **7**, 1–14 (2019).

109. Kawakita, T. *et al.* Functional expression of TWEAK in human hepatocellular carcinoma: Possible implication in cell proliferation and tumor angiogenesis. *Biochem Biophys Res Commun* **318**, 726–733 (2004).

110. Lin, B. R. *et al.* Prognostic significance of TWEAK expression in colorectal cancer and effect of its inhibition on invasion. *Ann Surg Oncol* **19**, (2012).

111. Yoriki, R. *et al.* Therapeutic potential of the TWEAK/FN14 pathway in intractable gastrointestinal cancer. *Exp Ther Med* **2**, 103–108 (2011).

112. Ho, D. H. *et al.* Soluble tumor necrosis factor-like weak inducer of apoptosis overexpression in HEK293 cells promotes tumor growth and angiogenesis in athymic nude mice. *Cancer Res* **64**, 8968–8972 (2004).

113. Hu, G., Zeng, W. & Xia, Y. TWEAK/Fn14 signaling in tumors. *Tumor Biology* **39**, (2017).

114. Dai, L., Gu, L., Ding, C., Qiu, L. & Di, W. TWEAK promotes ovarian cancer cell metastasis via NF-κB pathway activation and VEGF expression. *Cancer Lett* **283**, 159–167 (2009).

115. Hu, Y. *et al.* TWEAK-stimulated macrophages inhibit metastasis of epithelial ovarian cancer via exosomal shuttling of microRNA. *Cancer Lett* **393**, 60–67 (2017).

116. Cao, Q. *et al. MicroRNA-7 inhibits cell proliferation, migration and invasion in human non-small cell lung cancer cells by targeting FAK through ERK/MAPK signaling pathway*. vol. 7 www.impactjournals.com/oncotarget.

117. Liu, Z. *et al.* miR-7 inhibits glioblastoma growth by simultaneously interfering with the PI3K/ATK and Raf/MEK/ERK pathways. *Int J Oncol* **44**, 1571–1580 (2014).

118. Dhruv, H. *et al.* Structural basis and targeting of the interaction between fibroblast growth factor-inducible 14 and tumor necrosis factor-like weak inducer of apoptosis. *Journal of Biological Chemistry* **288**, 32261–32276 (2013).

119. Lassen, U. N. *et al.* A phase I monotherapy study of RG7212, a first-in- class monoclonal antibody targeting TWEAK signaling in patients with advanced cancers. *Clinical Cancer Research* **21**, 258–266 (2015).

120. Michaelson, J. S. *et al.* Development of an Fn14 agonistic antibody as an anti-tumor agent. *MAbs* **3**, (2011).

121. Chapman, M. S., Wu, L., Amatucci, A., Ho, S. N. & Michaelson, J. S. TWEAK signals through JAK-STAT to induce tumor cell apoptosis. *Cytokine* **61**, 210–217 (2013).

122. Michaelson, J. S. *et al.* The anti-Fn14 antibody BIIB036 inhibits tumor growth in xenografts and patient derived primary tumor models and enhances efficacy of chemotherapeutic agents in multiple xenograft models. *Cancer Biol Ther* **13**, 812–821 (2012).

123. Aido, A., Zaitseva, O., Wajant, H., Buzgo, M. & Simaite, A. Anti-Fn14 Antibody-Conjugated Nanoparticles Display Membrane TWEAK-Like Agonism. *Pharmaceutics* **13**, 1072 (2021).

124. Ye, S. *et al.* Enavatuzumab, a Humanized Anti-TWEAK Receptor Monoclonal Antibody, Exerts Antitumor Activity through Attracting and Activating Innate Immune Effector Cells. *J Immunol Res* **2017**, (2017).

125. Lam, E. T. *et al.* Phase I study of enavatuzumab, a first-in-class humanized monoclonal antibody targeting the TWEAK receptor, in patients with advanced solid tumors. *Mol Cancer Ther* **17**, 215–221 (2018).

126. Trebing, J. *et al.* A novel llama antibody targeting Fn14 exhibits anti-metastatic activity in vivo. *MAbs* **6**, 297–308 (2014).

127. Zaitseva, O. *et al.* Antibody-based soluble and membrane-bound TWEAK mimicking agonists with FcγR-independent activity. *Front Immunol* **14**, (2023).

128. Stirling, D. R. *et al.* CellProfiler 4: improvements in speed, utility and usability. *BMC Bioinformatics* **22**, 433 (2021).

129. Ljosa, V., Sokolnicki, K. L. & Carpenter, A. E. Annotated high-throughput microscopy image sets for validation. *Nat Methods* **9**, 637–637 (2012).

130. Wang, J., Sinnett-Smith, J., Stevens, J. V., Young, S. H. & Rozengurt, E. Biphasic Regulation of Yes-associated Protein (YAP) Cellular Localization, Phosphorylation, and Activity by G Protein-coupled Receptor Agonists in Intestinal Epithelial Cells. *Journal of Biological Chemistry* **291**, 17988–18005 (2016).

131. Hong, L., Wang, S., Li, W., Wu, D. & Chen, W. Tumor-associated macrophages promote the metastasis of ovarian carcinoma cells by enhancing CXCL16/CXCR6 expression. *Pathol Res Pract* **214**, 1345–1351 (2018).

132. Hagemann, T. *et al.* Macrophages Induce Invasiveness of Epithelial Cancer Cells Via NF-κB and JNK. *The Journal of Immunology* **175**, 1197–1205 (2005).

133. Chen, R. *et al.* Regulation of IKKβ by miR-199a affects NF-κB activity in ovarian cancer cells. *Oncogene* **27**, 4712–4723 (2008).

134. Shinin, V., Gayraud-Morel, B., Gomès, D. & Tajbakhsh, S. Asymmetric division and cosegregation of template DNA strands in adult muscle satellite cells. *Nat Cell Biol* **8**, 677–682 (2006).

135. Sunchu, B. & Cabernard, C. Principles and mechanisms of asymmetric cell division. *Development* **147**, (2020).

136. Pine, S. R. & Liu, W. Asymmetric cell division and template DNA co-segregation in cancer stem cells. *Front Oncol* **4 AUG**, (2014).

137. Charville, G. W. & Rando, T. A. Stem cell ageing and non-random chromosome segregation. *Philosophical Transactions of the Royal Society B: Biological Sciences* **366**, 85–93 (2011).

138. Fan, Y.-L., Zhao, H.-C., Li, B., Zhao, Z.-L. & Feng, X.-Q. Mechanical Roles of F-Actin in the Differentiation of Stem Cells: A Review. *ACS Biomater Sci Eng* **5**, 3788–3801 (2019).

139. Sliogeryte, K., Thorpe, S. D., Lee, D. A., Botto, L. & Knight, M. M. Stem cell differentiation increases membrane-actin adhesion regulating cell blebability, migration and mechanics. *Sci Rep* **4**, 7307 (2015).

140. Hernandez, L. *et al.* Characterization of ovarian cancer cell lines as in vivo models for preclinical studies. *Gynecol Oncol* **142**, 332–340 (2016).

141. Perez, J. G. *et al.* The TWEAK receptor Fn14 is a potential cell surface portal for targeted delivery of glioblastoma therapeutics. *Oncogene* vol. 35 2145–2155 Preprint at https://doi.org/10.1038/onc.2015.310 (2016).

142. Su, S. *et al.* CD10+GPR77+ Cancer-Associated Fibroblasts Promote Cancer Formation and Chemoresistance by Sustaining Cancer Stemness. *Cell* **172**, 841-856.e16 (2018).

143. Wu, A. Y. *et al.* Fn14 overcomes cisplatin resistance of high-grade serous ovarian cancer by promoting Mdm2-mediated p53-R248Q ubiquitination and degradation. *Journal of Experimental and Clinical Cancer Research* **38**, 1–14 (2019).

144. Haruta, H., Kato, A. & Todokoro, K. Isolation of a Novel Interleukin-1-inducible Nuclear Protein Bearing Ankyrin-repeat Motifs. *Journal of Biological Chemistry* **276**, 12485–12488 (2001).

145. Alexander, E. *et al.* IκBζ is a regulator for the senescence-associated secretory phenotype in DNA damage- and oncogene-induced senescence. *J Cell Sci* **126**, 3738–3745 (2013).

146. MaruYama, T. *et al.* Control of IFN-γ production and regulatory function by the inducible nuclear protein IκB-ζ in T cells. *J Leukoc Biol* **98**, 385–393 (2015).

147. Johansen, C. *et al.* IκBζ is a key driver in the development of psoriasis. *Proceedings of the National Academy of Sciences* **112**, E5825–E5833 (2015).

148. Liu, Q., Xiao, S. & Xia, Y. TWEAK/Fn14 Activation Participates in Skin Inflammation. *Mediators Inflamm* **2017**, (2017).

149. Bajar, B. T., Wang, E. S., Zhang, S., Lin, M. Z. & Chu, J. A guide to fluorescent protein FRET pairs. *Sensors (Switzerland)* **16**, 1–24 (2016).